NASA Technical Paper 3027

September 1990

Annoyance Caused by Advanced Turboprop Aircraft Flyover Noise

Counter-Rotating Propeller Configuration

David A. McCurdy

NASA

NASA Technical Paper 3027

1990

Annoyance Caused by Advanced Turboprop Aircraft Flyover Noise

Counter-Rotating Propeller Configuration

David A. McCurdy
Langley Research Center
Hampton, Virginia

National Aeronautics and Space Administration
Office of Management
Scientific and Technical Information Division

Summary

Two laboratory experiments were conducted to quantify the annoyance response of people to the flyover noise of advanced turboprop (propfan) aircraft with counter-rotating propellers. The specific objectives were (1) to determine the effects on annoyance of fundamental frequency (blade passage frequency) and tone-to-broadband noise ratio, (2) to compare annoyance response to counter-rotating advanced turboprop aircraft with annoyance responses to conventional turboprop and turbofan aircraft, and (3) to determine the ability of aircraft-noise measurement procedures and corrections to predict annoyance. Analyses of the data obtained from the two experiments are presented in this report.

The first experiment examined advanced turboprop aircraft with counter-rotating propellers having an equal number of blades on each rotor. A computer synthesis system was used to generate 27 realistic, time-varying simulations of takeoff noise in which the tonal content was systematically varied to represent the factorial combinations of 9 fundamental frequencies and 3 tone-to-broadband noise ratios. These advanced turboprop simulations, along with recordings of 5 conventional turboprop takeoffs and 5 conventional turbofan takeoffs, were presented at 3 sound pressure levels to 64 subjects in an anechoic chamber.

The second experiment examined advanced turboprop aircraft with counter-rotating propellers having an unequal number of blades on each rotor. The computer synthesis system was used to generate 35 simulations of takeoff noise representing combinations of 15 fundamental-frequency pairs and 3 tone-to-broadband noise ratios. As in the first experiment, these simulations, along with recordings of 5 conventional turboprop takeoffs and 5 conventional turbofan takeoffs, were presented at 3 sound pressure levels to 64 subjects in an anechoic chamber.

Analyses of the subjects' annoyance judgments in both experiments showed that annoyance was significantly affected by the interaction of fundamental frequency with tone-to-broadband noise ratio and by the interaction of tone-to-broadband noise ratio with noise level. No significant differences in annoyance between the conventional turbofan aircraft and the advanced turboprop aircraft with counter-rotating propellers were found for configurations having either an equal or unequal number of blades. The use of a duration correction and a modified tone correction improved the annoyance prediction for the stimuli in both experiments. An A-weighted sound pressure level with duration and tone corrections provided the most accurate annoyance prediction.

Introduction

The return of the propeller to long-haul commercial service may be rapidly approaching in the form of the advanced turboprop (propfan) aircraft as illustrated in figure 1. The advanced turboprop propeller is vastly different from conventional propellers in shape and number of blades. Also, it will most likely be a counter-rotating propeller (CRP) instead of the conventional single-rotating propeller (SRP) configuration found on almost all of today's propeller-driven aircraft. The counter-rotating propeller, shown in figure 2, consists of two rotors (or rows) of blades rotating in opposite directions around the same axis. The advanced turboprop aircraft offers substantial savings in operating costs through improved energy efficiency. However, such an aircraft will come into general usage only if its noise, which has unique spectral characteristics, especially in the counter-rotating configuration, meets the standards of community acceptability currently applied to existing aircraft. Much research has been directed toward understanding and quantifying the annoyance caused by jet-aircraft flyover noise, but relatively little research has been conducted for conventional propeller noise. Reference 1 is a study of annoyance caused by advanced turboprop aircraft with single-rotating propellers. The present paper extends that work to include the counter-rotating propeller configuration. Two laboratory experiments were conducted to quantify the annoyance of people to the flyover noise of advanced turboprop aircraft with counter-rotating propellers.

The primary concern in quantifying advanced turboprop noise annoyance is the unique spectral characteristics of the noise. In general, propeller noise consists of a number of harmonically related pure tone components that are superimposed on broadband noise as illustrated in figure 3. The fundamental frequency of these tones, which can dominate the total noise produced by the aircraft, occurs at the propeller blade passage frequency. The frequency envelope shape is described in terms of the sound pressure levels of the harmonics relative to the fundamental. Tone-to-broadband noise ratio can be defined in a number of ways. As used in these studies, it is defined to be the difference between the level of the fundamental tone and the level of the highest 1/3-octave band of broadband noise. The fundamental frequency ranges from 50 Hz to about 150 Hz for conventional propeller aircraft. For advanced turboprop aircraft, the fundamental frequency is expected to range from 150 Hz to as high as 300 Hz.

Figure 4(a) illustrates the tonal content and frequency-envelope-shape characteristic of the single-rotating propeller configuration. The counter-rotating propeller configuration produces a second set of harmonically related pure tone components and a set of interaction pure tone components. For the counter-rotating configuration in which the number of blades on each rotor is equal, the second set of harmonic tones and the interaction tones are produced at the same frequencies as the first set of harmonic tones (assuming that both rotors rotate at the same speed). This can affect the frequency envelope shape as illustrated in figure 4(b). For the counter-rotating configuration in which the number of blades on each rotor is unequal, the second set of harmonic tones occurs at frequencies different from the first set, as shown in figure 4(c). In addition, the interaction tones occur at combinations of the frequencies of the two sets of harmonic tones. Thus, the tonal content is increased and the frequency envelope shape is affected as shown in the example presented in figure 4(d). The directivity patterns of interaction tones also differ significantly from those of harmonic tones, as illustrated in figure 5.

The annoyance caused by noise sources with strong tonal components has historically been more difficult to quantify than the annoyance caused by broadband noise (refs. 2 5). The uncertainty in accounting for tonal content is increased in this case because less basic psychoacoustic research has been conducted in the lower frequency range of tones from conventional and advanced turboprop propellers than in the higher frequency range of tones from jet aircraft.

The first laboratory experiment examined the effects on annoyance of the tonal characteristics of counter-rotating propeller configurations with an equal number of blades on each rotor. The second laboratory experiment examined the effects on annoyance of the tonal characteristics of counter-rotating propeller configurations with an unequal number of blades on each rotor. Included in each experiment were five conventional turboprop aircraft takeoffs and five conventional turbofan aircraft takeoffs. Both experiments had three specific objectives. The first objective was to determine the effects on annoyance of fundamental frequency and tone-to-broadband noise ratio. The second objective was to compare the annoyance response to counter-rotating advanced turboprop aircraft with the annoyance responses to conventional turboprop and turbofan aircraft. The final objective was to determine the ability of aircraft-noise measurement procedures and corrections to predict annoyance to the combined set of aircraft types.

Noise Metrics, Symbols, and Abbreviations

Noise Metrics

EPNL	effective perceived noise level, dB
L_A	A-weighted sound pressure level, dB
L_D	D-weighted sound pressure level, dB
L_E	E-weighted sound pressure level, dB
L_1	weighted sound pressure level based on modified frequency weighting from reference 6 (see "Acoustic Data Analyses" section), dB
LL	loudness level (Stevens Mark VI procedure), dB
LL_Z	Zwicker loudness level, dB
PL	perceived level (Stevens Mark VII procedure), dB
PNL	perceived noise level, dB
PNL_K, PNL_M, PNL_W	perceived noise level with critical-band corrections (see "Acoustic Data Analyses" section), dB

Detailed descriptions of the noise metrics used in this report can be found in references 6, 7, and 8.

Symbols and Abbreviations

ATP	advanced turboprop
CRP	counter-rotating propeller
F_o	fundamental frequency (blade passage frequency), Hz
F_{oa}	fundamental frequency (blade passage frequency) of aft rotor, Hz
F_{of}	fundamental frequency (blade passage frequency) of forward rotor, Hz
FAR	Federal Aviation Regulation
L_S	subjective noise level, dB

$n \times m$	unequal number of blades in each rotor of counter-rotating propeller (n blades in forward rotor, m blades in aft rotor)
$n \times n$	equal number of blades in each rotor of counter-rotating propeller (n blades in forward rotor and in aft rotor)
p	probability
SPL	sound pressure level, dB
SRP	single-rotating propeller
T_1	EPNL tone-correction method (ref. 7)
T_2	tone-correction method identical to T_1 except that no corrections are applied for tones below the 500-Hz 1/3-octave band
T/N	tone-to-broadband noise ratio (defined as the difference between the level of the fundamental tone and the level of the highest 1/3-octave band of broadband noise), dB

Experimental Method

Test Facility

The Anechoic Listening Room in the Langley Acoustics Research Laboratory (fig. 6) was used as the test facility in both experiments. This room, which has a volume of 20 m^3 and an A-weighted ambient noise level of 15 dB, provides an essentially echo-free environment. This eliminates any possibility of standing waves affecting the data. The monophonic recordings of the aircraft noise stimuli were played on a studio-quality tape recorder using a noise reduction system to reduce tape hiss. The noise reduction system provided a nominal 30-dB increase in signal-to-noise ratio and reduced tape hiss to inaudible levels. In the first experiment, the stimuli were presented to the subjects using a special speaker system consisting of one high-frequency unit and one low-frequency unit. The high-frequency unit had a frequency range from 100 to 10 000 Hz, and the low-frequency unit had a frequency range from 30 to 100 Hz. In the second experiment the speaker system was modified so that it consisted of one unit with a usable frequency range from 40 to 10 000 Hz.

Test Subjects

One hundred and twenty-eight subjects, 64 for each experiment, were randomly selected from a pool of local residents with a wide range of socioeconomic backgrounds and were paid to participate in the experiments. All test subjects were given audiograms prior to the experiment to verify normal hearing. Table I gives the sex and age data for the subjects in each experiment.

Noise Stimuli

Advanced turboprop stimuli in the first experiment. The advanced turboprop stimuli in the first experiment represented noise from an aft-mounted, pusher, counter-rotating propeller configuration with an equal number of blades on each rotor. The Aircraft Noise Synthesis System described in reference 9 was used to generate these noise stimuli. The computer-based system generates realistic, time-varying, audio simulations of aircraft flyover noise at a specified observer location on the ground. The synthesis takes into account the time-varying aircraft position relative to the observer; specified reference spectra consisting of broadband, narrowband, and pure tone components; directivity patterns; Doppler shift; atmospheric effects; and ground effects. These parameters can be specified and controlled in such a way as to generate stimuli in which certain noise characteristics such as fundamental frequency or duration are independently varied while the remaining characteristics such as broadband content are held constant. The synthesis system was used to generate 27 simulations of advanced turboprop aircraft flyover noise in which the tonal content was systematically varied to represent the factorial combinations of 9 fundamental frequencies and 3 tone-to-broadband noise ratios.

The first step in generating the simulations was to define a synthesis-system input data set for each of the 27 flyovers. A literature review was conducted to determine typical characteristics of advanced turboprop aircraft and expected ranges of the tonal characteristics (refs. 10–24). Because of testing time constraints, the simulations were limited to one takeoff flight profile, one observer location, one broadband noise spectrum, and one broadband noise directivity pattern. Each of these parameters was the same for each simulation. Aircraft speed was 70 m/sec (a Mach number of 0.2). The selected takeoff flight profile resulted in an altitude at closest approach to the observer of 380 m, about the altitude expected at the FAR 36 takeoff noise measurement location (ref. 7). The observer was located on the centerline of the ground track. Since predictions of advanced

turboprop broadband noise were not available, the broadband spectral content was based on measurements of an existing, large, turboprop aircraft, the Lockheed P-3. The broadband 1/3-octave spectrum and the broadband directivity pattern are given in figures 7 and 8, respectively.

The tonal components, frequency envelope shape, and tone directivity patterns for each of the 27 advanced turboprop noise simulations were chosen based on a review of the available literature (refs. 25–43). This information was then used in the synthesis-system input data sets. The numbers of blades chosen for each rotor were 5, 6, 7, 8, 9, 10, 11, 12, and 13. When combined with the assumed rotation speed of 1350 rpm, the blade numbers yielded the following nine fundamental frequencies: 112.5, 135, 157.5, 180, 202.5, 225, 247.5, 270, and 292.5 Hz. The frequency envelope shape used for the simulations is shown in figure 9. The directivity patterns for the fundamental tone and each harmonic tone are given in figure 10. The desired tone-to-broadband noise ratios of 0, 15, and 30 dB were obtained by specifying the relative levels of the tonal content and the broadband noise in the synthesis-system input data sets.

For each of the 27 input data sets, the synthesis system generated an audio simulation that was recorded on tape. Each of these recordings was presented to the test subjects at peak D-weighted sound pressure levels of 70, 80, and 90 dB. The factorial combinations of 9 fundamental frequencies, 3 tone-to-broadband noise ratios, and 3 sound levels resulted in 81 advanced turboprop aircraft flyover noise stimuli. The L_A time history and the 1/3-octave band spectrum at peak L_A of the highest level presentation of each of the 27 flyover noises are given in figure 11. To illustrate the tonal content of the noise stimuli, figure 12 gives the narrowband spectrum of the 30-dB tone-to-broadband noise ratio condition for each fundamental frequency.

Advanced turboprop stimuli in the second experiment. Thirty-five simulations of advanced turboprop aircraft takeoff noise were used in the second experiment. The simulations were based on an aft-mounted, pusher, counter-rotating propeller configuration having an unequal number of blades on each rotor. The aft rotor had either one or two blades less than the forward rotor. All 35 simulations were generated using the Aircraft Noise Synthesis System in the manner previously described for the first experiment. Except for the tonal content, the input data set parameters were the same in both experiments. The tonal content of 30 of the 35 simulations was systematically varied to represent the factorial combinations of 15 fundamental-frequency pairs and 2 tone-to-broadband noise ratios. As in the first experiment, the tonal components, frequency envelope shape, and tone directivity patterns for each of the advanced turboprop noise simulations were chosen based on a review of the available literature (refs. 25–43). The blade combinations chosen for the rotors were 6×5, 7×5, 7×6, 8×6, 8×7, 9×7, 9×8, 10×8, 10×9, 11×9, 11×10, 12×10, 12×11, 13×11, and 13×12. When combined with the assumed rotation speed of 1350 rpm, the blade numbers yielded the following fundamental-frequency pairs: 135×112.5, 157.5×112.5, 157.5×135, 180×135, 180×157.5, 202.5×157.5, 202.5×180, 225×180, 225×202.5, 247.5×202.5, 247.5×225, 270×225, 270×247.5, 292.5×247.5, and 292.5×270 Hz. The frequency envelope shape used for the simulation is shown in figure 13. The directivity patterns for the fundamentals and each harmonic tone are given in figure 14. The desired tone-to-broadband noise ratios of 15 and 30 dB were obtained by specifying the relative levels of the tonal content and the broadband noise in the synthesis-system input data sets. (Tone-to-broadband noise ratio was defined to be the difference between the level of the aft-rotor fundamental tone and the level of the highest 1/3-octave band of the broadband noise.) The five other simulations had tone-to-broadband noise ratios of 0 dB. These five simulations were at blade numbers of 7×5, 8×7, 10×8, 11×10, and 13×11. These represented frequency pairs of 157.5×112.5, 180×157.5, 225×180, 247.5×225, and 292.5×247.5 Hz.

As in the first experiment, each simulation generated by the synthesis system was recorded on tape and presented to the test subjects at peak D-weighted sound pressure levels of 70, 80, and 90 dB. This resulted in 105 advanced turboprop aircraft takeoff noise stimuli in the second experiment. The L_A time history and the 1/3-octave band spectrum at peak L_A of the highest level presentation of each flyover noise are given in figure 15. The narrowband spectrum of the 30-dB tone-to-broadband noise ratio condition for each fundamental-frequency pair is given in figure 16.

Conventional turboprop and turbofan stimuli in both experiments. Recordings of five conventional turboprop aircraft takeoffs and five conventional turbofan aircraft takeoffs were included in each experiment for comparison with the advanced turboprop noise stimuli. The types of aircraft used and some specifications of each are given in table II. The recordings of the turbofan aircraft were made on the extended-runway centerline approximately 5000 m from the brake-release point. All conventional

turboprop aircraft had maximum takeoff weights greater than 5700 kg. The turboprop aircraft recordings were made at several different airports, and the distances from brake release varied. At each location, the turboprop aircraft recordings were made on or near the extended-runway centerline. Because of the higher flight profiles and lower source noise levels of the turboprop aircraft, the recording sites for the turboprop aircraft were located closer to the brake-release point than those for the jet aircraft. Each takeoff was presented to the test subjects at peak D-weighted sound pressure levels of 70, 80, and 90 dB for a total of 15 conventional turboprop noise stimuli and 15 conventional turbofan noise stimuli in each experiment. The L_A time histories and the 1/3-octave band spectra at peak L_A of the highest level presentations of the conventional turboprop and turbofan takeoffs are given in figure 17.

Other stimuli in both experiments. Boeing 727 takeoff noise stimuli were included in both experiments as a reference noise for converting subjective responses to subjective decibel levels in the analyses of the experiments. In addition to the three presentations made as part of the conventional turbofan stimuli, the Boeing 727 takeoff recording was also presented at peak L_D levels of 65, 75, 85, 95, and 99 dB. This resulted in a total of eight Boeing 727 stimuli, ranging in peak L_D levels from 65 to 95 dB in 5-dB increments plus one at 99 dB, being presented to the test subjects in each experiment. The test subjects were presented a total of 116 stimuli in the first experiment and a total of 140 stimuli in the second experiment.

Experiment Design

Numerical category scaling was chosen as the psychophysical method for both experiments. The choice was made to maximize the number of stimuli that could be judged in the fixed amount of time available. The scale selected was a unipolar, 11-point scale from 0 to 10. The end points of the scale were labeled "EXTREMELY ANNOYING" and "NOT ANNOYING AT ALL." The term "ANNOYING" was defined in the subject instructions as "UNWANTED, OBJECTIONABLE, DISTURBING, OR UNPLEASANT."

For each experiment, the stimuli were divided into two sets of four tapes. The first set of four tapes contained all the stimuli in the experiment. The second set contained the same stimuli as the first but in reverse order. There were 29 stimuli per tape in the first experiment and 35 per tape in the second experiment. The stimuli were divided between tapes so that each blade count, tone-to-broadband noise ratio, noise level, and/or aircraft type were about equally represented on each tape. The order of the stimuli on the tape was then randomly selected. The orders for each tape are given in tables III and IV. (The first four characters of the codes in tables III and IV indicate the type of aircraft and the number of propeller blades if the aircraft type is advanced turobprop. The fifth character indicates the tone-to-broadband noise ratio for the advanced turboprop noises and the type of operation for the conventional turboprop and turbojet noises. The last two characters give the peak L_D level at which the noise was presented to the test subjects. For example, "B707 T 80" is a Boeing 707 takeoff noise presented at a peak L_D level of 80 dB, and "0808 3 70" is an eight- by eight-bladed counter-rotating advanced turboprop noise having a tone-to-broadband noise ratio of 30 dB and presented at a peak L_D level of 70 dB.) A period of approximately 10 sec was provided after each stimulus for the subjects to make and record their judgments. Each tape served as one of four test sessions for the subjects and required approximately 30 minutes for playback in the first experiment and 35 minutes in the second experiment.

The 64 test subjects in each experiment were divided into 32 groups of 2 subjects. In each experiment the first 4 tapes were presented to 16 groups of subjects and the second 4 tapes were presented to the other 16 groups of subjects. To prevent subject fatigue and other temporal effects from unduly influencing the results, the order in which the tapes were presented was varied to provide a balanced presentation. Table V gives the order of presentation used for the tapes in both experiments.

Procedure

Upon arrival at the laboratory, the subjects were seated in the test facility and each was given a set of instructions and a consent form. Copies of these items for the first experiment are given in the appendix. In the second experiment, these items were identical except that the length of the session was changed from 30 to 35 minutes, and the number of aircraft sounds was changed from 29 to 35. After reading the instructions and completing the consent form, the subjects were given a brief verbal explanation of the cards used for recording judgments and were asked if they had any questions. Three practice stimuli were then presented to the subjects while the test conductor remained in the test facility. In order for the subjects to gain experience in scoring the sounds, they were instructed to make and record judgments of the practice stimuli. After asking again for any questions about the test, the test conductor

issued scoring cards for the first session and left the facility. Then, the first of four test sessions began. After the conclusion of each session, the test conductor reentered the test facility, collected the scoring cards, and issued new scoring cards for the next session. Between the second and third sessions, the subjects were given a 15-minute rest period outside the test facility.

Results and Discussion

Acoustic Data Analyses

Each noise stimulus in each experiment was analyzed to provide 1/3-octave-band sound pressure levels from 20 Hz to 20 kHz for use in computing a selected group of noise metrics. The measurements were made with a 1.27-cm-diameter condenser microphone and a real-time, 1/3-octave analysis system that used digital filtering. In both experiments the microphone was located at ear level at a point midway between the two seats. No subjects were present during the measurements. A total of 11 noise metrics were computed in the analyses. They included the simple weighting procedures L_A, L_D, L_E, and L_1 and the more complex calculation procedures LL, LL_Z, PL, and PNL. In addition, three types of critical-band corrections were applied to PNL.

The noise metric L_1 is based on a modified frequency weighting developed in a study of annoyance to simulated helicopter rotor noise (ref. 6). That study found that annoyance prediction error was more correlated with the logarithm of the subjectively dominant frequency (approximated by the 1/3-octave-band center frequency with the greatest D-weighted energy) than with impulsiveness measures. Based on this result, a modified frequency weighting was developed that provided improved annoyance prediction when implemented as the L_1 noise metric. For 1/3-octave bands with center frequencies less than or equal to 1000 Hz, the modified frequency weighting falls between the A and D weightings. D-weighting values are used for bands above 1000 Hz. The L_1 metric uses the same energy summation method used for L_A, L_D, and L_E.

The first critical-band correction procedure applied to PNL was suggested by Kryter (ref. 44). In this procedure, the increased bandwidths of critical bands below 400 Hz are approximated by groups of 1/3-octave bands. The groups are the bands with center frequencies: 315 and 250 Hz; 200, 160, and 125 Hz; and 100, 80, 63, and 50 Hz. Within each group the band levels are summed on an energy basis. The summed band levels are assigned to the band center frequency having the greatest intensity within the group. The PNL calculation procedure then uses these "critical bands" instead of the 1/3-octave bands below 400 Hz. The metric using this procedure is designated as PNL_K in further discussions in this report.

The second critical-band correction procedure used the same groups for summing the 1/3-octave bands. The summed band levels, however, were assigned to the band center frequency responsible for the greatest "noy" value within the group before summing. The metric using this procedure is designated as PNL_M.

The third critical-band correction procedure also used the same groups of 1/3-octave bands. In this case, the noy values of the 1/3-octave-band levels were added on an energy basis within each group. The resultant noy values for all critical bands were then summed using the PNL procedure. The metric using this procedure is designated as PNL_W.

Six different variations of each of the 11 previously described noise metrics were calculated. The first was the peak or maximum level occurring during the flyover noise. Two other variations were calculated by applying two different tone corrections. Three more variations were attained by applying duration corrections to the non tone-corrected level and the two tone-corrected levels. The duration correction and the first tone correction T_1 are identical to those used in the effective perceived noise level procedure defined in the Federal Aviation Administration FAR 36 regulation (ref. 7). The second tone correction T_2 is identical to the first except that no corrections are applied for tones identified in bands with center frequencies less than 500 Hz.

Subjective Data Analyses

The means (across subjects) of the judgments were calculated for each stimulus in each experiment. In order to obtain a subjective scale with meaningful units of measure, these mean annoyance scores were converted to subjective noise levels L_S having decibel-like properties through the following process. Included in each experiment for the purpose of converting the mean annoyance scores to L_S values were eight presentations of a Boeing 727 takeoff recording. The L_D levels of the eight presentations were 65, 70, 75, 80, 85, 90, 95, and 99 dB. Third-order polynomial regression analyses were performed separately for each experiment on data obtained for these eight stimuli. The dependent variable was the calculated PNL, and the independent variable was the mean annoyance score for each of the eight stimuli. Figure 18 presents the two sets of data and the resulting best-fit curves. The regression equations were then used to predict the level of the Boeing 727 takeoff noise that would produce the same mean annoyance score

as each of the other noise stimuli in the separate experiments. These levels were then considered as the subjective noise level for each stimulus. Comparisons in these studies and in previous studies indicate that analyses using subjective noise levels yield the same results as analyses using mean annoyance scores.

Comparison of Noise Metrics

In order to investigate the prediction ability of the noise measurement procedures and corrections, the differences between the subjective noise level L_S and the calculated noise level for each of the six variations of the measurement procedures and corrections were determined for each stimulus in each experiment. These differences were considered to be the "prediction error" for each stimulus and noise metric variation. The standard deviation of the prediction errors for each noise metric variation is a measurement of how accurately the variation predicts annoyance. The smaller the standard deviation is, the greater the prediction accuracy.

It should be noted that because of interrelationships between the data cases, statistical tests for significance of differences in the standard deviations of prediction error are not straightforward. The following results are based primarily on the consistent trends found in the data. Approximate statistical tests indicate that differences in standard deviations as small as 0.13 dB in the first experiment and 0.05 dB in the second experiment could be significant ($p \leq 0.05$).

First experiment. Table VI gives the standard deviations of prediction error for each noise metric variation examined for the combined set of 111 advanced turboprop, conventional turboprop, and conventional turbofan stimuli in the first experiment. Comparisons of the standard deviations indicate that annoyance prediction ability was improved by the addition of duration corrections. The T_2 tone correction improved prediction ability in every case, but the results for the T_1 tone correction were mixed. When the T_1 tone correction was applied to the noise metric variations without duration corrections, it sometimes improved prediction ability (but not as much as the T_2 tone correction) and sometimes degraded prediction ability. When the T_1 correction was applied to the noise metric variations with duration corrections, it always improved prediction ability, but usually not as much as the T_2 tone correction and never significantly more than the T_2 tone correction. Duration-corrected L_A with T_1 tone corrections and duration-corrected L_A with T_2 tone corrections had the smallest standard deviations of prediction error. The difference between the standard deviations for the two noise metric variations was not significant. The addition of critical-band corrections to PNL did not significantly improve its prediction ability. Comparisons of the standard deviations of prediction error in table VI clearly indicate that L_A with duration and tone corrections most accurately predicted the annoyance caused by the combined set of advanced turboprop, conventional turboprop, and conventional turbofan stimuli in the first experiment.

Second experiment. Table VII gives the standard deviations of prediction error for each noise metric variation examined for the combined set of 135 advanced turboprop, conventional turboprop, and conventional turbofan stimuli in the second experiment. Comparisons of the standard deviations indicate that annoyance prediction ability was improved by the addition of duration corrections. The T_2 tone correction improved prediction ability in every case. The T_1 tone correction usually improved prediction ability, but not as much as the T_2 tone correction. Duration-corrected L_A with T_2 tone corrections and duration-corrected L_A with T_1 tone corrections had the smallest standard deviations of prediction error. The difference between the standard deviations for the two noise metric variations was not significant. All three of the critical-band corrections applied to PNL improved prediction ability. The $\mathrm{PNL_K}$ and $\mathrm{PNL_W}$ cases, in particular, clearly showed a significant improvement in prediction ability. Comparisons of the standard deviations of prediction error in table VII clearly indicate that L_A with duration and tone corrections most accurately predicted the annoyance caused by the combined set of advanced turboprop, conventional turboprop, and conventional turbofan stimuli in the second experiment.

The following analyses of the advanced turboprop stimuli in both experiments will be presented in terms of L_A, PNL, and $\mathrm{LL_Z}$. Both $\mathrm{L_A}$ and PNL are used because they are the two most commonly used procedures and because the results for the remaining noise measurement procedures are similar. The $\mathrm{LL_Z}$ procedure is included because the results using $\mathrm{LL_Z}$ differ somewhat from the results using the other noise measurement procedures.

Effects of Tone Characteristics

Analyses of the annoyance prediction errors in each experiment indicated two major results regarding the tonal characteristics considered. In both experiments, annoyance was significantly affected by the interaction of fundamental frequency with tone-to-broadband noise ratio and by the interaction of

tone-to-broadband noise ratio with noise level. However, the magnitudes and trends of the effects of the interactions varied depending on the combination of duration and tone corrections used with the noise measurement procedures.

Interaction of fundamental frequency and tone-to-broadband noise ratio. For the two experiments, respectively, figures 19 and 20 illustrate the interaction of fundamental frequency with tone-to-broadband noise ratio for each combination of duration and tone corrections applied to L_A, PNL, and LL_Z. Annoyance relative to the noise metric prediction is plotted versus fundamental frequency for each of the three tone-to-broadband noise ratios. "Annoyance relative to noise metric prediction" is the prediction error (subjective noise level minus the calculated level of the metric) normalized by subtracting the average (across all stimuli) prediction error for the metric. When defined in this manner, a positive number represents annoyance greater than that predicted by the metric, and results for different metrics can be directly compared. As is apparent from the figures, the interaction of fundamental frequency and tone-to-broadband noise ratio is complex and its effects are not consistent across metrics. In general, annoyance increased as tone-to-broadband noise ratio increased. The magnitude of the change in annoyance usually increased as fundamental frequency increased. The addition of duration corrections tended to increase the effect of tone-to-broadband noise ratio. The addition of tone corrections tended to decrease the effect of tone-to-broadband noise ratio. The interaction effects were slightly more pronounced for the LL_Z procedure. Of most interest is the result that for the counter-rotating configuration, annoyance usually was greater at the higher tone-to-broadband noise ratios. Similar studies of single-rotating configurations of advanced turboprop aircraft also found an interaction of fundamental frequency and tone-to-broadband noise ratio. However, in those studies (ref. 1), annoyance decreased as tone-to-broadband noise ratio increased.

Interaction of tone-to-broadband noise ratio and noise level. For the two experiments, respectively, figures 21 and 22 illustrate the interaction of tone-to-broadband noise ratio with noise level for each combination of duration and tone corrections applied to L_A, PNL, and LL_Z. Annoyance relative to the noise metric prediction is plotted versus tone-to-broadband noise ratio for each of the three noise levels at which the stimuli were presented to the test subjects. "Annoyance relative to noise metric prediction" is defined the same as in figures 19 and 20. In both experiments, annoyance increased with tone-to-broadband noise ratio at a greater rate for the low-level stimuli than it did for the middle- and high-level stimuli. In general, the interaction was similar for all combinations of noise measurement procedures and corrections, except that in some cases in the first experiment the annoyance of the middle- and high-level stimuli did not increase with tone-to-broadband noise ratio. Also, the magnitude of the interaction was greater for the LL_Z cases.

Effect of Blade Number Difference

The $n \times m$ CRP advanced turboprop aircraft in the second experiment were divided into two groups based on the blade number difference between the front and aft rotors. The blade combinations in the first group (6×5, 7×6, 8×7, 9×8, 10×9, 11×10, 12×11, and 13×12) had a blade number difference of 1. The blade combinations in the second group (7×5, 8×6, 9×7, 10×8, 11×9, 12×10, and 13×11) had a blade number difference of 2. The two groups of stimuli were compared by using indicator (dummy) variable analyses. The results, which were consistent across noise metrics, indicated no differences in annoyance response to the two groups of $n \times m$ CRP advanced turboprop stimuli. Blade number difference did not affect annoyance response.

Comparison of Aircraft Types

Figure 23 compares the annoyance responses to $n \times n$ CRP advanced turboprop, conventional turboprop, and conventional turbofan aircraft flyover noises obtained in the first experiment. The figure shows subjective noise level plotted against duration-corrected L_A for each of the three categories of aircraft. Simple linear regression lines for each of the aircraft types are also shown. Indicator (dummy) variable analyses for the duration-corrected L_A metric found no significant differences in slope or intercept between the appropriate regressions for the $n \times n$ CRP advanced turboprop noises, the conventional turboprop noises, and the conventional turbofan noises. Therefore, for duration-corrected L_A, annoyance to all three categories of aircraft can be represented by one simple linear regression equation. Figure 24 compares the annoyance responses to $n \times n$ CRP advanced turboprop, conventional turboprop, and conventional turbofan aircraft flyover noises using EPNL. (The EPNL is duration-corrected PNL with T_1 tone corrections.) For EPNL, indicator variable analyses show a significant difference in intercept, but not in slope, between the appropriate regressions for the combined set of $n \times n$ CRP advanced turboprop and conventional turbofan

noises and the conventional turboprop noises. For a given EPNL value, the conventional turboprop noises were slightly less annoying than the combined set of $n \times n$ CRP advanced turboprop and conventional turbofan noises. Almost all the noise metrics considered yielded this result. No differences between the $n \times n$ CRP advanced turboprop noises and the conventional turbofan noises were found for any noise metric.

Figure 25 compares the annoyance responses to $n \times m$ CRP advanced turboprop, conventional turboprop, and conventional turbofan aircraft flyover noises obtained in the second experiment. The figure plots subjective noise level versus duration-corrected L_A for each of the three categories of aircraft in the experiment. Simple linear regression lines for each of the aircraft types are also shown. Indicator (dummy) variable analyses for the duration-corrected L_A metric show a significant difference in slope and intercept between the appropriate regressions for the combined set of $n \times m$ CRP advanced turboprop and conventional turbofan noises and the conventional turboprop noises. However, no consistent difference in annoyance between the conventional turboprops and the other aircraft types is apparent over the range of levels considered in the experiment.

Figure 26 compares the annoyance responses to $n \times m$ CRP advanced turboprop, conventional turboprop, and conventional turbofan aircraft flyover noises using EPNL. For EPNL, indicator variable analyses also showed a significant difference in intercept and slope between the appropriate regressions for the combined set of $n \times m$ CRP advanced turboprop and conventional turbofan noises and the conventional turboprop noises. For a given EPNL value in the lower range of levels considered, the conventional turboprop noises appear to be slightly less annoying than the combined set of advanced turboprop and conventional turbofan noises. Almost all the metrics considered yielded this result. No differences in annoyance between the advanced turboprop noises and the conventional turbofan noises were found for any metric.

Conclusions

Two laboratory experiments were conducted to provide information on quantifying the annoyance response of people to the flyover noise of advanced turboprop (propfan) aircraft with counter-rotating propellers. In both experiments, a computer synthesis system was used to generate realistic simulations of advanced turboprop aircraft takeoff noise. In the first experiment, the simulations were based on an aft-mounted, pusher, counter-rotating propeller configuration with an equal number of blades on each rotor. The first experiment examined 27 advanced turboprop simulations representing the factorial combinations of 9 fundamental frequencies and 3 tone-to-broadband noise ratios. In the second experiment, the simulations were based on an aft-mounted, pusher, counter-rotating propeller with an unequal number of blades on each rotor. The second experiment examined 35 advanced turboprop simulations representing combinations of 15 fundamental-frequency pairs and 3 tone-to-broadband noise ratios. In each experiment the advanced turboprop simulations along with recordings of 5 conventional turboprop takeoffs and 5 conventional turbofan takeoffs were presented at 3 sound pressure levels to 64 subjects in an anechoic listening room. Analyses of the annoyance responses were conducted in terms of several variations of seven conventional noise metrics (A-, D-, and E-weighted sound pressure level, loudness level (Stevens Mark VI procedure), Zwicker's loudness level, perceived level (Stevens Mark VII procedure), and perceived noise level) and one other recently developed noise metric (L_1) based on a modified frequency weighting.

Based on the results presented in this paper, the following conclusions were noted:

1. In both experiments, the annoyance prediction ability of the noise metrics was improved by the addition of a duration correction.

2. In both experiments, the annoyance prediction ability of the noise metrics was improved by the addition of a tone correction similar to the one used in effective perceived noise level (EPNL) but limited to tones in 1/3-octave bands with center frequencies greater than or equal to 500 Hz. Addition of the effective perceived noise level (EPNL) tone correction to the noise metrics did not improve prediction ability as consistently as the limited tone correction.

3. Critical-band corrections to perceived noise level (PNL) did not significantly improve annoyance prediction in the first experiment. However, in the second experiment, two of the three critical-band correction methods did significantly improve annoyance prediction.

4. In both experiments, A-weighted sound pressure level (L_A) with duration and tone corrections provided the most accurate annoyance prediction.

5. The interaction of fundamental frequency and tone-to-broadband noise ratio did have a complex effect on annoyance to the noise of advanced turboprop aircraft with counter-rotating propellers. Although the indicated interaction varied somewhat between noise metrics and between the two experiments, in most cases the annoyance to the higher tone-to-broadband noise ratio flyovers was greater

than the annoyance to the other flyovers. This is the opposite of the effect found for single-rotating configurations in previous studies. The difference in annoyance between the higher tone-to-broadband noise ratio flyovers and the other flyovers varied with fundamental frequency.

6. The interaction of tone-to-broadband noise ratio and noise level did have a significant effect on annoyance to the noise of advanced turboprop aircraft with counter-rotating propellers. Although the indicated interaction varied somewhat between noise metrics and between the two experiments, annoyance increased with tone-to-broadband noise ratio at a greater rate for the low-level stimuli than it did for the middle- and high-level stimuli.

7. Annoyance was not significantly affected by the difference in number of blades between the front and aft rotors of the advanced turboprop aircraft with counter-rotating propellers having an unequal number of blades on each rotor.

8. No significant differences in annoyance response between the advanced turboprop aircraft with counter-rotating propellers and the conventional turbofans were found in either experiment.

NASA Langley Research Center
Hampton, VA 23665-5225
July 26, 1990

Appendix

Instructions and Consent Form

INSTRUCTIONS

The experiment in which you are participating will help us understand the characteristics of aircraft sounds which can cause annoyance in airport communities. We would like you to judge how ANNOYING some of these aircraft sounds are. By ANNOYING we mean - UNWANTED, OBJECTIONABLE, DISTURBING, OR UNPLEASANT.

The experiment consists of four 30 minute sessions. During each session 29 aircraft sounds will be presented for you to judge. You will record your judgments of the sounds on computer cards like the one below:

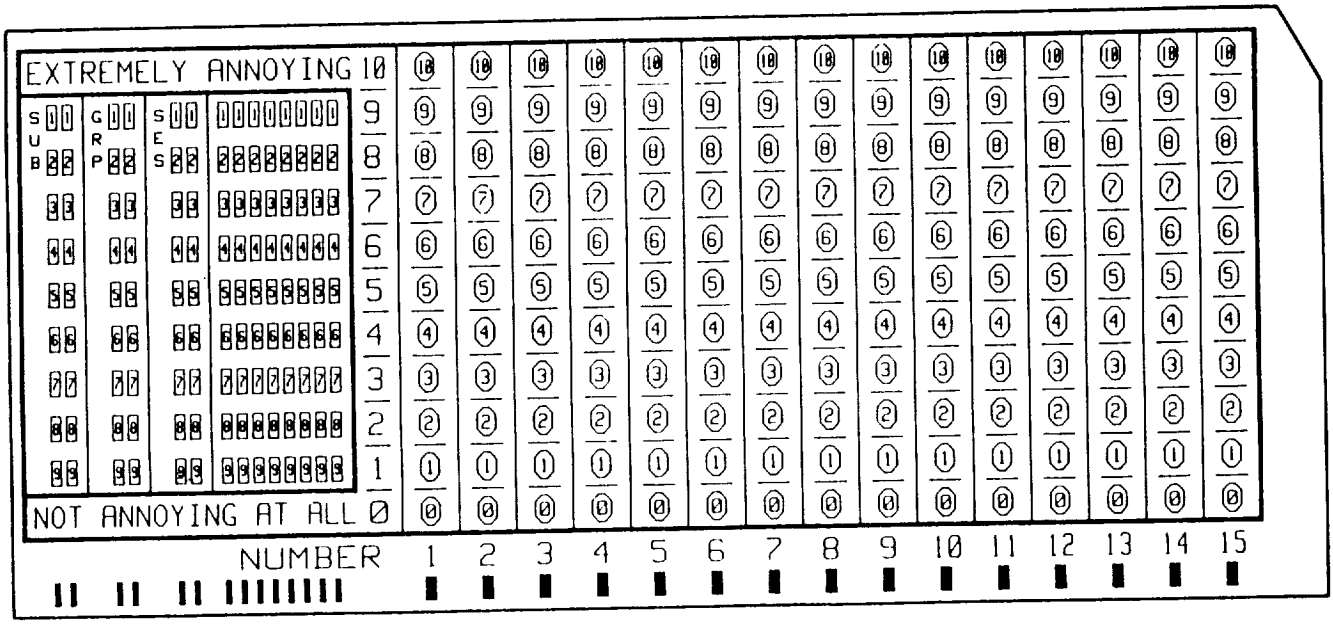

After each sound there will be a few seconds of silence. During this interval, please indicate how annoying you judge the sound to be by marking the appropriate numbered circle on the computer card. The number of each sound is indicated across the bottom of the card. If you judge a sound to be only slightly annoying, mark one of the numbered circles close to the NOT ANNOYING AT ALL end of the scale, that is a low numbered circle near the bottom of the card. Similarly, if you judge a sound to be very annoying, then mark one

of the numbered circles close to the EXTREMELY ANNOYING end of the scale, that is a high numbered circle near the top of the card. A moderately annoying judgment should be marked in the middle portion of the scale. In any case, make your mark so that the circle that most closely indicates your annoyance to the sound is completely filled in. There are no right or wrong answers; we are only interested in your judgment of each sound.

Before the first session begins you will be given a practice computer card and three sounds will be presented to familiarize you with making and recording judgments. I will remain in the testing room with you during the practice time to answer any questions you may have.

Thank you for your help in conducting the experiment.

VOLUNTARY CONSENT FORM FOR SUBJECTS

FOR HUMAN RESPONSE TO AIRCRAFT NOISE AND VIBRATION

I understand the purpose of the research and the technique to be used, including my participation in the research, as explained to me by the Principal Investigator (or qualified designee).

I do voluntarily consent to participate as a subject in the human response to aircraft noise experiment to be conducted at NASA Langley Research Center on _____.
date

I understand that I may at any time withdraw from the experiment and that I am under no obligation to give reasons for withdrawal or to attend again for experimentation.

I undertake to obey the regulations of the laboratory and instruction of the Principal Investigator regarding safety, subject only to my right to withdraw declared above.

I affirm that, to my knowledge, my state of health has not changed since the time at which I completed and signed the medical report form required for my participation as a test subject.

_____
PRINT NAME

_____
SIGNATURE

References

1. McCurdy, David A.: *Annoyance Caused by Advanced Turboprop Aircraft Flyover Noise Single-Rotating Propeller Configuration.* NASA TP-2782, 1988.
2. Pearsons, Karl S.: *Combination Effects of Tone and Duration Parameters on Perceived Noisiness.* NASA CR-1283, 1969.
3. Kryter, K. D.; Johnson, P. J.; and Young, J. R.: *Judgment Tests of Flyover Noise From Various Aircraft.* NASA CR-1635, 1970.
4. Scharf, B.; and Hellman, R.: *Comparison of Various Methods for Predicting the Loudness and Acceptability of Noise. Part 2: Effects of Spectral Pattern and Tonal Components.* Rep. EPA-550/9-79-102, U.S. Environmental Protection Agency, Nov. 1979. (Available from NTIS as PB82 138 702.)
5. Kryter, Karl D.: *Physiological, Psychological, and Social Effects of Noise.* NASA RP-1115, 1984.
6. Powell, Clemans A.; and McCurdy, David A.: *Effects of Repetition Rate and Impulsiveness of Simulated Helicopter Rotor Noise on Annoyance.* NASA TP-1969, 1982.
7. *Noise Standards: Aircraft Type and Airworthiness Certification.* Federal Aviation Regulations, vol. III, pt. 36, Federal Aviation Adm., 1978.
8. Pearsons, Karl S.; and Bennett, Ricarda L.: *Handbook of Noise Ratings.* NASA CR-2376, 1974.
9. McCurdy, David A.; and Grandle, Robert E.: *Aircraft Noise Synthesis System.* NASA TM-89040, 1987.
10. Stern, John A.: Aircraft Propulsion A Key to Fuel Conservation, An Aircraft Manufacturer's View. SAE Paper 760538, May 1976.
11. Kraus, E. F.; and Van Abkoude, J. C.: *Cost/Benefit Tradeoffs for Reducing the Energy Consumption of the Commercial Air Transportation System Summary Report.* NASA CR-137925, 1976.
12. Douglas Aircraft Co.: *Cost/Benefit Tradeoffs for Reducing the Energy Consumption of the Commercial Air Transportation System. Volume I: Technical Analysis.* NASA CR-137923, 1976.
13. Hanson, Donald B.: Near Field Noise of High Tip Speed Propellers in Forward Flight. AIAA Paper No. 76-565, July 1976.
14. Dugan, J. F.; Miller, B. A.; and Sagerser, D. A.: Status of Advanced Turboprop Technology. CTOL Transport Technology 1978, NASA CP-2036, Part I, 1978, pp. 139 166.
15. Dugan, James F., Jr.; Gatzen, Bernard S.; and Adamson, William M.: Prop-Fan Propulsion Its Status and Potential. SAE Tech. Paper Ser. 780995, Nov. 1978.
16. Hanson, Donald B.: The Influence of Propeller Design Parameters on Far Field Harmonic Noise in Forward Flight. AIAA Paper 79-0609, Mar. 1979.
17. Dittmar, James H.; Jeracki, Robert J.; and Blaha, Bernard J.: *Tone Noise of Three Supersonic Helical Tip Speed Propellers in a Wind Tunnel.* NASA TM-79167, [1979].
18. Rennison, D. C.; Wilby, J. F.; Marsh, A. H.; and Wilby, E. G.: *Interior Noise Control Prediction Study for High-Speed Propeller-Driven Aircraft.* NASA CR-159200, 1979.
19. Brooks, Bennett M.; and Metzger, F. B.: *Acoustic Test and Analysis of Three Advanced Turboprop Models.* NASA CR-159667, 1980.
20. Revell, J. D.; Balena, F. J.; and Koval, L. R.: *Analytical Study of Interior Noise Control by Fuselage Design Techniques on High-Speed, Propeller-Driven Aircraft.* NASA CR-159222, 1980.
21. Dugan, James F.; Miller, Brent A.; Graber, Edwin J.; and Sagerser, David A.: *The NASA High-Speed Turboprop Program.* NASA TM-81561, [1980].
22. Muehlbauer, J. C.; Hewell, J. G., Jr.; Lindenbaum, S. P.; Randall, C. C.; Searle, N.; and Stone, F. R., Jr.: *Turboprop Cargo Aircraft Systems Study, Phase 1.* NASA CR-159355, 1980.
23. Muehlbauer, J. C.; Hewell, J. G., Jr.; Lindenbaum, S. P.; Randall, C. C.; Searle, N.; and Stone, F. R., Jr.: *Turboprop Cargo Aircraft Systems Study.* NASA CR-165813, 1981.
24. Arndt, William E.: Fuel Efficient and Mach 0.8, Too. *Lockheed Horiz.*, Issue 10, Spring 1982, pp. 27 34.
25. French-Developed Propfan Demonstrates Performance in Wind Tunnel Tests. *Aviation Week & Space Technol.*, vol. 124, no. 1, Jan. 1986, p. 67.
26. Allison Propfan Development Centers on Gearbox Design. *Aviation Week & Space Technol.*, vol. 123, no. 25, Dec. 1985, pp. 46 47.
27. Douglas Plans Continuing Upgrades To Maintain MD-80 Competitiveness. *Aviation Week & Space Technol.*, vol. 123, no. 19, Nov. 1985, pp. 52, 57, 59, 61, and 65.
28. DeMeis, Richard: Propfans Gear Up. *Aerosp. America*, vol. 24, no. 10, Oct. 1985, pp. 22 and 24.
29. Full-Power Tests on Propfan Progress at Wright-Patterson. *Aviation Week & Space Technol.*, vol. 123, no. 13, Sept. 1985, p. 55.
30. Rolls Royce Favoring Geared Propfan Design for New Development Program. *Aviation Week & Space Technol.*, vol. 122, no. 13, Apr. 1985, p. 64.
31. DeMeis, Richard: Propfans: Fuel Saving but Ear Splitting. *Aerosp. America*, vol. 22, no. 10, Oct. 1984, pp. 37, 40 and 88.
32. Brown, David A.: Propfan Concepts Gain in Development. *Aviation Week & Space Technol.*, vol. 121, no. 12, Sept. 1984, pp. 54 55.
33. Brahney, James H.: Propfan Engine Designs Examined. *Aerosp. Eng.*, vol. 6, no. 2, Feb. 1986, pp. 16 22.
34. Holt, Daniel J.: Will 1990s Aircraft be Powered by Propfan or Advanced Turbofan? *Aerosp. Eng.*, vol. 6, no. 2, Feb. 1986, pp. 8 12.
35. Brown, David A.: Rolls Attacks Technical Obstacles in Propfan Development Program. *Aviation Week & Space Technol.*, vol. 122, no. 10, Mar. 1985, p. 38 39.
36. Mordoff, Keith F.: NASA/Lockheed Propfan System Completes Ground Tests. *Aviation Week & Space Technol.*, vol. 125, no. 3, July 1986, pp. 93–95.
37. Mordoff, Keith F.: Douglas Studies MD-92X Production. *Aviation Week & Space Technol.*, vol. 125, no. 7, Aug. 1986, pp. 33 34.
38. Mordoff, Keith F.: General Electric Flies First Unducted Fan Demonstrator. *Aviation Week & Space Technol.*, vol. 125, no. 8, Aug. 1986, pp. 31 32.

39. Bradley, A. J.: A Study of the Rotor/Rotor Interaction Tones From a Contra-Rotating Propeller Driven Aircraft. AIAA-86-1894, July 1986.

40. Parzych, David; and Shattuck, Colman: Noise of the Fairey Gannet Counter Rotating Propeller. AIAA-86-1895, July 1986.

41. Block, P. J. W.: Noise Radiation Patterns of Counter-Rotation and Unsteadily Loaded Single-Rotation Propellers. *J. Aircr.*, vol. 22, no. 9, Sept. 1985, pp. 776–783.

42. Hanson, D. B.: Noise of Counter Rotation Propellers. AIAA-84-2305, Oct. 1984.

43. Woodward, Richard P.: *Noise of a Model High Speed Counterrotation Propeller at Simulated Takeoff/Approach Conditions (F7/A7).* NASA TM-100206, 1987. (Available as AIAA-87-2657.)

44. Kryter, K. D.: *Possible Modifications to the Calculation of Perceived Noisiness.* NASA CR-1636, 1970.

Table I. Data on Test Subjects

Experiment	Sex	Number of participants	Mean age	Median age	Age range
1	Male	22	34	32	18–70
	Female	42	41	41	21–73
	All subjects	64	39	38.5	18–73
2	Male	18	39	36	18–70
	Female	46	42	42.5	18–64
	All subjects	64	41	41.5	18–70

Table II. Conventional Turboprop and Turbofan Aircraft in Both Experiments

Aircraft	Number of engines	Engine type	Maximum takeoff weight, kg
de Havilland Canada DHC-7 Dash 7	4	Turboprop	20 000
Lockheed P-3	4	↓	61 200
NAMC YS-11	2	↓	24 500
Nord 262	2	↓	10 600
Shorts 330	2	↓	10 300
Airbus Industrie A-300	2	Turbofan	≥142 000
Boeing 707	4	↓	≥117 000
Boeing 727-200	3	↓	86 900
McDonnell Douglas DC-9	2	↓	≥41 100
McDonnell Doublas DC-10	3	↓	≥206 400

Table III. Presentation Order of Stimuli on Tapes in First Experiment

PRACTICE TAPE	TAPE 1 ↓	TAPE 2 ↓	TAPE 3 ↓	TAPE 4 ↓
B707 T 80	0606 3 70	B727 T 85	1212 1 90	N262 T 70
0808 3 70	0707 1 90	1313 3 70	1111 3 70	0909 1 80
YS11 T 90	1313 3 90	0606 1 90	0707 2 90	B727 T 90
	B727 T 80	0707 1 70	1313 3 80	0505 3 70
	1212 2 90	1010 2 90	S330 T 90	0707 2 70
	1111 1 80	DD-7 T 80	0707 1 80	1212 3 90
	0505 1 70	B727 T 99	0808 3 70	1313 1 80
	DD-7 T 70	1010 3 70	0606 2 90	0606 2 80
	1010 3 90	0505 1 80	B727 T 70	DC-9 T 70
	0808 2 90	1111 2 90	0505 3 80	0909 2 90
	0909 3 80	DC-9 T 80	0909 1 70	1212 1 80
	B707 T 70	YS11 T 90	DC10 T 90	0808 3 80
	S330 T 80	0606 2 70	1111 2 80	1010 1 70
	1313 1 70	0808 3 90	DC-9 T 90	LP-3 T 90
	B727 T 95	0909 2 80	0606 1 70	1212 2 70
	0909 2 70	A300 T 70	1010 3 80	0606 3 90
	N262 T 90	1010 1 80	1313 1 90	B707 T 80
	0707 3 80	1111 3 90	B727 T 65	1111 1 70
	1212 3 70	S330 T 70	1212 2 80	DD-7 T 90
	1313 2 80	0707 2 80	1010 1 90	1313 2 70
	A300 T 90	1313 2 90	0808 2 80	B727 T 75
	0606 1 80	1212 1 70	YS11 T 70	0707 3 90
	1111 2 70	0909 3 70	0707 3 70	DC10 T 70
	0808 1 80	LP-3 T 80	N262 T 80	0808 1 90
	0505 3 90	0606 3 80	1111 1 90	1010 2 80
	DC10 T 80	B707 T 90	0505 2 70	1111 3 80
	1010 2 70	0505 2 90	A300 T 80	0808 2 70
	0505 2 80	0808 1 70	0909 3 90	0505 1 90
	0909 1 90	1212 3 80	LP-3 T 70	YS11 T 80
	TAPE 5 ↑	TAPE 6 ↑	TAPE 7 ↑	TAPE 8 ↑

STIMULI KEY				
AIRCRAFT TYPE AND/OR NUMBER OF BLADES			OPERATION TYPE OR TONE-TO-BROADBAND NOISE RATIO	NOMINAL L_D
ADVANCED TURBOPROP	CONVENTIONAL TURBOPROP	CONVENTIONAL TURBOFAN		
ffaa ff = # of forward blades aa = # of aft blades	DD-7 = Dash 7 LP-3 = P-3 YS11 = YS-11 N262 = Nord 262 S330 = Shorts 330	A300 = Airbus A-300 B707 = Boeing 707 B727 = Boeing 727 DC-9 = DC-9 DC10 = DC-10	T = Takeoff 1 = 0 dB 2 = 15 dB 3 = 30 dB	65 = 65 dB 70 = 70 dB 75 = 75 dB 80 = 80 dB 85 = 85 dB 90 = 90 dB 95 = 95 dB 99 = 99 dB

Table IV. Presentation Order of Stimuli on Tapes in Second Experiment

PRACTICE TAPE	TAPE 1 ↓	TAPE 2 ↓	TAPE 3 ↓	TAPE 4 ↓
B727 T 80	B727 T 75	1311 2 90	0907 2 90	A300 T 90
0908 3 70	0605 3 90	1109 3 70	0705 2 70	1210 3 70
DD-7 T 90	0806 2 70	1008 3 80	1210 3 90	S330 T 80
	1311 1 80	N262 T 90	0807 3 80	1110 2 90
	A300 T 70	0706 2 80	B727 T 65	0807 1 80
	1312 2 90	1311 1 70	1110 1 90	0705 3 70
	0806 3 90	0806 2 90	YS11 T 70	DD-7 T 90
	1109 2 80	1109 3 80	1311 2 70	1311 3 70
	0907 3 70	S330 T 70	0806 3 80	0706 2 90
	B707 T 80	DC10 T 90	0706 3 90	B727 T 80
	0807 1 70	1110 2 80	1110 2 70	1110 3 80
	1311 3 90	0908 2 70	LP-3 T 80	1109 2 90
	B727 T 99	0807 1 90	1312 2 80	0806 3 70
	1009 2 70	1110 3 70	1109 3 90	YS11 T 90
	1211 3 80	DD-7 T 80	DD-7 T 70	1110 1 70
	S330 T 90	B707 T 90	0807 2 70	0908 2 80
	DC-9 T 90	0705 3 90	0705 3 80	1311 2 80
	0807 2 80	0605 2 80	N262 T 80	1008 3 70
	0908 3 70	0706 3 70	1311 1 90	0705 2 90
	1210 2 70	1108 2 90	0706 2 70	1312 3 70
	0706 3 80	1312 3 80	1009 3 70	DC10 T 80
	1110 3 90	0807 3 90	0908 3 80	0908 3 90
	0908 2 90	B727 T 85	B727 T 90	0907 2 80
	0705 1 70	1009 2 90	DC10 T 70	1312 3 90
	1211 2 70	0705 1 80	1210 2 80	1109 2 70
	YS11 T 80	0605 3 70	1008 3 90	B727 T 95
	1008 1 90	DC-9 T 80	1312 2 70	0806 2 80
	1210 3 80	0907 2 70	1211 3 90	1009 3 80
	0605 2 70	LP-3 T 90	A300 T 80	0807 3 70
	1008 2 80	1211 3 70	0605 2 90	DC-9 T 70
	0907 3 90	0907 3 80	B707 T 70	0807 2 90
	N262 T 70	1210 2 90	1009 2 80	1008 1 80
	1110 1 80	1008 1 70	0705 1 90	0605 3 80
	0705 2 80	B727 T 70	1311 3 80	LP-3 T 70
	1009 3 90	1211 2 80	1008 2 70	1211 2 90
	TAPE 5 ↑	TAPE 6 ↑	TAPE 7 ↑	TAPE 8 ↑

STIMULI KEY				
AIRCRAFT TYPE AND/OR NUMBER OF BLADES			OPERATION TYPE OR TONE-TO-BROADBAND NOISE RATIO	NOMINAL L_D
ADVANCED TURBOPROP	CONVENTIONAL TURBOPROP	CONVENTIONAL TURBOFAN		
ffaa ff = # of forward blades aa = # of aft blades	DD-7 = Dash 7 LP-3 = P-3 YS11 = YS-11 N262 = Nord 262 S330 = Shorts 330	A300 = Airbus A-300 B707 = Boeing 707 B727 = Boeing 727 DC-9 = DC-9 DC10 = DC-10	T = Takeoff 1 = 0 dB 2 = 15 dB 3 = 30 dB	65 = 65 dB 70 = 70 dB 75 = 75 dB 80 = 80 dB 85 = 85 dB 90 = 90 dB 95 = 95 dB 99 = 99 dB

Table V. Order of Tapes Presented to Test Subjects in Both Experiments

Test subject group	Tapes presented during session			
	1	2	3	4
1	1	2	3	4
2	2	1	4	3
3	3	4	1	2
4	4	3	2	1
5	5	6	7	8
6	6	5	8	7
7	7	8	5	6
8	8	7	6	5
9	1	3	4	2
10	2	4	3	1
11	3	1	2	4
12	4	2	1	3
13	5	7	8	6
14	6	8	7	5
15	7	5	6	8
16	8	6	5	7
17	4	1	2	3
18	1	4	3	2
19	2	3	4	1
20	3	2	1	4
21	8	5	6	7
22	5	8	7	6
23	6	7	8	5
24	7	6	5	8
25	3	2	1	4
26	2	3	4	1
27	1	4	3	2
28	4	1	2	3
29	7	6	5	8
30	6	7	8	5
31	5	8	7	6
32	8	5	6	7

Table VI. Standard Deviations of Prediction Error for Advanced Turboprop ($n \times n$), Conventional Turboprop, and Conventional Turbofan Stimuli in First Experiment

Metric	Standard deviation, dB, for					
	No duration correction			Duration corrected		
	No tone correction	T_1	T_2	No tone correction	T_1	T_2
L_A	2.33	2.23	2.10	2.05	1.76	1.78
L_D	3.13	3.16	3.00	2.78	2.58	2.51
L_E	3.07	3.09	2.87	2.68	2.48	2.38
L_1	2.80	2.85	2.76	2.55	2.33	2.39
LL	3.31	3.24	3.10	3.06	2.79	2.77
LL_Z	3.05	2.89	2.80	2.84	2.52	2.57
PL	3.14	3.05	2.88	3.01	2.72	2.70
PNL	2.91	2.94	2.78	2.74	2.50	2.45
PNL_K	2.89	2.93	2.76	2.66	2.44	2.38
PNL_M	2.98	3.01	2.84	2.69	2.46	2.41
PNL_W	2.92	3.00	2.86	2.63	2.46	2.39

Table VII. Standard Deviations of Prediction Error for Advanced Turboprop ($n \times m$), Conventional Turboprop, and Conventional Turbofan Stimuli in Second Experiment

Metric	Standard deviation, dB, for					
	No duration correction			Duration corrected		
	No tone correction	T_1	T_2	No tone correction	T_1	T_2
L_A	2.99	2.94	2.85	2.71	2.58	2.55
L_D	3.70	3.70	3.57	3.32	3.22	3.12
L_E	3.70	3.69	3.54	3.27	3.17	3.07
L_1	3.32	3.33	3.24	3.04	2.94	2.89
LL	4.19	4.11	3.95	3.83	3.66	3.58
LL_Z	3.79	3.69	3.60	3.51	3.33	3.27
PL	3.91	3.82	3.68	3.70	3.51	3.45
PNL	3.71	3.68	3.52	3.40	3.25	3.16
PNL_K	3.62	3.63	3.47	3.31	3.19	3.09
PNL_M	3.69	3.67	3.52	3.35	3.23	3.12
PNL_W	3.59	3.60	3.45	3.31	3.20	3.10

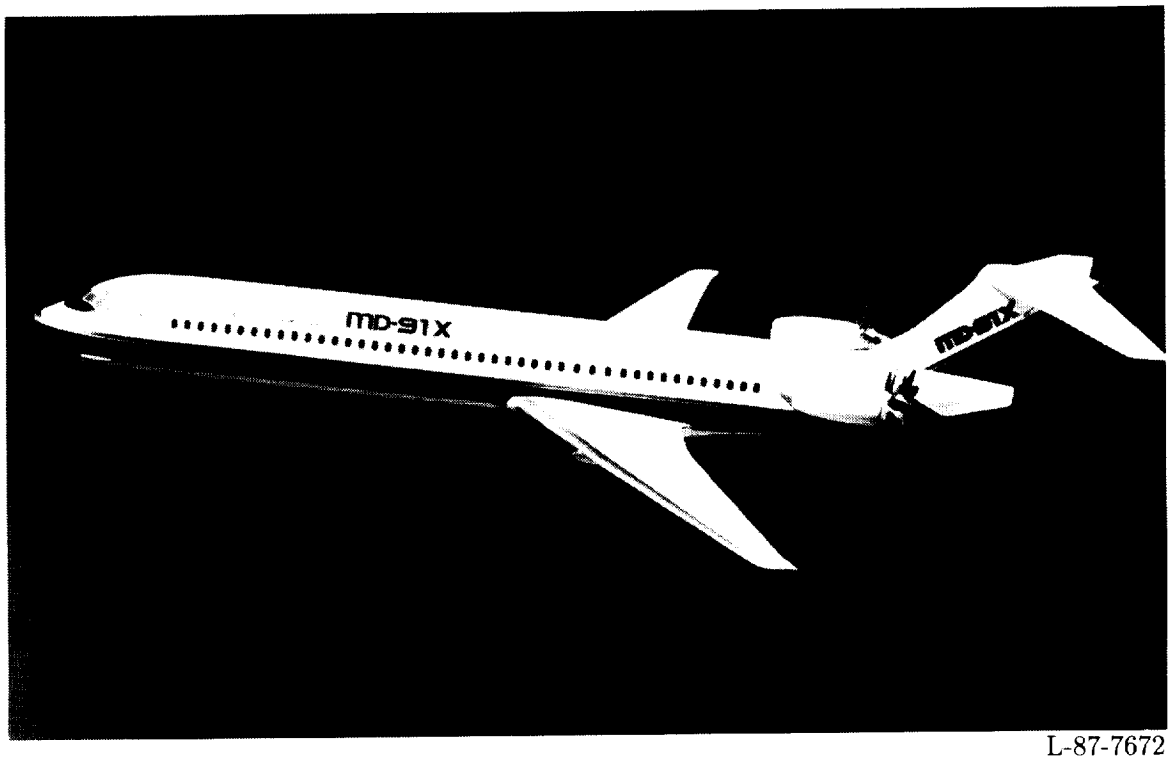

L-87-7672

Figure 1. An aft-mounted, pusher, counter-rotating propeller configuration of an advanced turboprop aircraft.

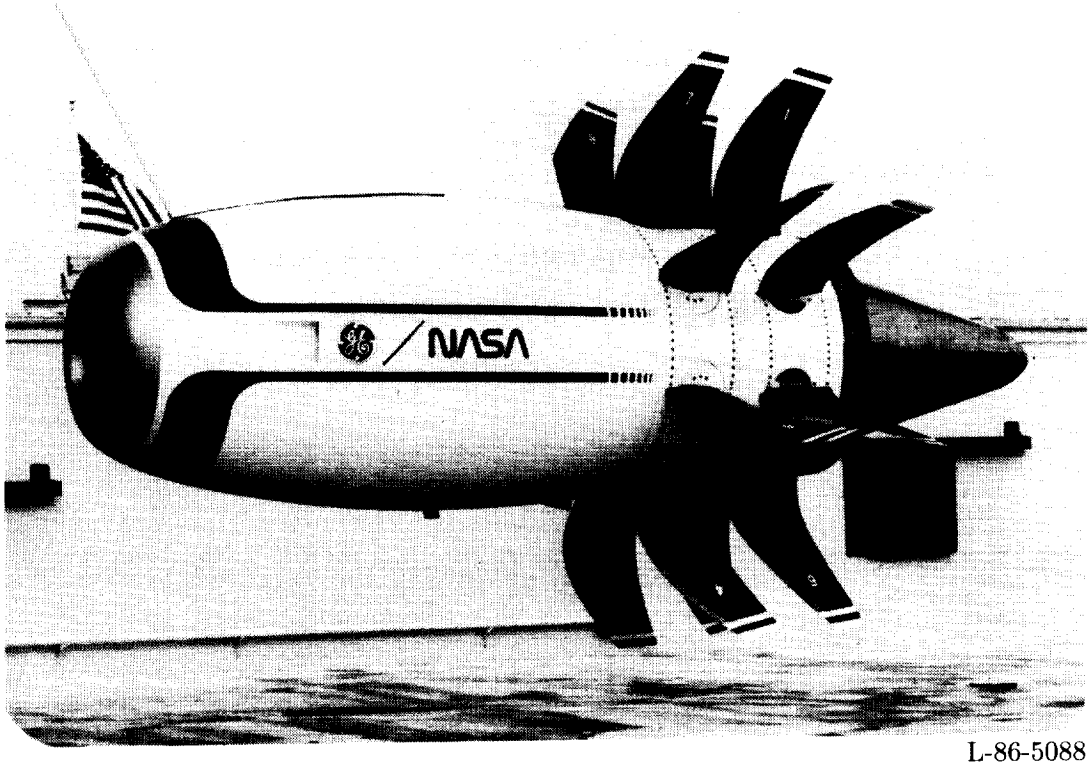

L-86-5088

Figure 2. Advanced turboprop engine with counter-rotating propeller.

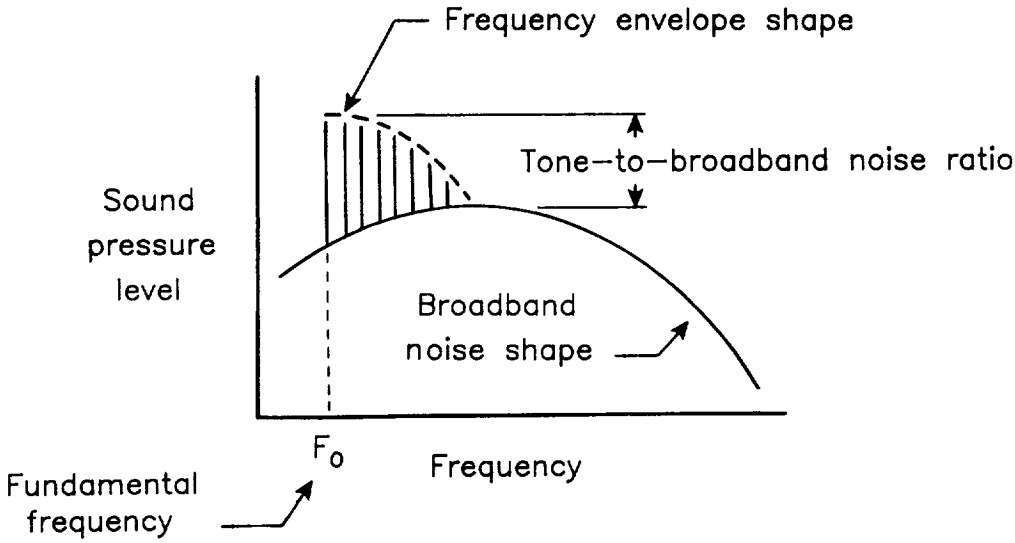

Figure 3. Noise characteristics of propeller aircraft.

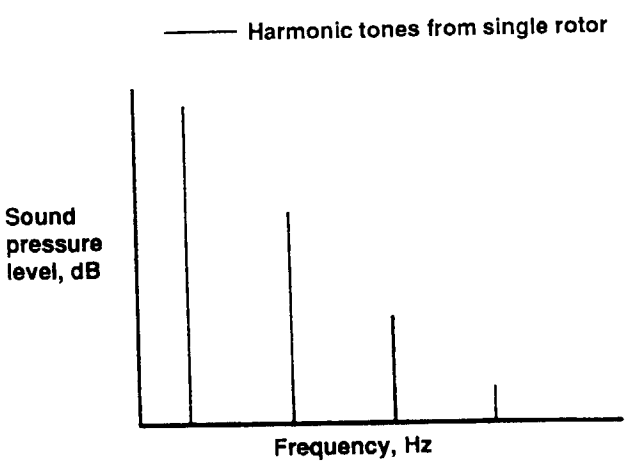

(a) SRP.

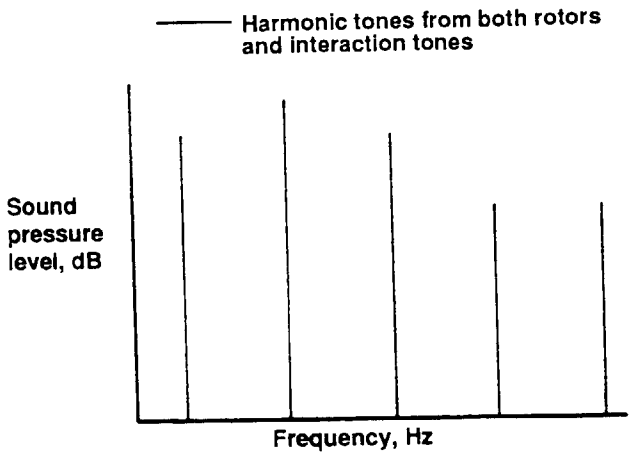

(b) $n \times n$ CRP.

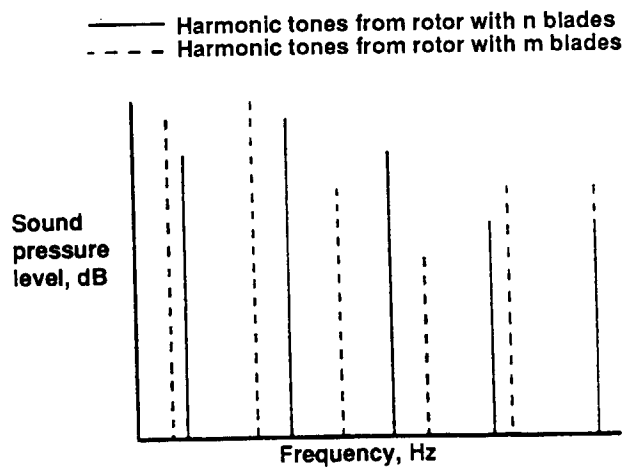

(c) $n \times m$ CRP (harmonic tones only).

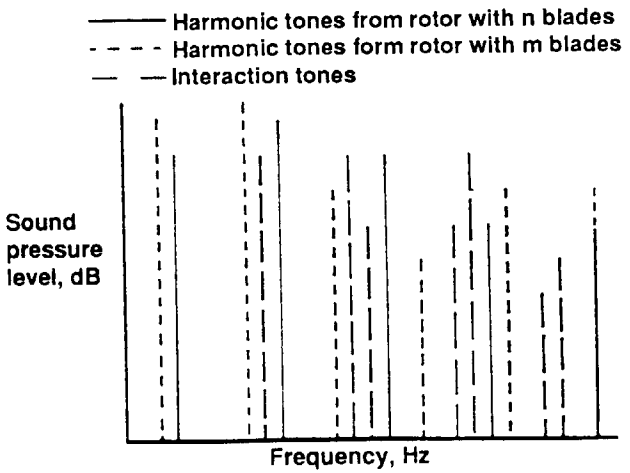

(d) $n \times m$ CRP (harmonic and interaction tones).

Figure 4. Examples of tonal content and frequency envelope shape for different advanced turboprop propeller configurations.

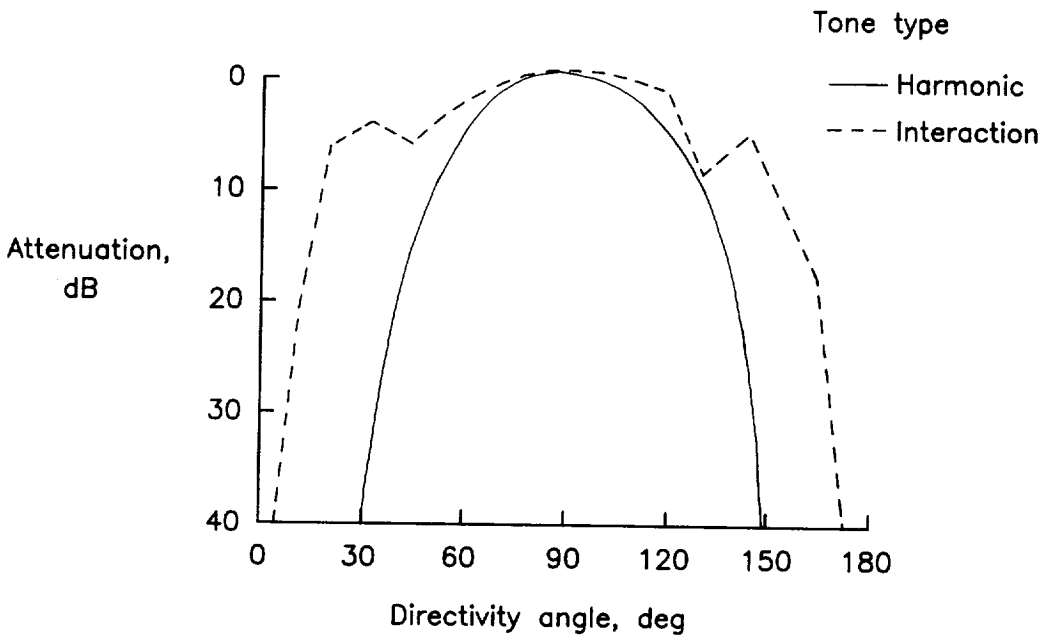

Figure 5. Examples of directivity patterns for different types of advanced turboprop propeller tones.

ORIGINAL PAGE
BLACK AND WHITE PHOTOGRAPH

L-80-6613

Figure 6. Subjects in Anechoic Listening Room in the Langley Acoustics Research Laboratory.

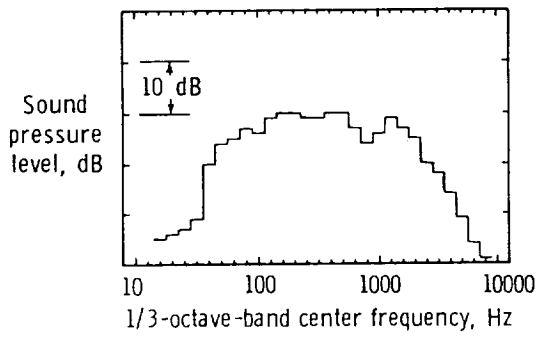

Figure 7. Broadband 1/3-octave spectrum used in synthesis of advanced turboprop aircraft flyover noise for both experiments.

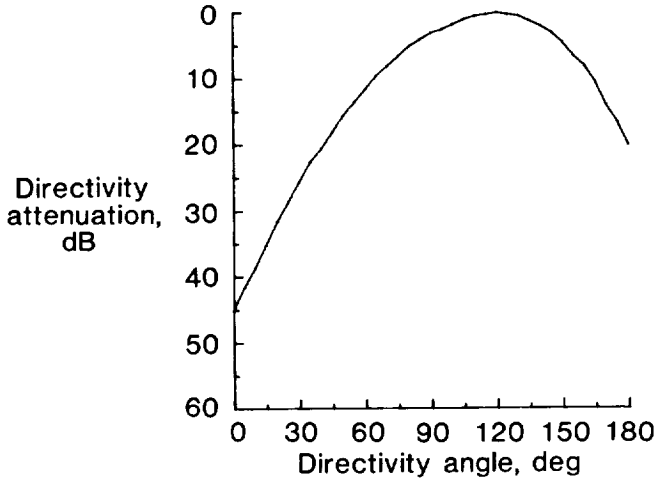

Figure 8. Directivity pattern of broadband 1/3-octave spectrum used in synthesis of advanced turboprop aircraft flyover noise for both experiments.

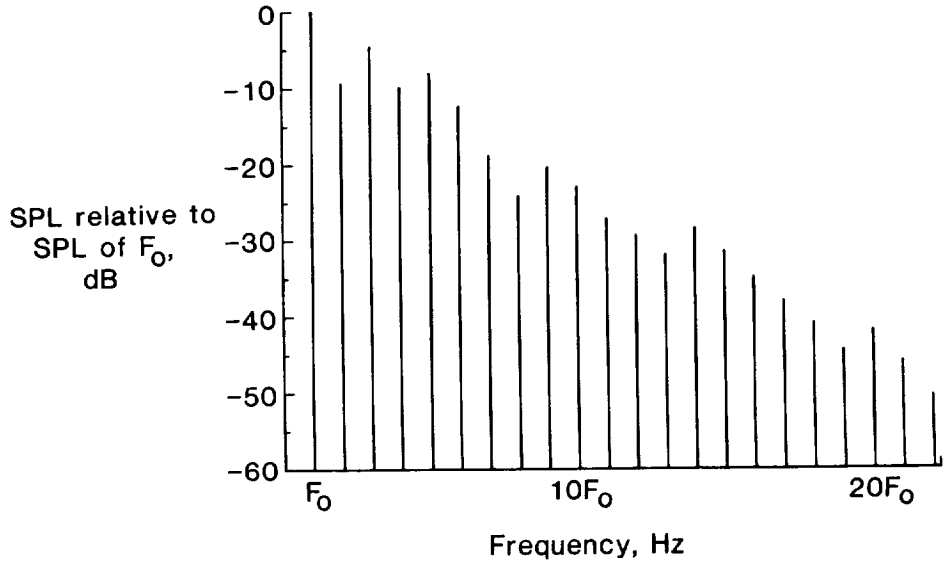

Figure 9. Tonal components used in synthesis of advanced turboprop aircraft flyover noises in first experiment.

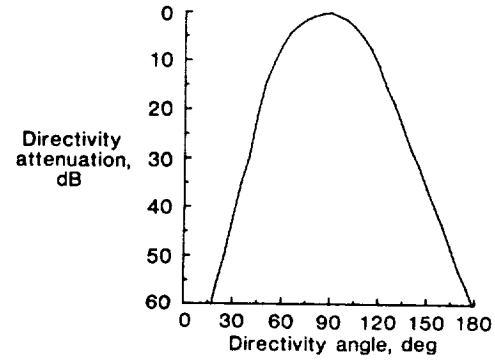

(a) F_o.

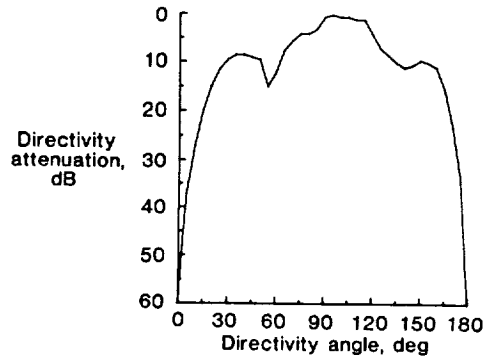

(b) $2F_o$.

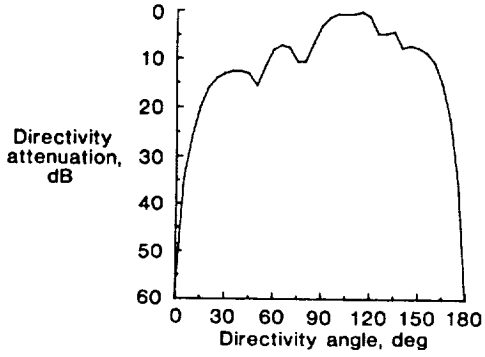

(c) $3F_o$.

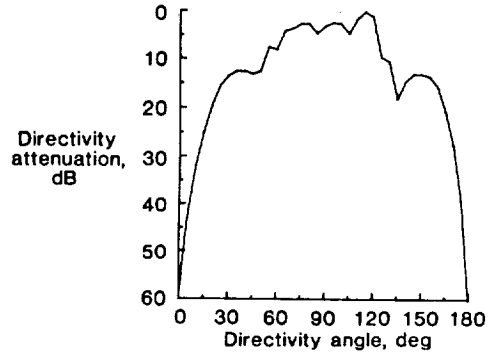

(d) $4F_o$.

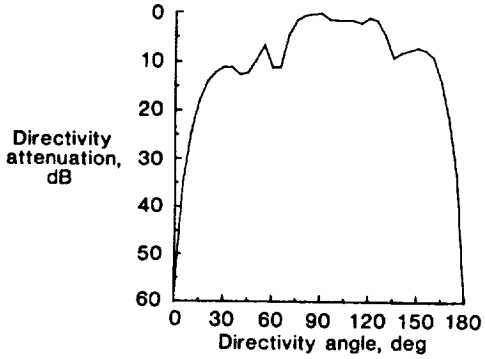

(e) $5F_o$.

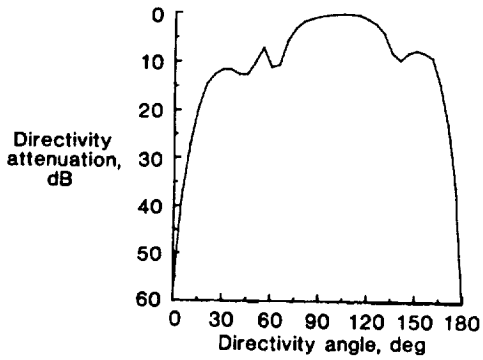

(f) nF_o where $n \geq 6$.

Figure 10. Directivity patterns of tonal components used in synthesis of advanced turboprop aircraft flyover noise in first experiment.

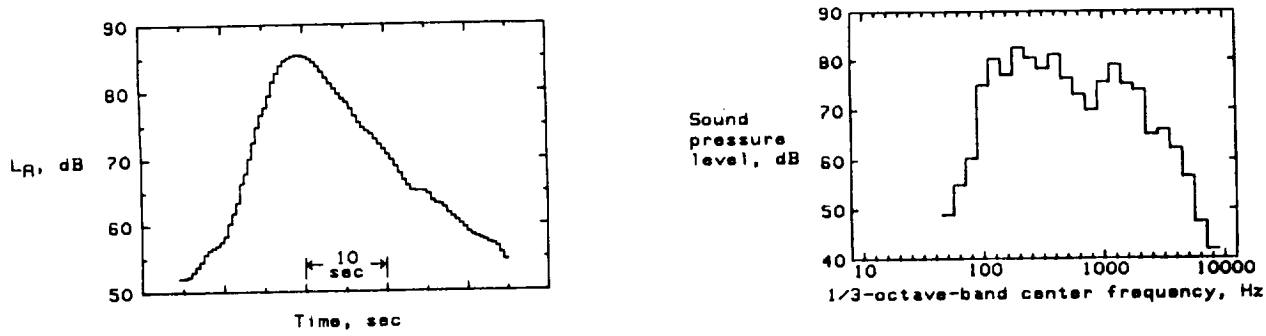

(a) $F_o = 112.5$ Hz; $T/N = 0$ dB.

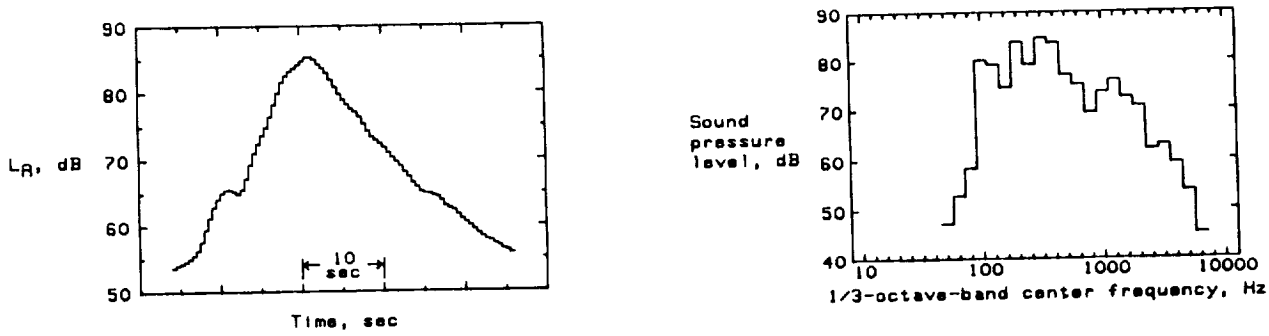

(b) $F_o = 112.5$ Hz; $T/N = 15$ dB.

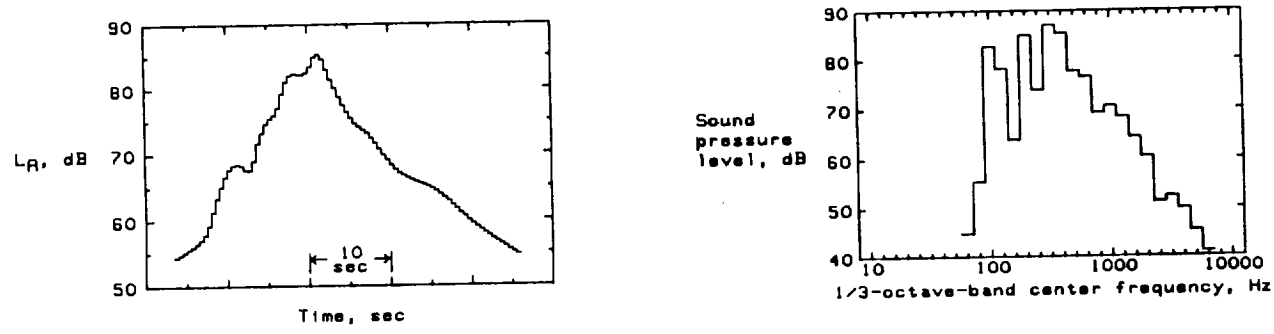

(c) $F_o = 112.5$ Hz; $T/N = 30$ dB.

Figure 11. L_A time history and 1/3-octave-band spectrum at peak L_A of highest level presentation of each advanced turboprop flyover noise in first experiment.

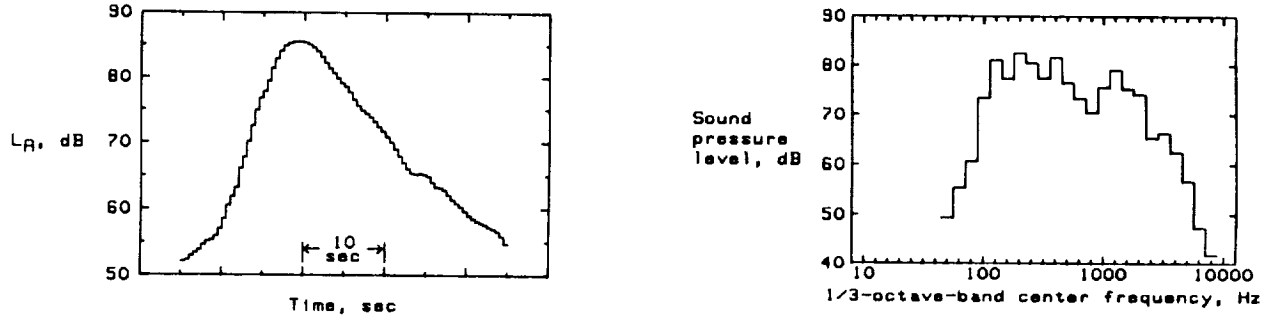

(d) $F_o = 135$ Hz; $T/N = 0$ dB.

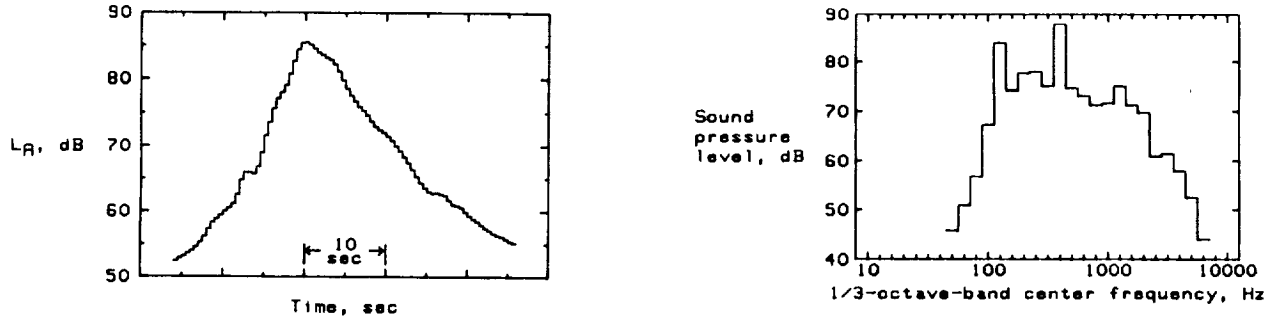

(e) $F_o = 135$ Hz; $T/N = 15$ dB.

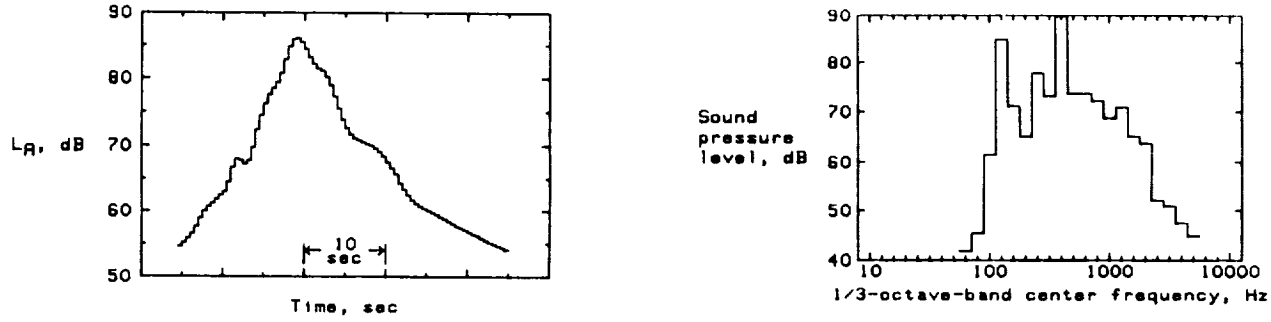

(f) $F_o = 135$ Hz; $T/N = 30$ dB.

Figure 11. Continued.

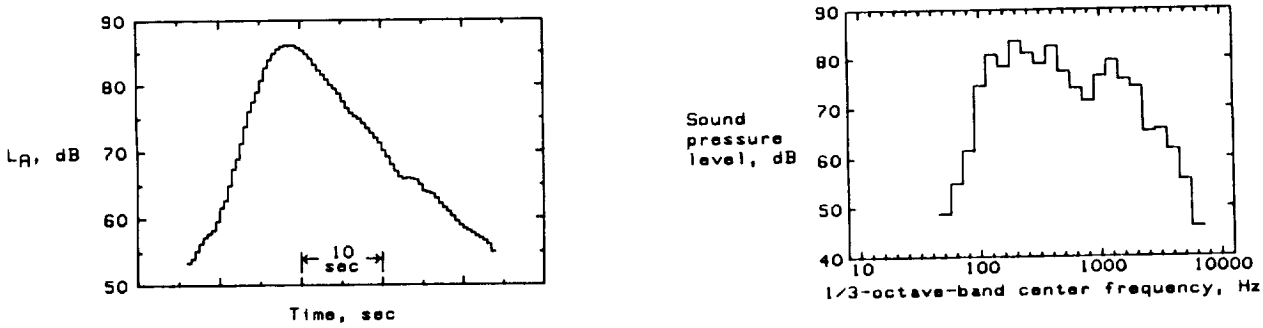

(g) $F_o = 157.5$ Hz; $T/N = 0$ dB.

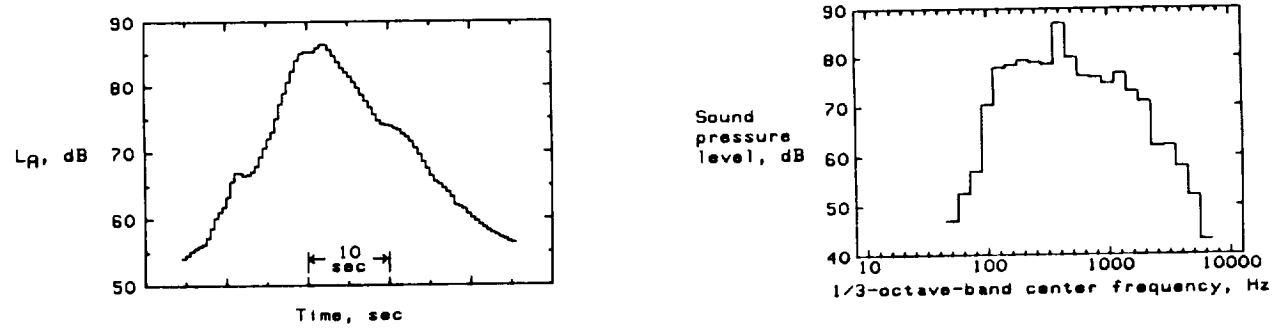

(h) $F_o = 157.5$ Hz; $T/N = 15$ dB.

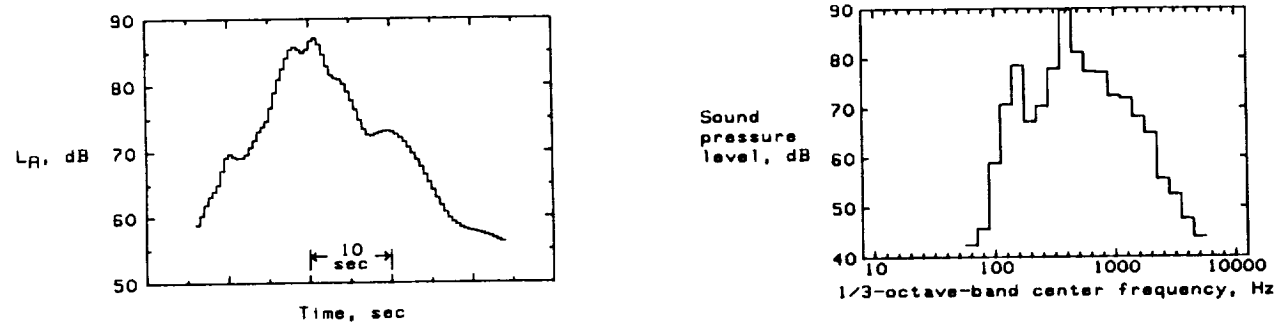

(i) $F_o = 157.5$ Hz; $T/N = 30$ dB.

Figure 11. Continued.

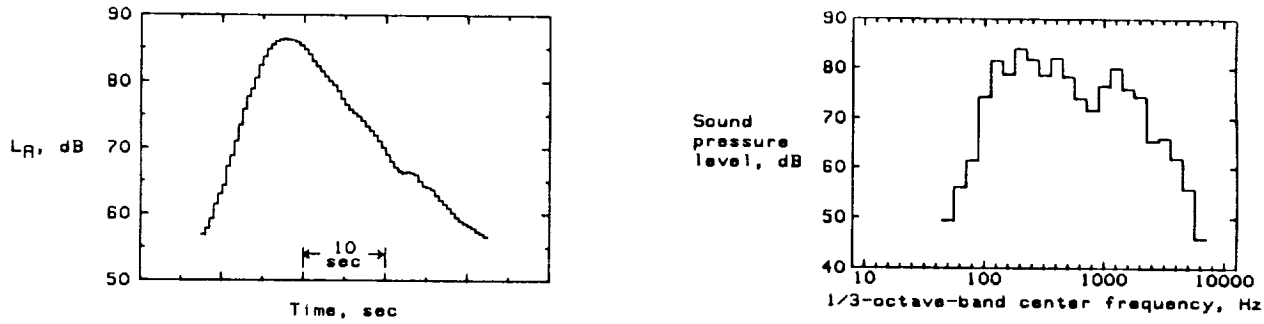

(j) $F_o = 180$ Hz; $T/N = 0$ dB.

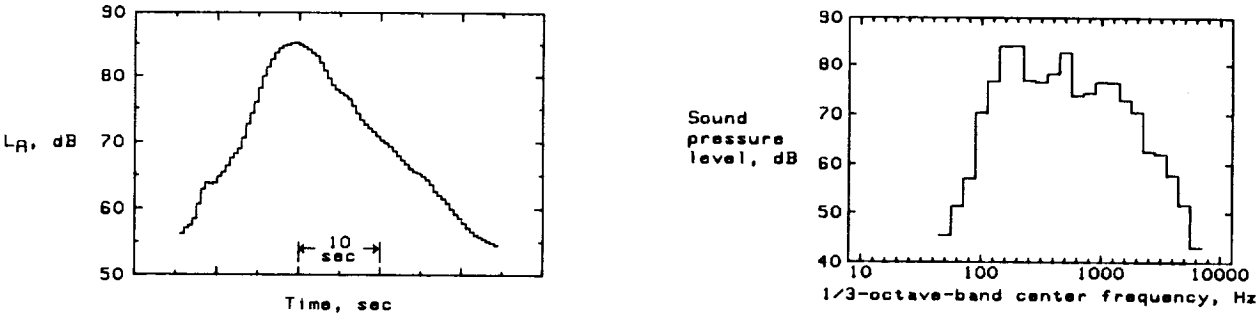

(k) $F_o = 180$ Hz; $T/N = 15$ dB.

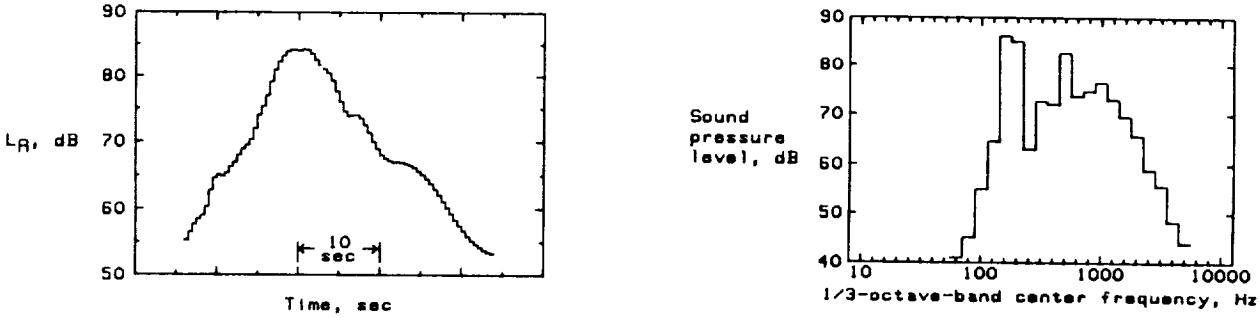

(l) $F_o = 180$ Hz; $T/N = 30$ dB.

Figure 11. Continued.

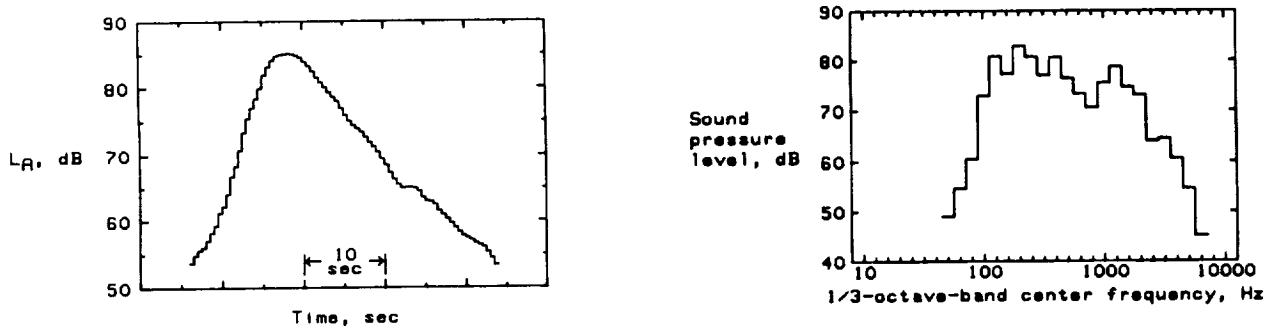

(m) $F_o = 202.5$ Hz; $T/N = 0$ dB.

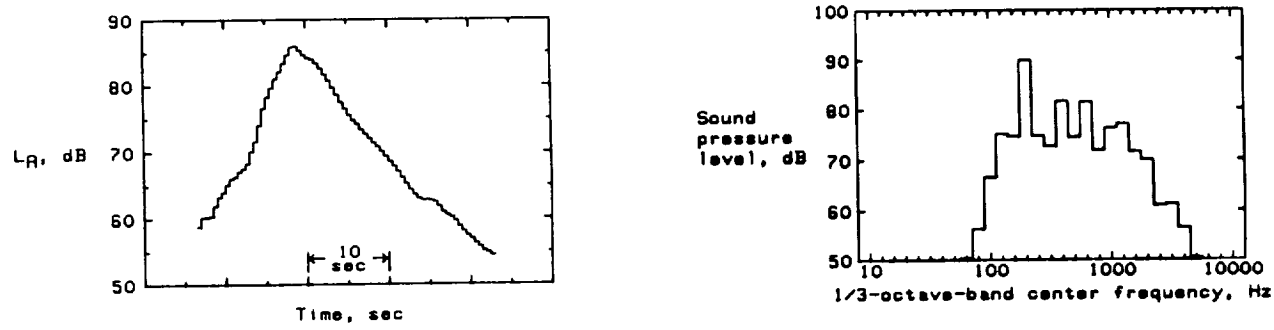

(n) $F_o = 202.5$ Hz; $T/N = 15$ dB.

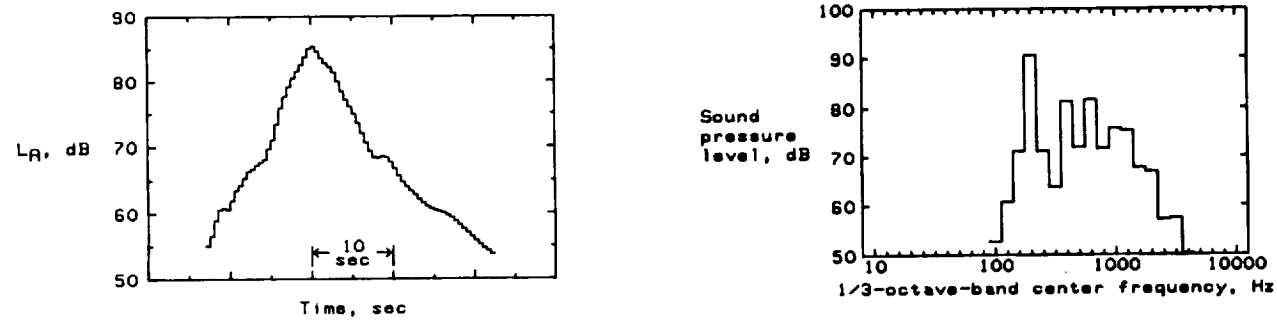

(o) $F_o = 202.5$ Hz; $T/N = 30$ dB.

Figure 11. Continued.

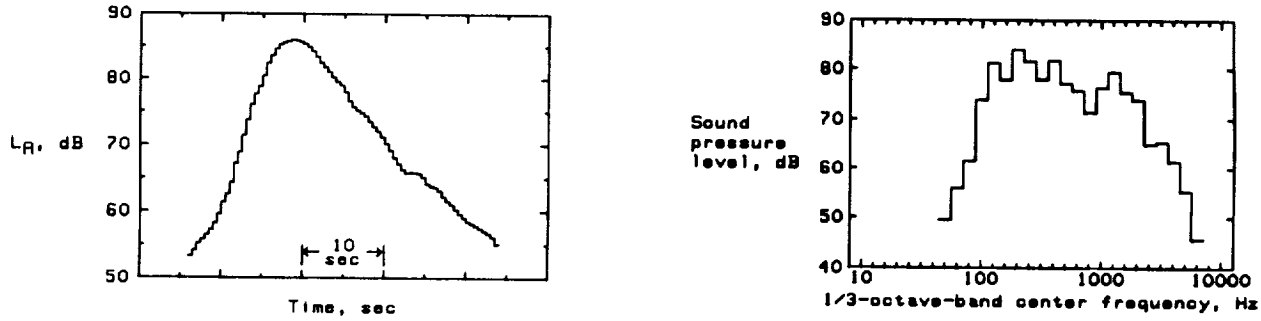

(p) $F_o = 225$ Hz; $T/N = 0$ dB.

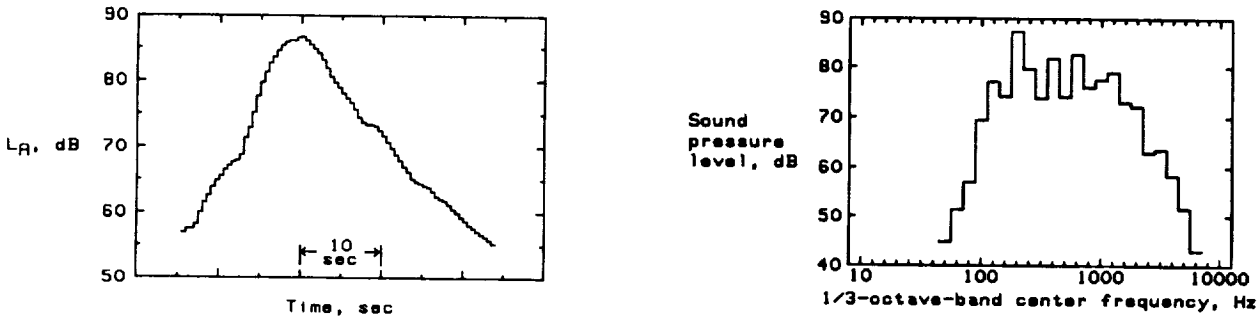

(q) $F_o = 225$ Hz; $T/N = 15$ dB.

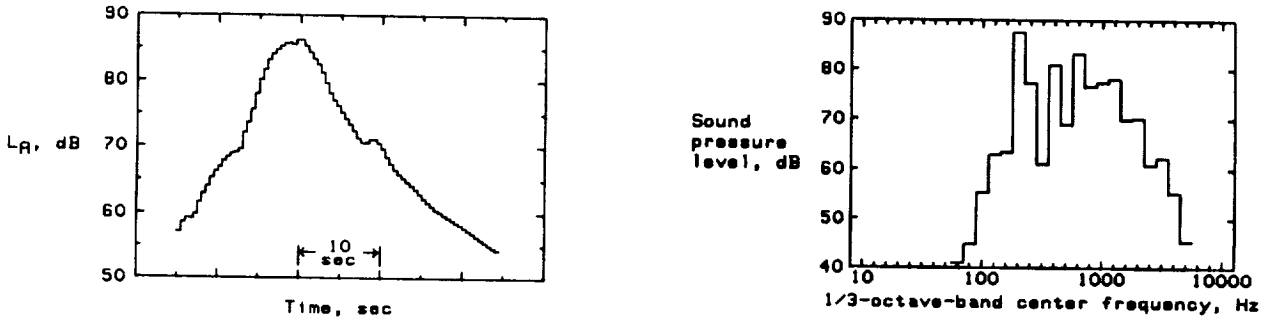

(r) $F_o = 225$ Hz; $T/N = 30$ dB.

Figure 11. Continued.

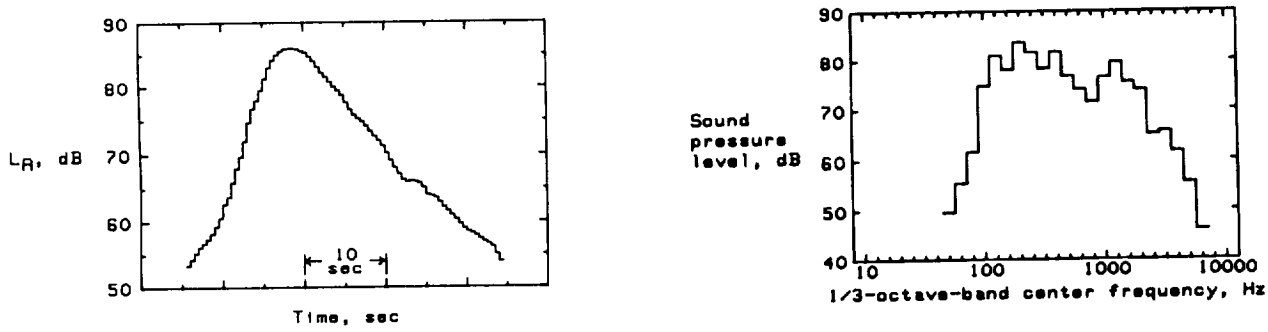

(s) $F_o = 247.5$ Hz; $T/N = 0$ dB.

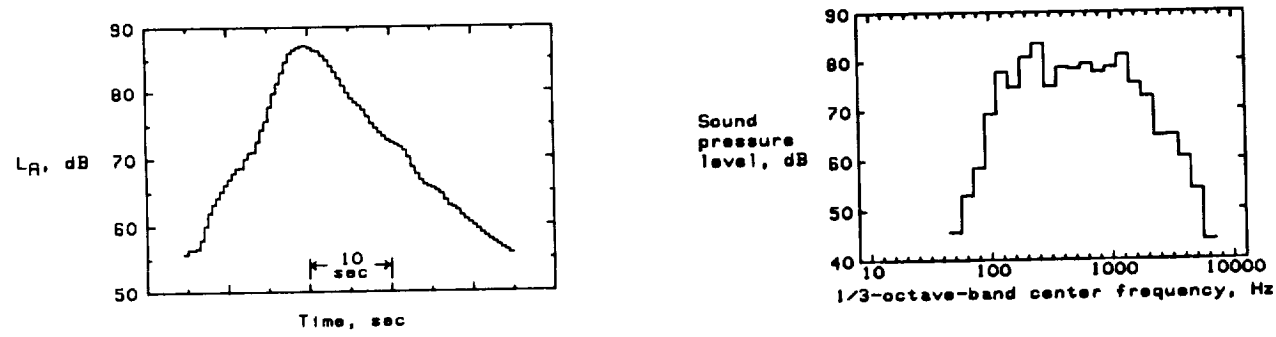

(t) $F_o = 247.5$ Hz; $T/N = 15$ dB.

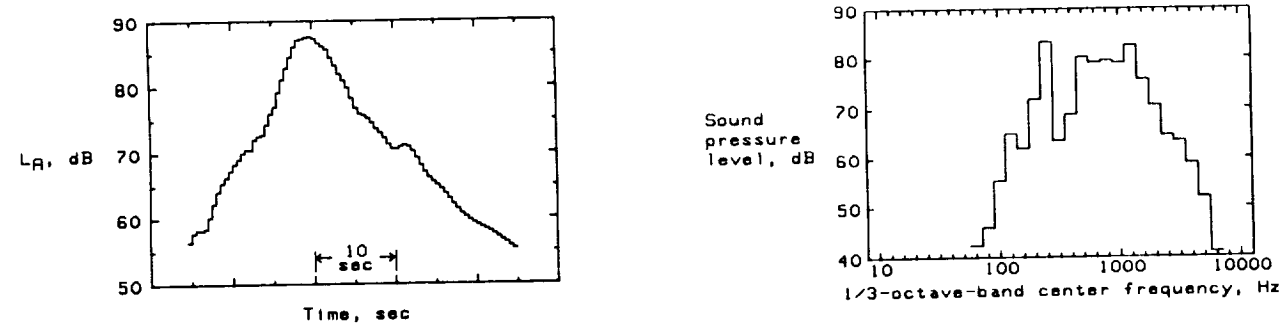

(u) $F_o = 247.5$ Hz; $T/N = 30$ dB.

Figure 11. Continued.

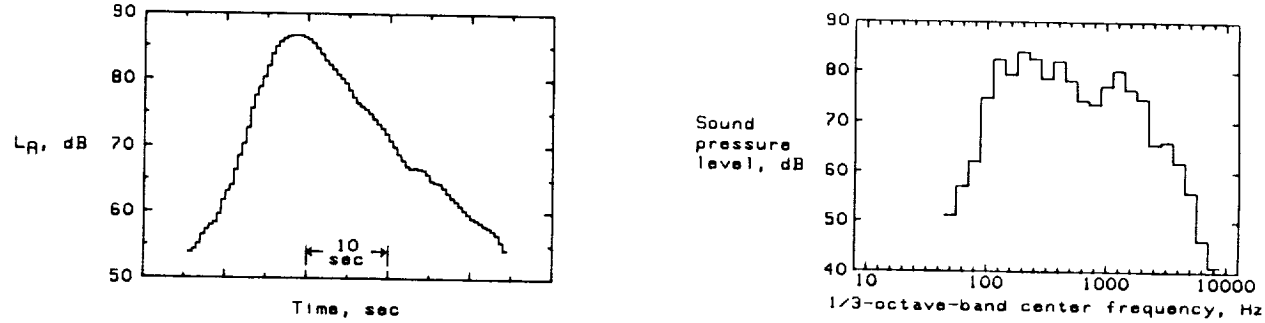

(v) $F_o = 270$ Hz; $T/N = 0$ dB.

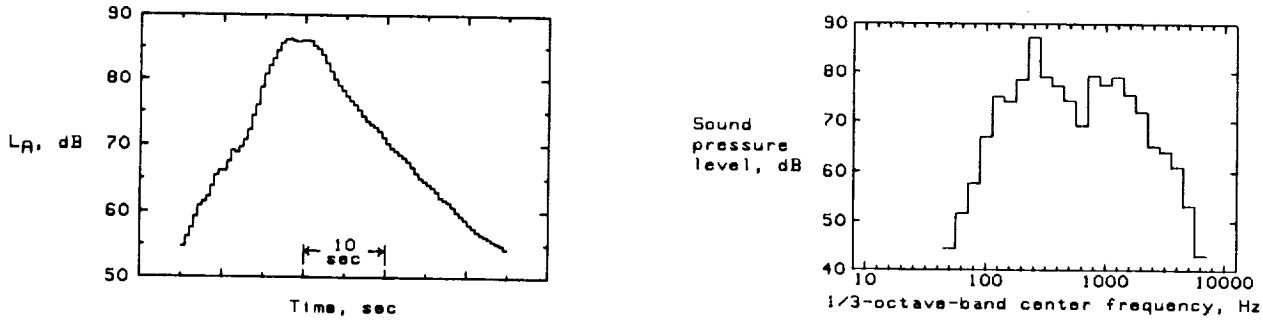

(w) $F_o = 270$ Hz; $T/N = 15$ dB.

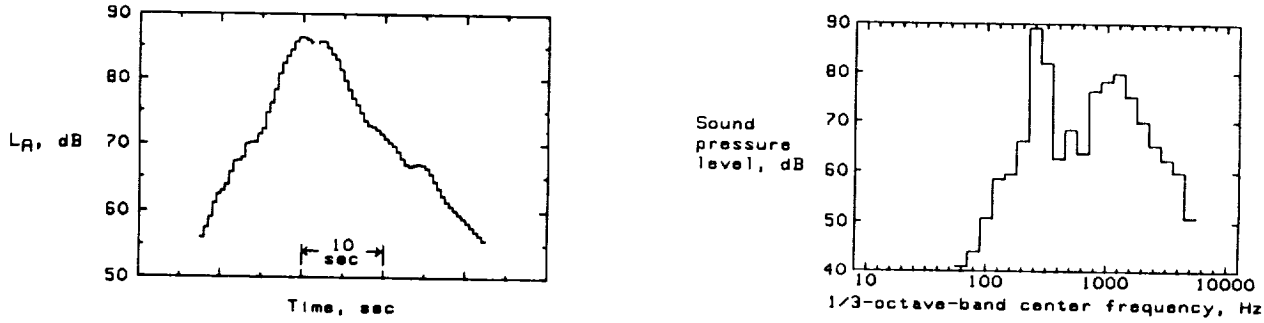

(x) $F_o = 270$ Hz; $T/N = 30$ dB.

Figure 11. Continued.

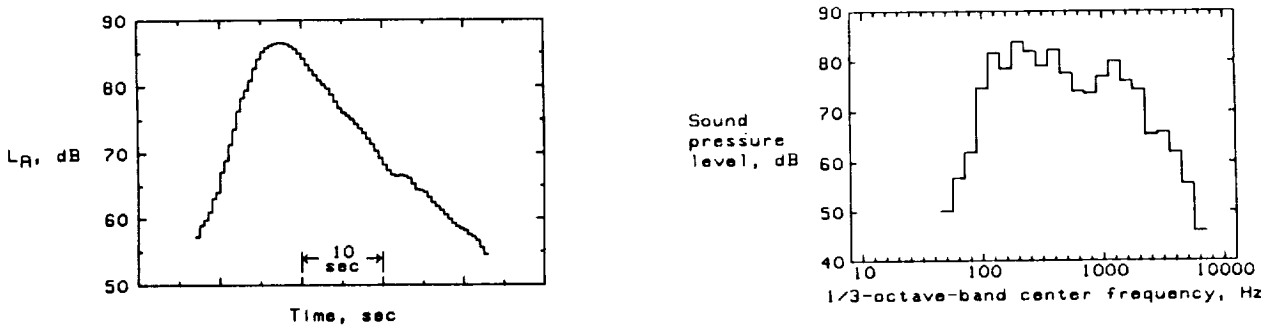

(y) $F_o = 292.5$ Hz; $T/N = 0$ dB.

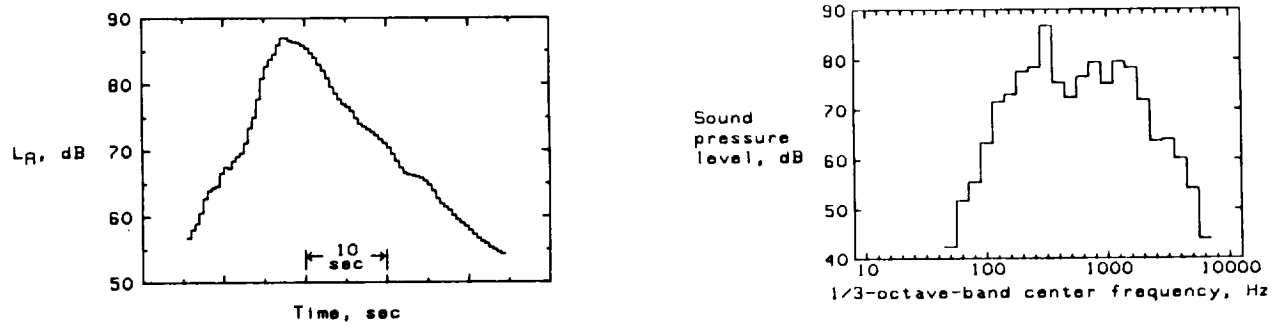

(z) $F_o = 292.5$ Hz; $T/N = 15$ dB.

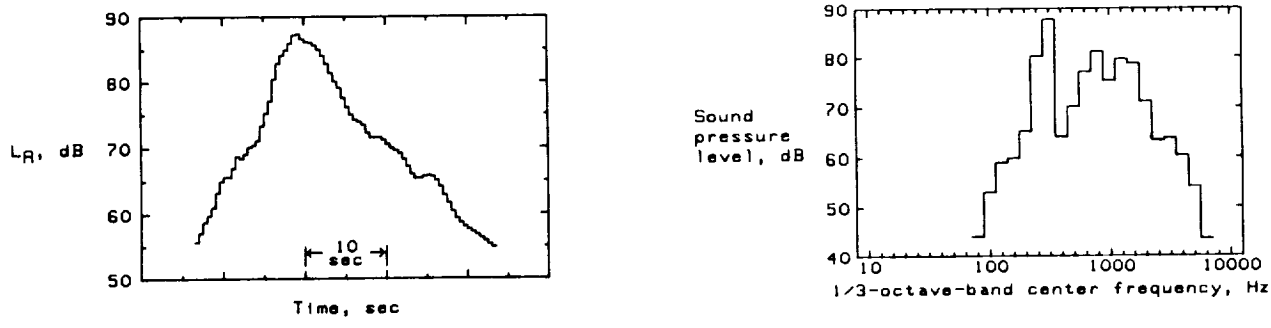

(aa) $F_o = 292.5$ Hz; $T/N = 30$ dB.

Figure 11. Concluded.

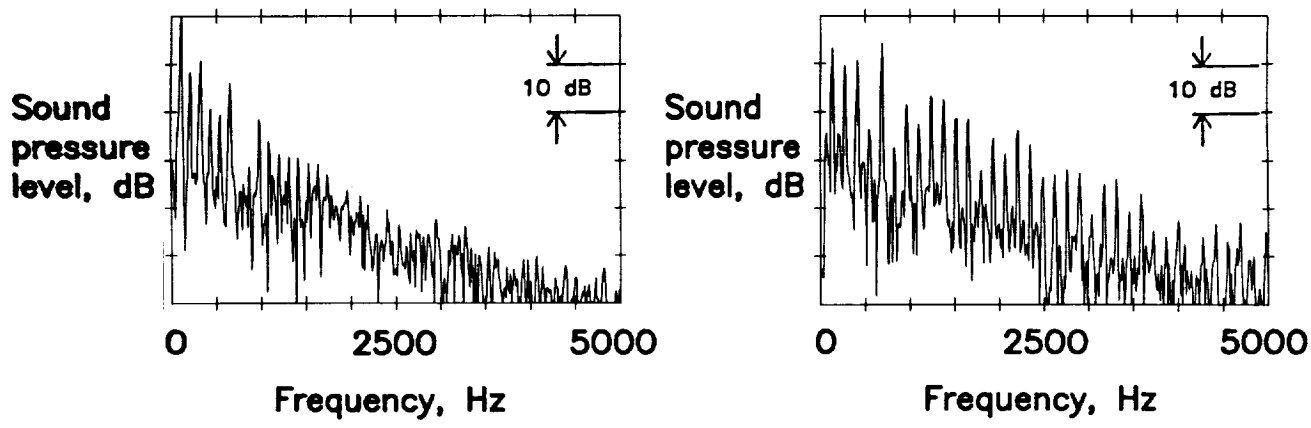

(a) $F_o = 112.5$ Hz.

(b) $F_o = 135$ Hz.

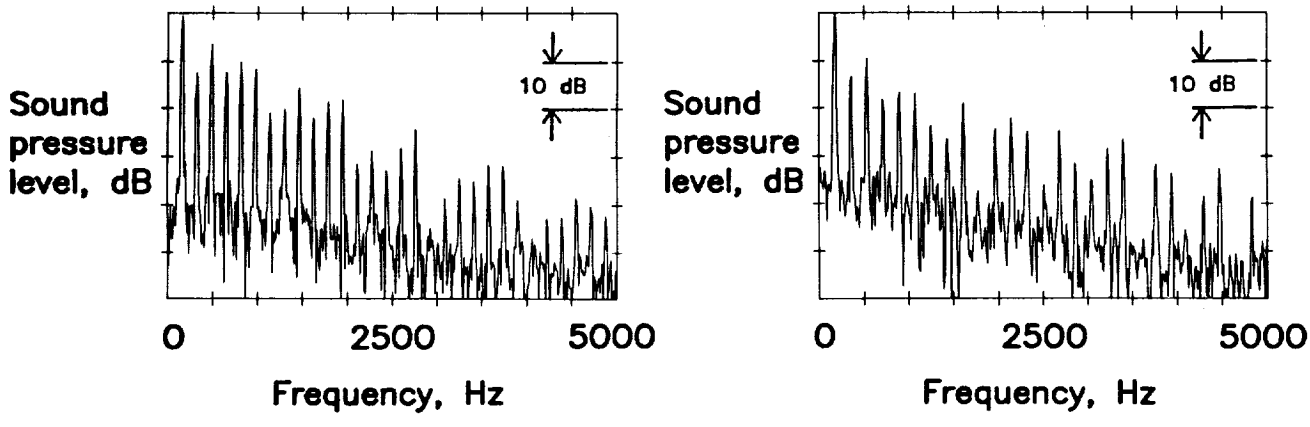

(c) $F_o = 157.5$ Hz.

(d) $F_o = 180$ Hz.

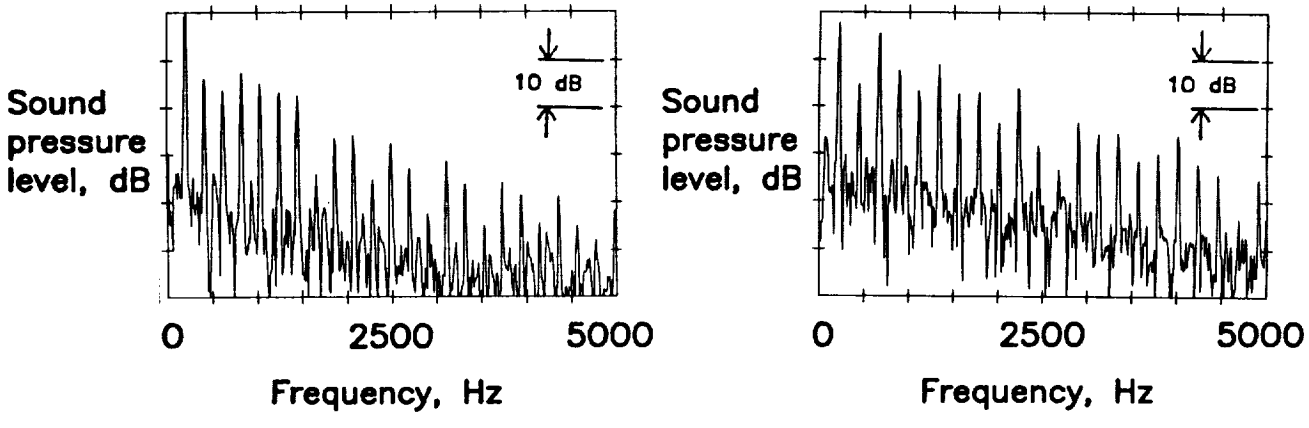

(e) $F_o = 202.5$ Hz.

(f) $F_o = 225$ Hz.

Figure 12. Narrowband spectrum of each advanced turboprop flyover noise with 30-dB tone-to-broadband noise ratio in first experiment.

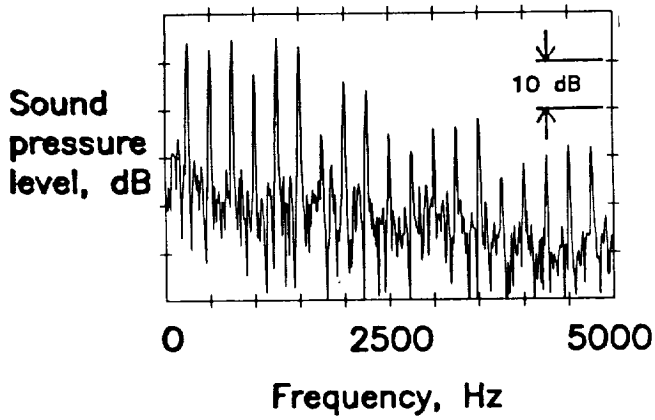

(g) $F_o = 247.5$ Hz.

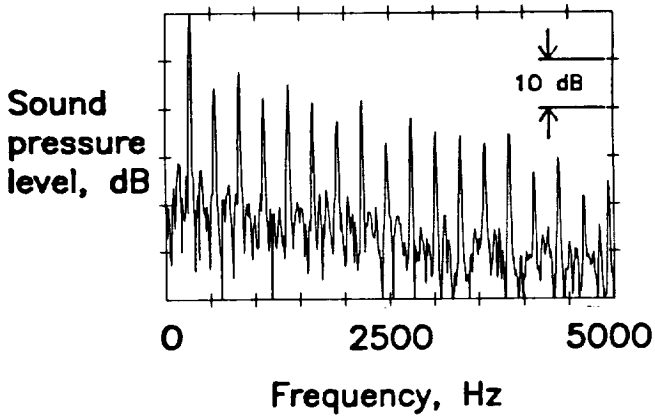

(h) $F_o = 270$ Hz.

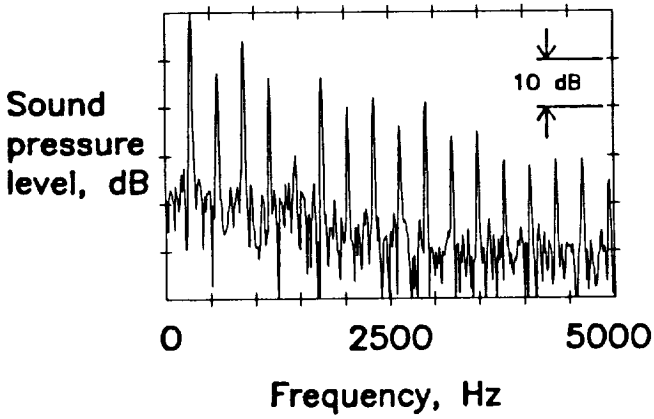

(i) $F_o = 292.5$ Hz.

Figure 12. Concluded.

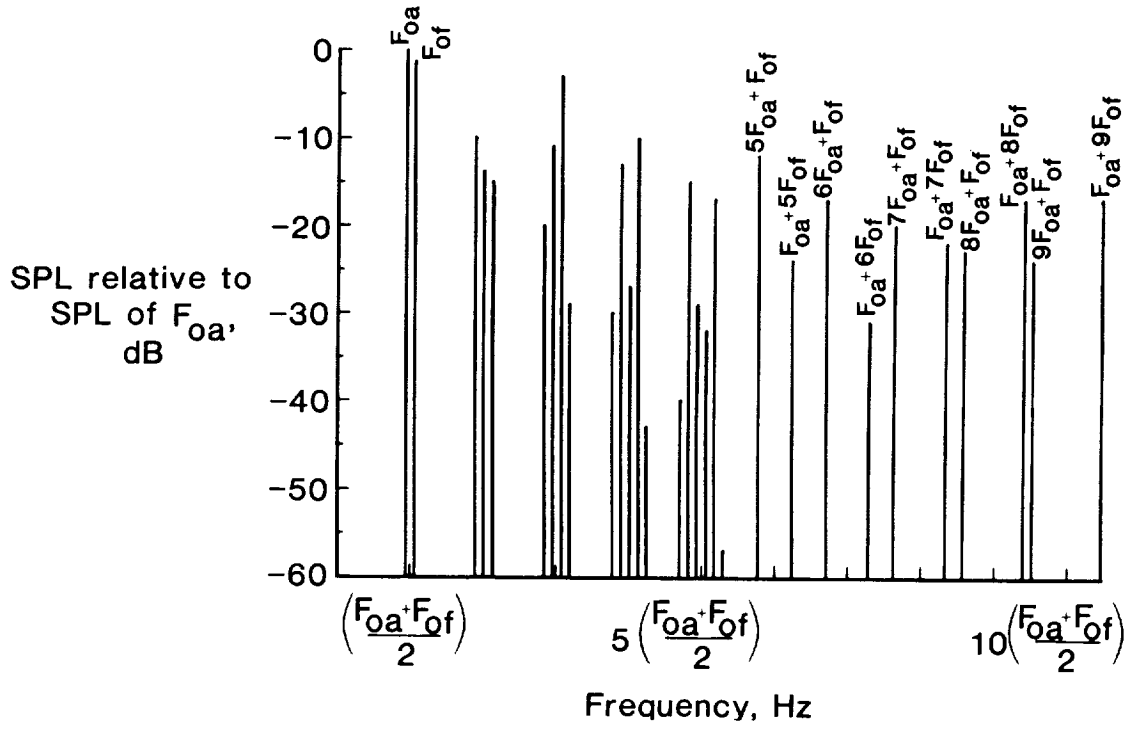

Figure 13. Tonal components used in synthesis of advanced turboprop aircraft flyover noises in second experiment.

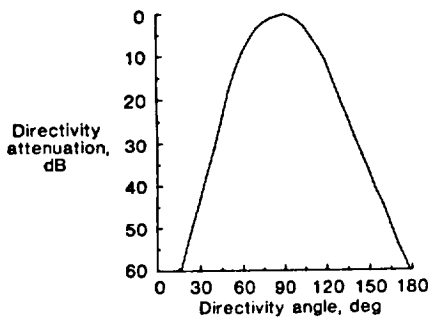

(a) F_{oa}.

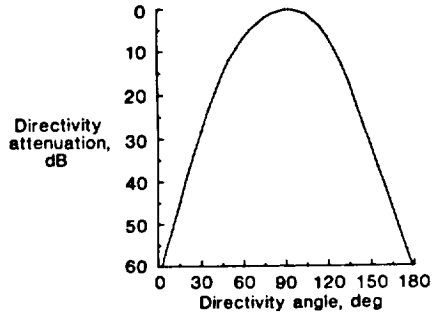

(b) F_{of}.

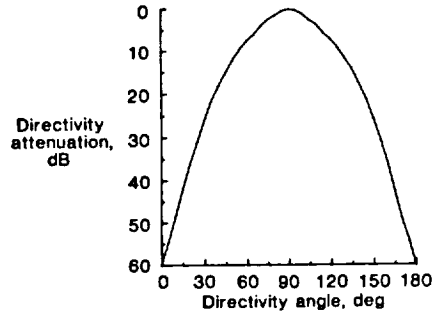

(c) nF_{oa} or nF_{of} where $n \geq 2$.

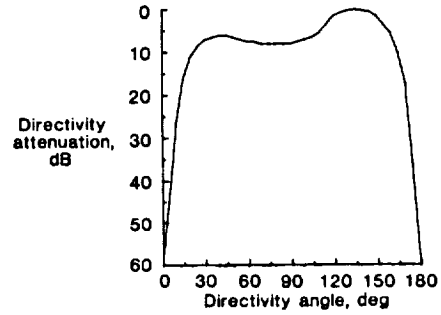

(d) $F_{oa} + F_{of}$.

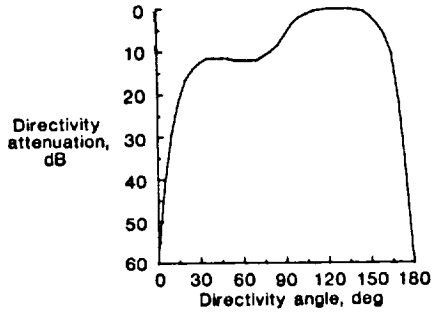

(e) $2F_{oa} + F_{of}$.

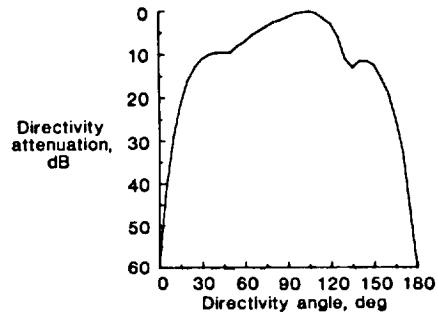

(f) $F_{oa} + 2F_{of}$.

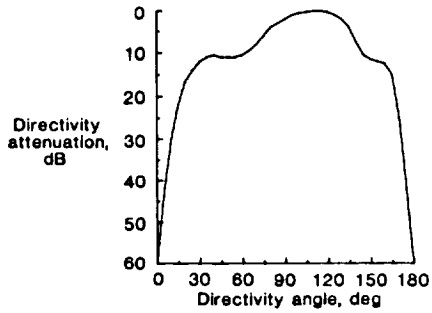

(g) $mF_{oa} + nF_{of}$ where $m \geq 1$, $n \geq 1$, and $m + n \geq 4$.

Figure 14. Directivity patterns of tonal components used in synthesis of advanced turboprop aircraft flyover noises in second experiment.

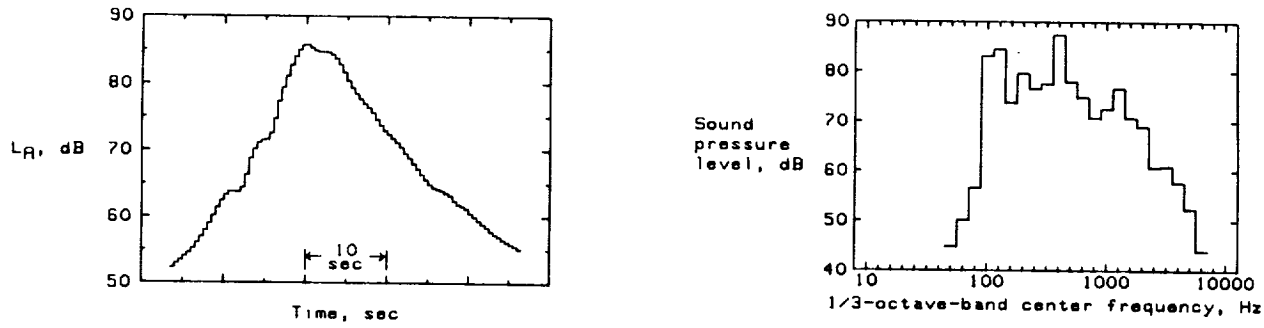

(a) $F_{of} = 135$ Hz; $F_{oa} = 112.5$ Hz; $T/N = 15$ dB.

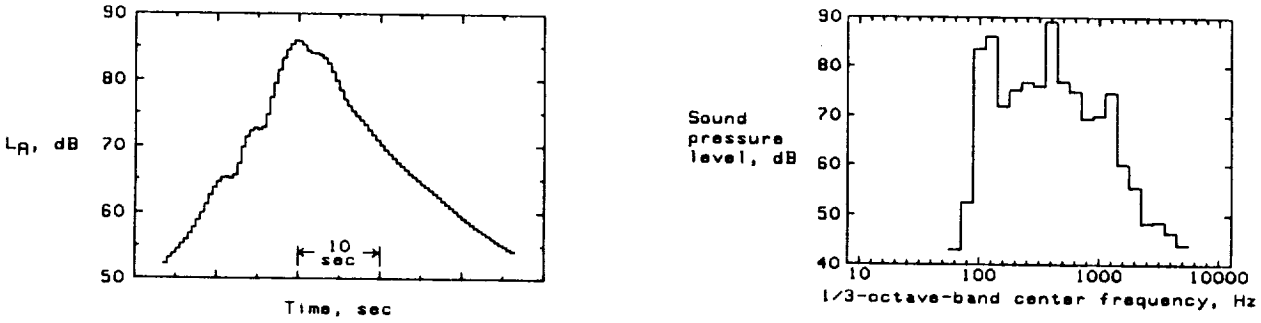

(b) $F_{of} = 135$ Hz; $F_{oa} = 112.5$ Hz; $T/N = 30$ dB.

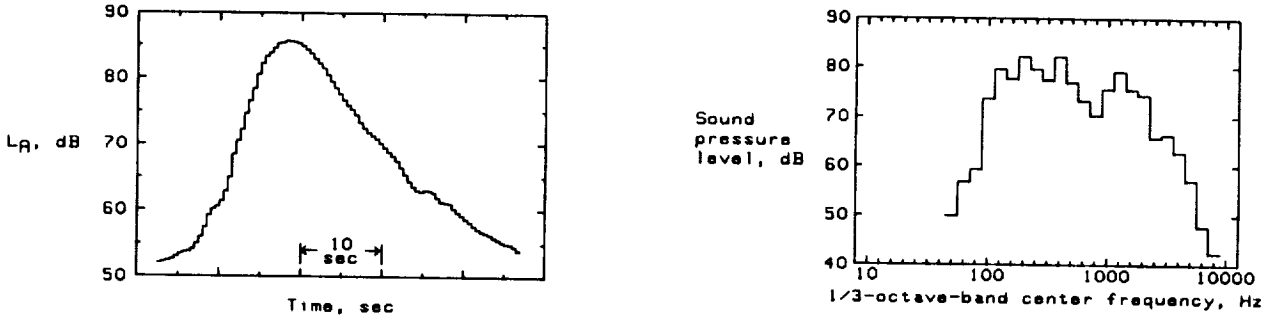

(c) $F_{of} = 157.5$ Hz; $F_{oa} = 112.5$ Hz; $T/N = 0$ dB.

Figure 15. L_A time history and 1/3-octave-band spectrum at peak L_A of highest level presentation of each advanced turboprop flyover noise in second experiment.

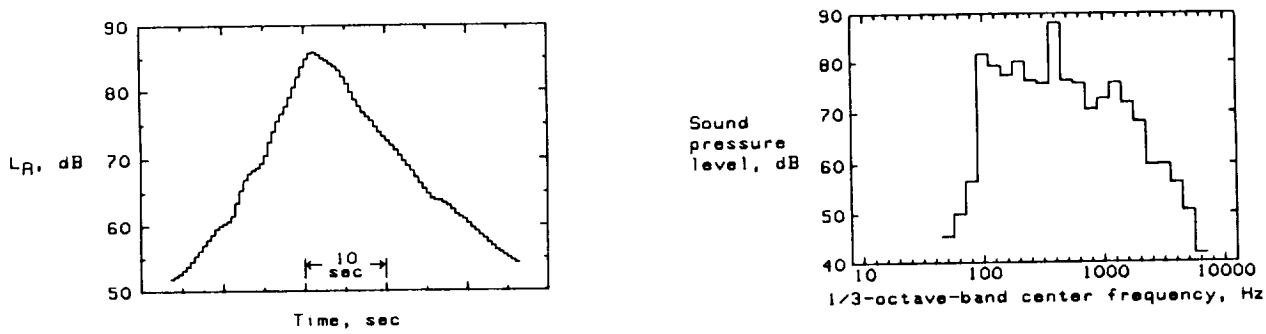

(d) $F_{of} = 157.5$ Hz; $F_{oa} = 112.5$ Hz; $T/N = 15$ dB.

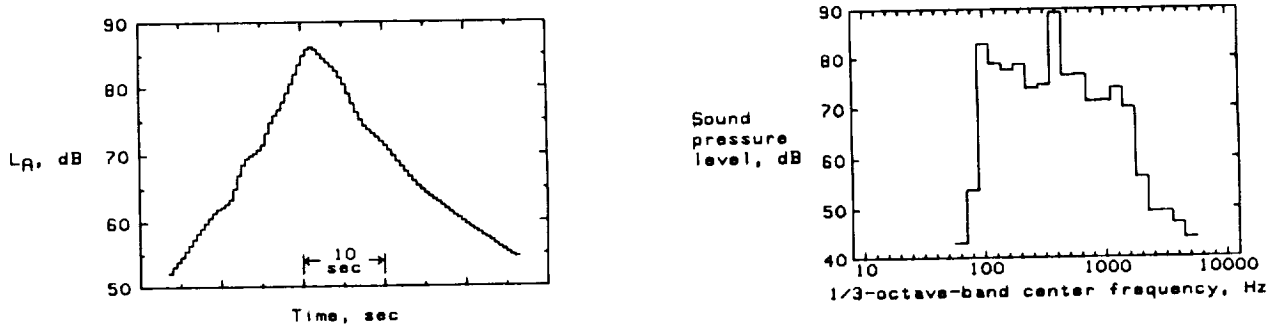

(e) $F_{of} = 157.5$ Hz; $F_{oa} = 112.5$ Hz; $T/N = 30$ dB.

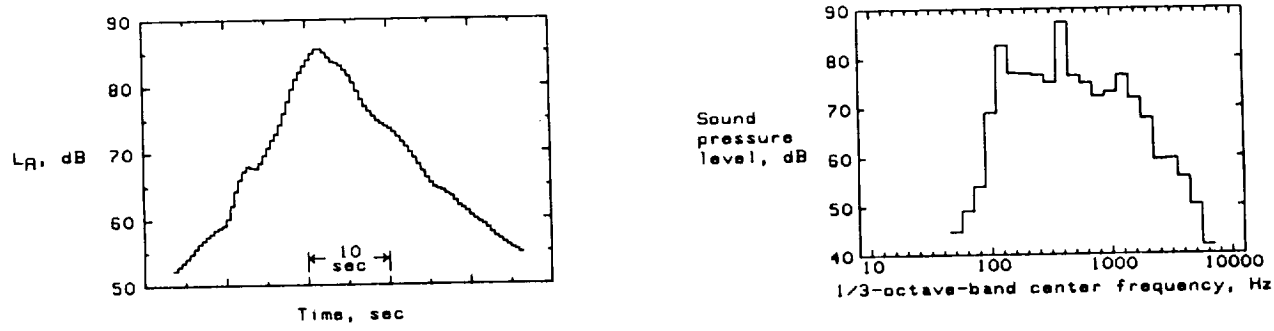

(f) $F_{of} = 157.5$ Hz; $F_{oa} = 135$ Hz; $T/N = 20$ dB.

Figure 15. Continued.

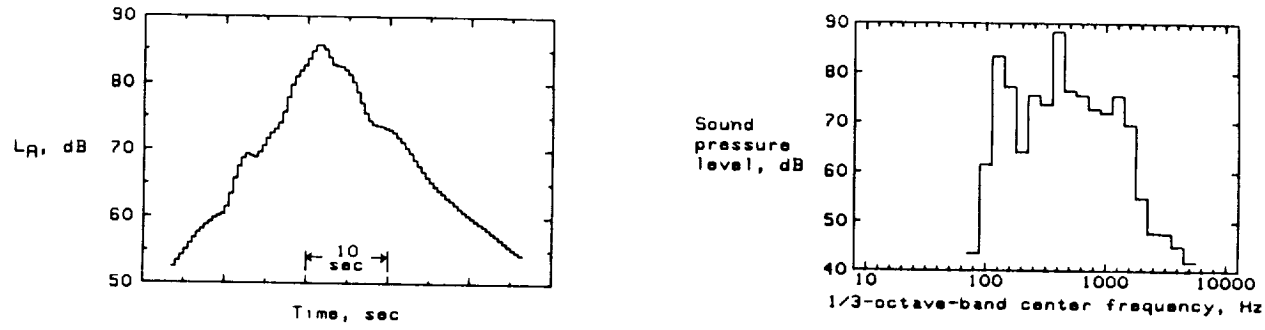

(g) $F_{of} = 157.5$ Hz; $F_{oa} = 135$ Hz; $T/N = 30$ dB.

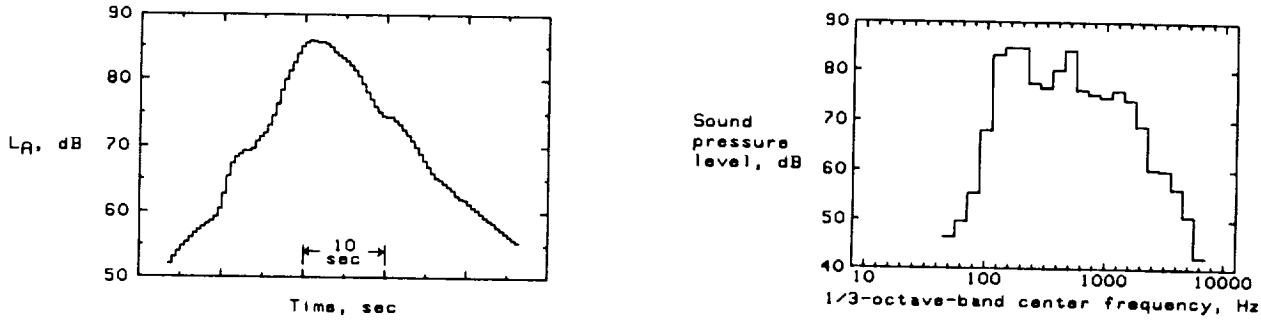

(h) $F_{of} = 180$ Hz; $F_{oa} = 135$ Hz; $T/N = 20$ dB.

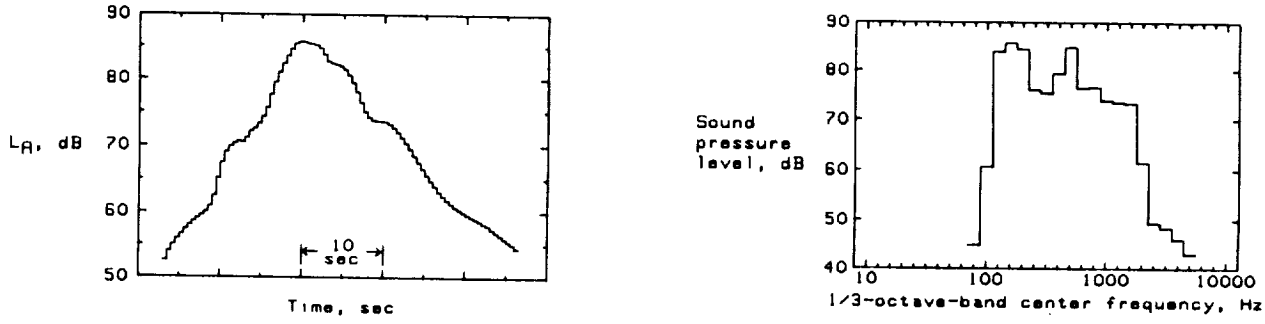

(i) $F_{of} = 180$ Hz; $F_{oa} = 135$ Hz; $T/N = 30$ dB.

Figure 15. Continued.

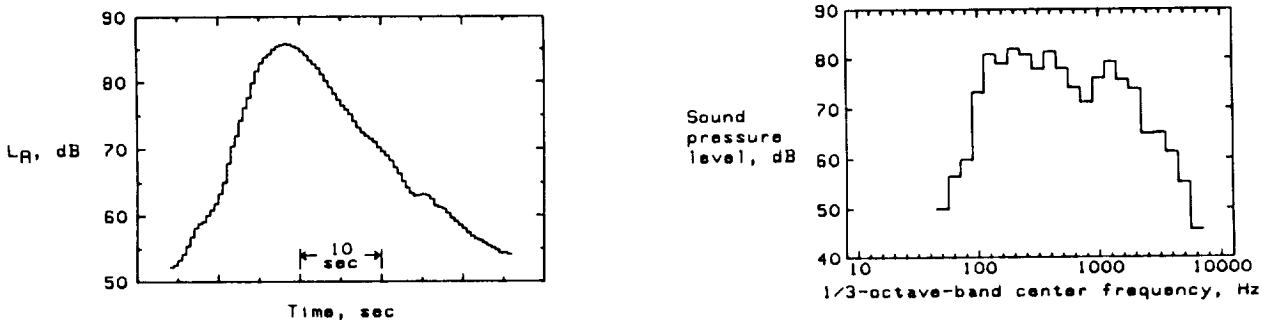

(j) $F_{of} = 180$ Hz; $F_{oa} = 157.5$ Hz; $T/N = 0$ dB.

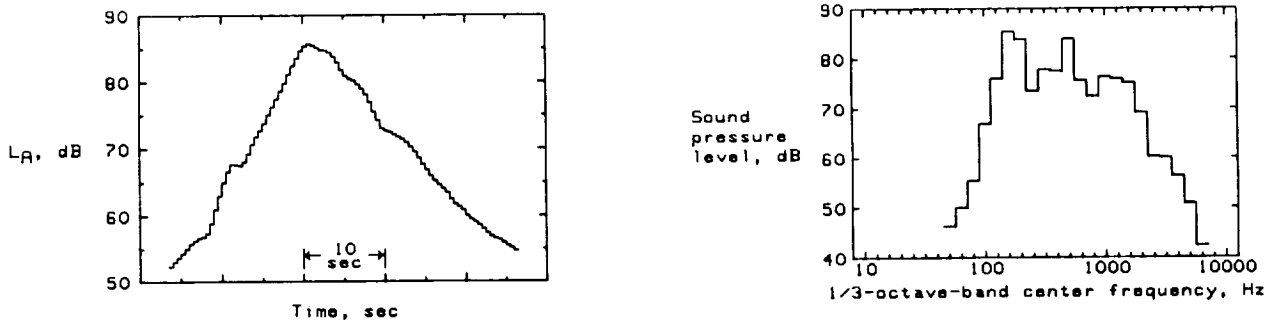

(k) $F_{of} = 180$ Hz; $F_{oa} = 157.5$ Hz; $T/N = 15$ dB.

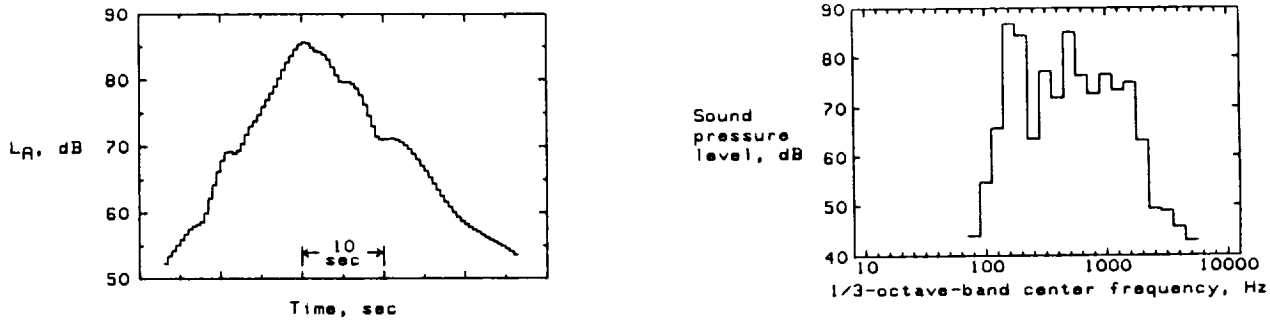

(l) $F_{of} = 180$ Hz; $F_{oa} = 157.5$ Hz; $T/N = 30$ dB.

Figure 15. Continued.

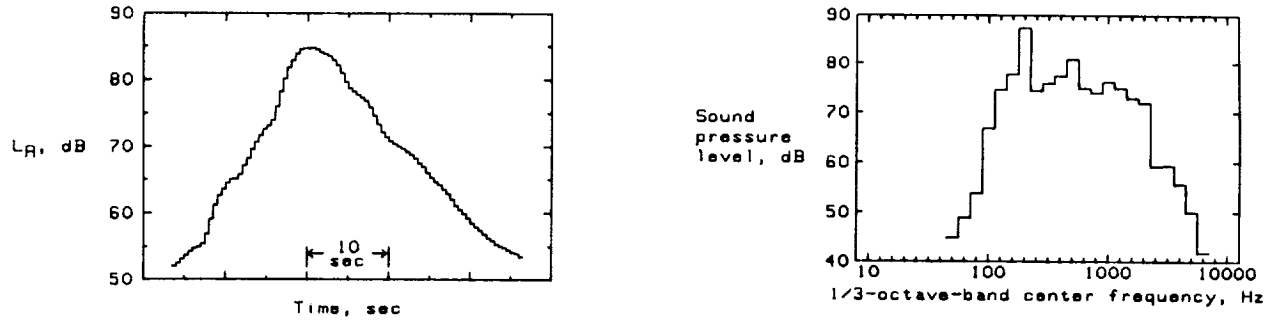

(m) $F_{of} = 202.5$ Hz; $F_{oa} = 157.5$ Hz; $T/N = 15$ dB.

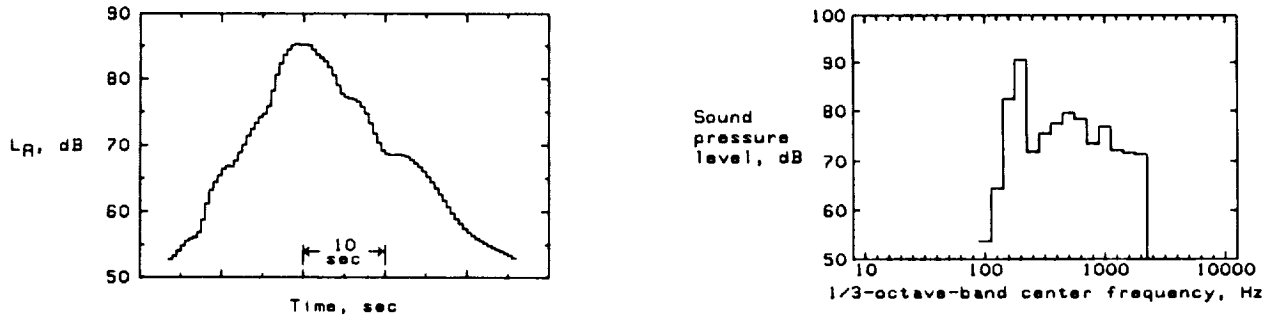

(n) $F_{of} = 202.5$ Hz; $F_{oa} = 157.5$ Hz; $T/N = 30$ dB.

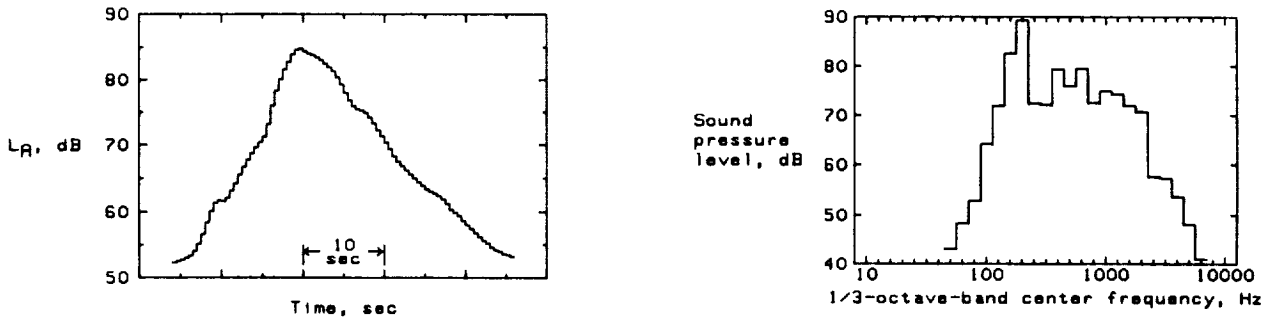

(o) $F_{of} = 202.5$ Hz; $F_{oa} = 180$ Hz; $T/N = 15$ dB.

Figure 15. Continued.

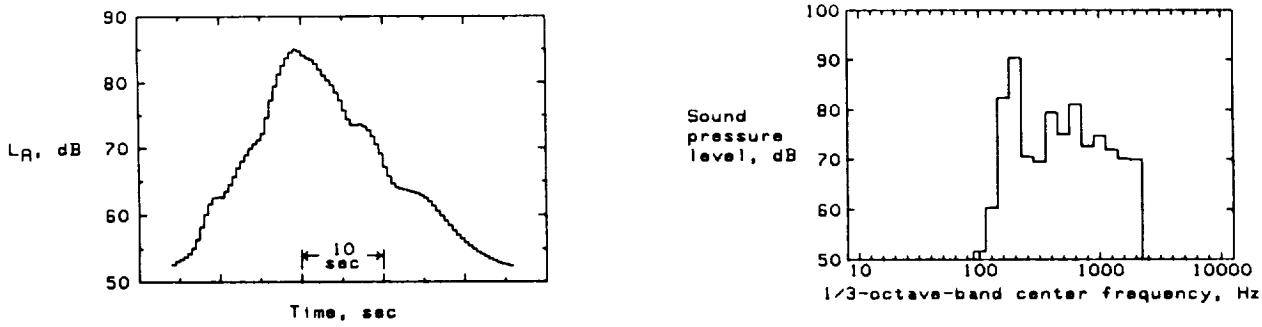

(p) $F_{of} = 202.5$ Hz; $F_{oa} = 180$ Hz; $T/N = 30$ dB.

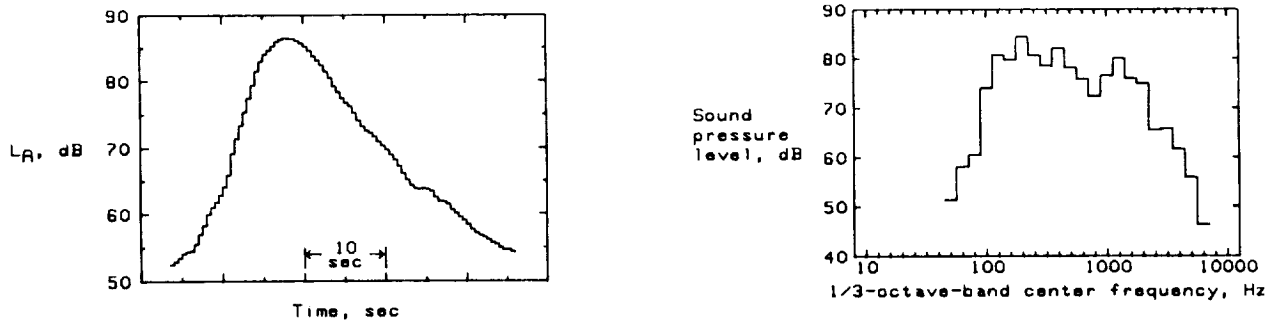

(q) $F_{of} = 225$ Hz; $F_{oa} = 180$ Hz; $T/N = 0$ dB.

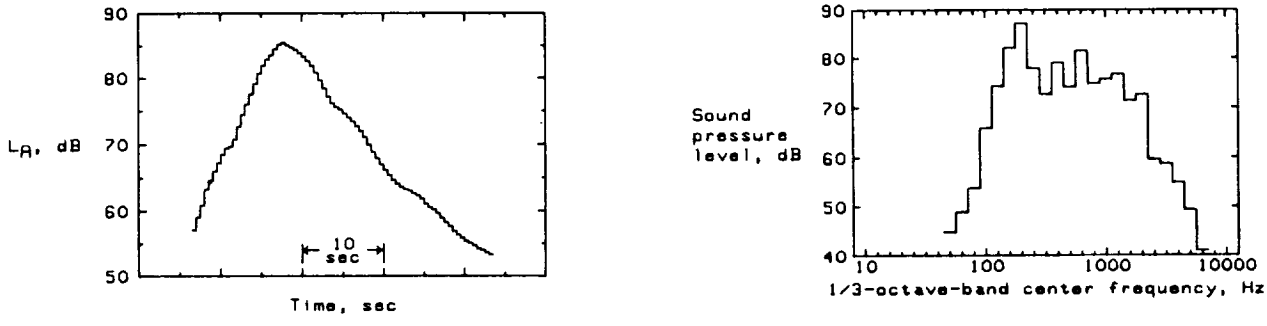

(r) $F_{of} = 225$ Hz; $F_{oa} = 180$ Hz; $T/N = 15$ dB.

Figure 15. Continued.

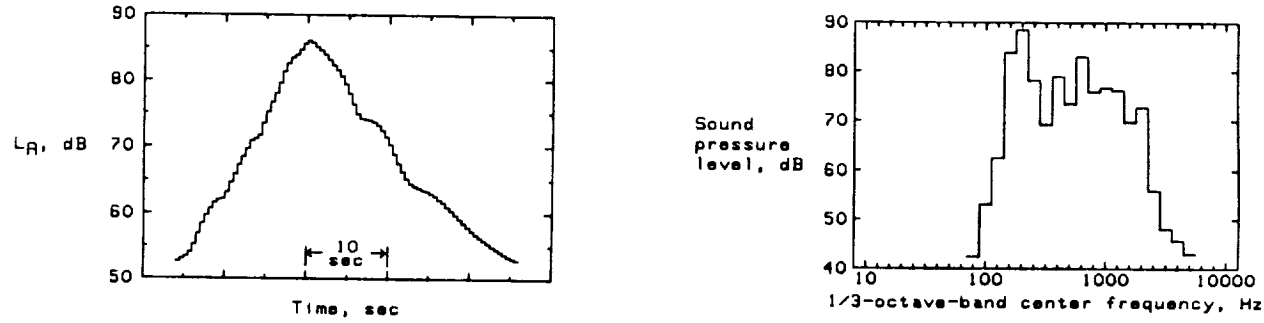

(s) $F_{of} = 225$ Hz; $F_{oa} = 180$ Hz; $T/N = 30$ dB.

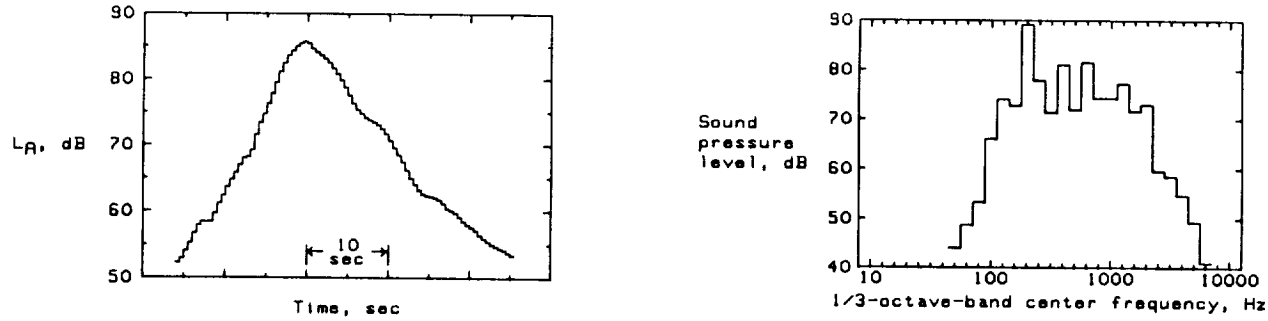

(t) $F_{of} = 225$ Hz; $F_{oa} = 202.5$ Hz; $T/N = 15$ dB.

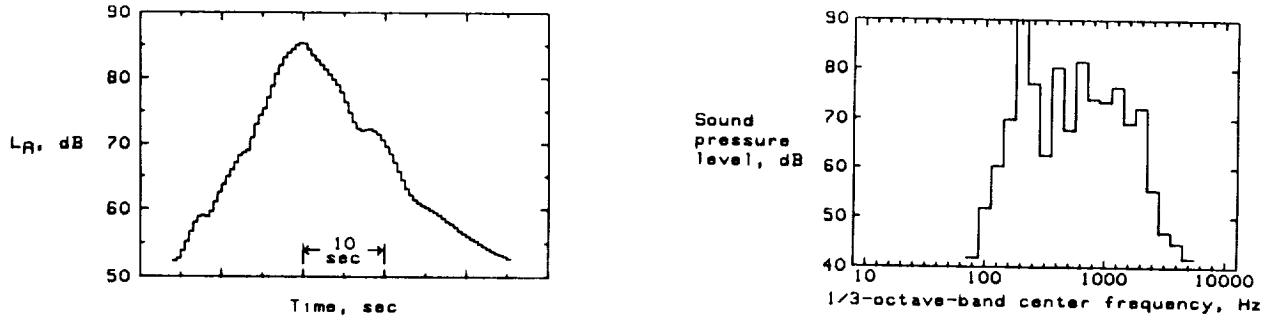

(u) $F_{of} = 225$ Hz; $F_{oa} = 202.5$ Hz; $T/N = 30$ dB.

Figure 15. Continued.

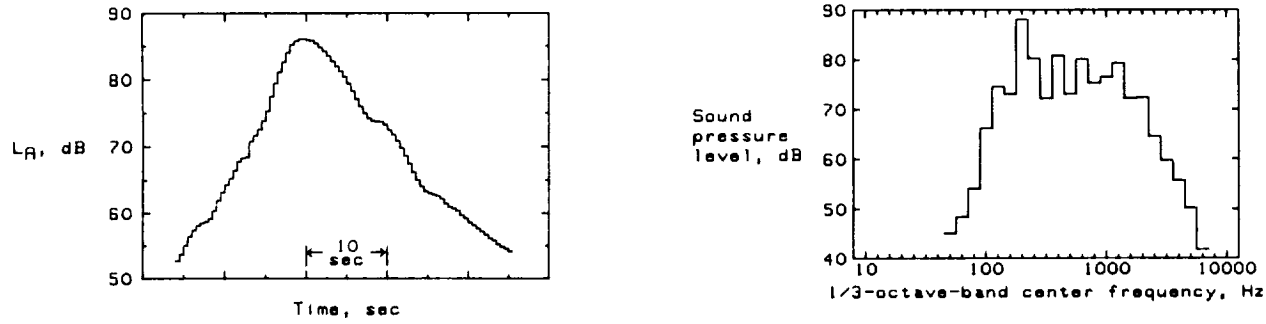

(v) $F_{of} = 247.7$ Hz; $F_{oa} = 202.5$ Hz; $T/N = 15$ dB.

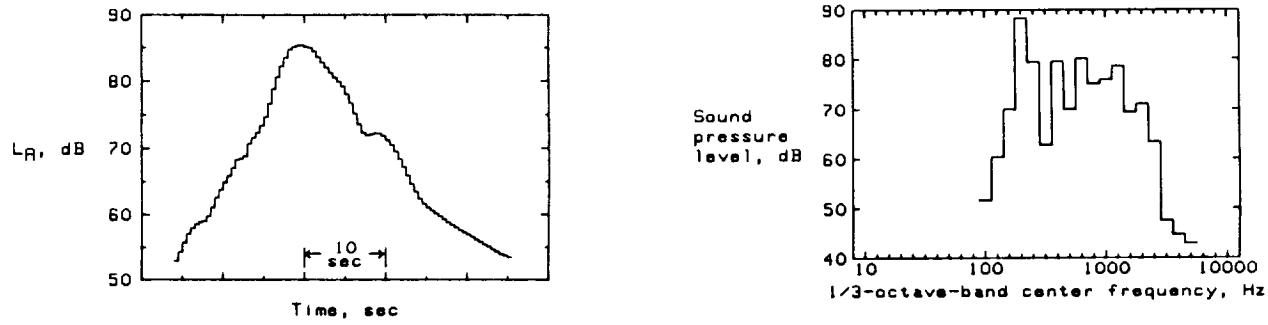

(w) $F_{of} = 247.5$ Hz; $F_{oa} = 202.5$ Hz; $T/N = 30$ dB.

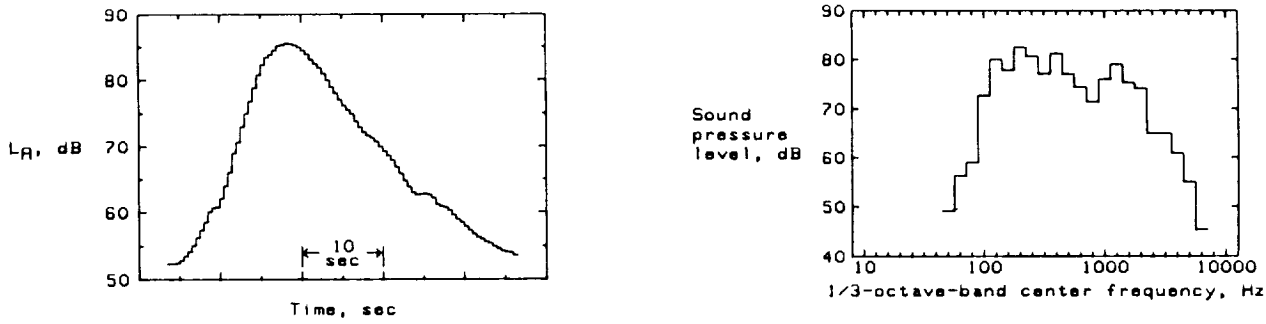

(x) $F_{of} = 247.5$ Hz; $F_{oa} = 225$ Hz; $T/N = 0$ dB.

Figure 15. Continued.

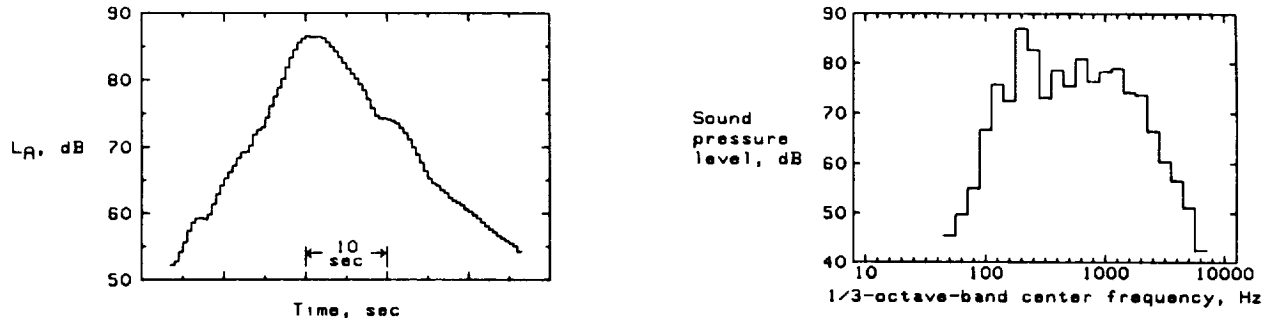

(y) $F_{of} = 247.5$ Hz; $F_{oa} = 225$ Hz; $T/N = 15$ dB.

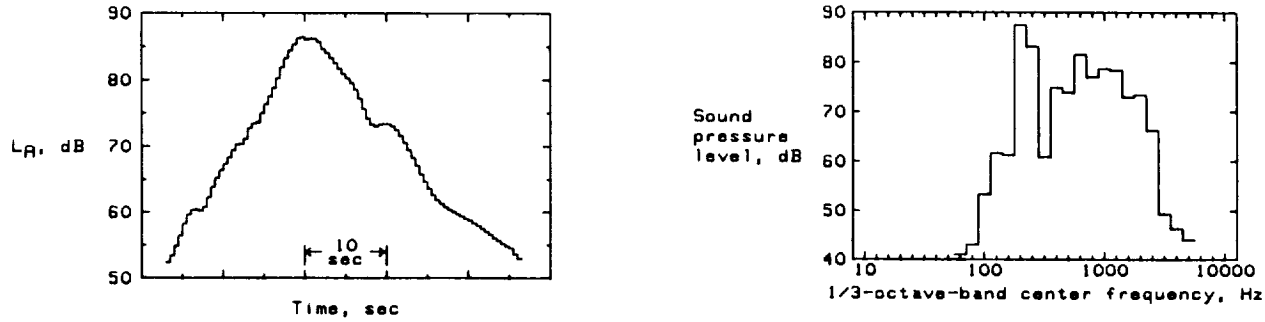

(z) $F_{of} = 247.5$ Hz; $F_{oa} = 225$ Hz; $T/N = 30$ dB.

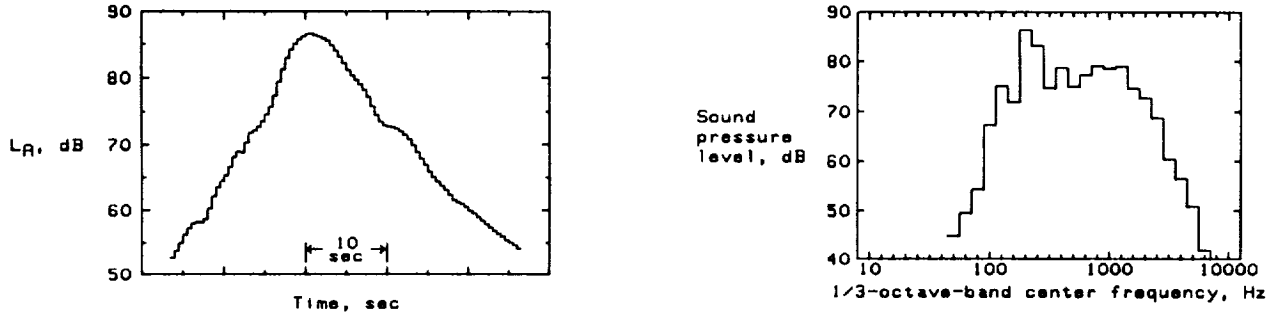

(aa) $F_{of} = 270$ Hz; $F_{oa} = 225$ Hz; $T/N = 15$ dB.

Figure 15. Continued.

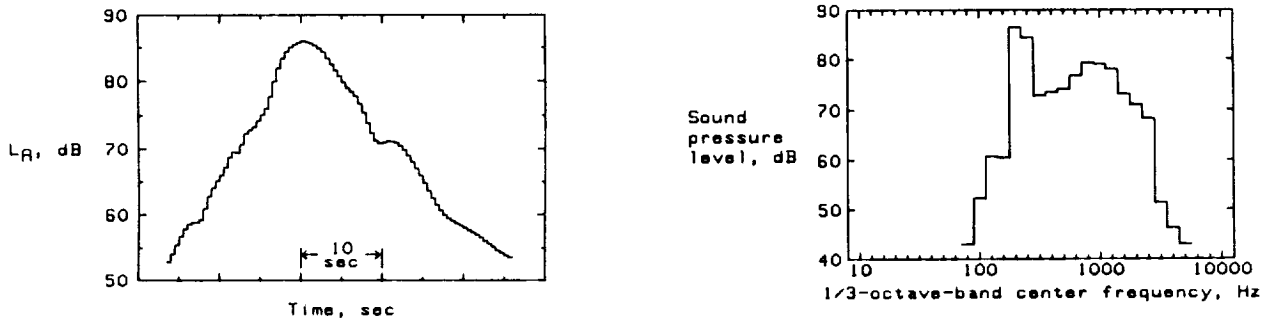

(bb) $F_{of} = 270$ Hz; $F_{oa} = 225$ Hz; $T/N = 30$ dB.

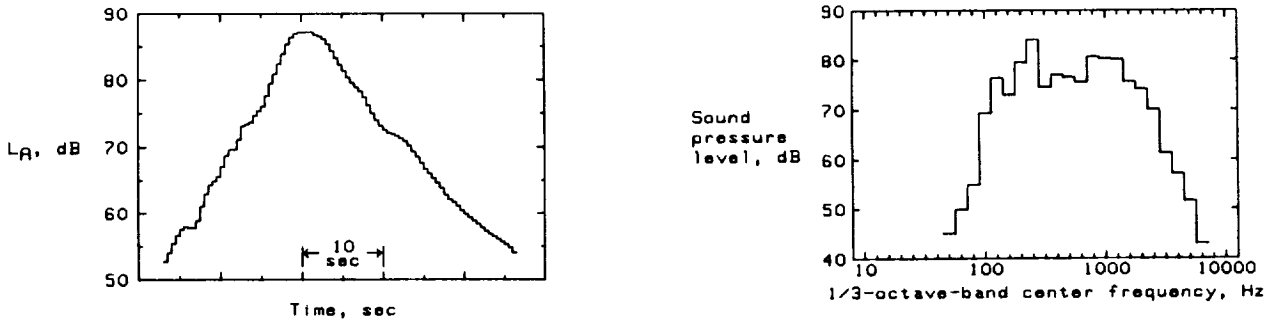

(cc) $F_{of} = 270$ Hz; $F_{oa} = 247.5$ Hz; $T/N = 15$ dB.

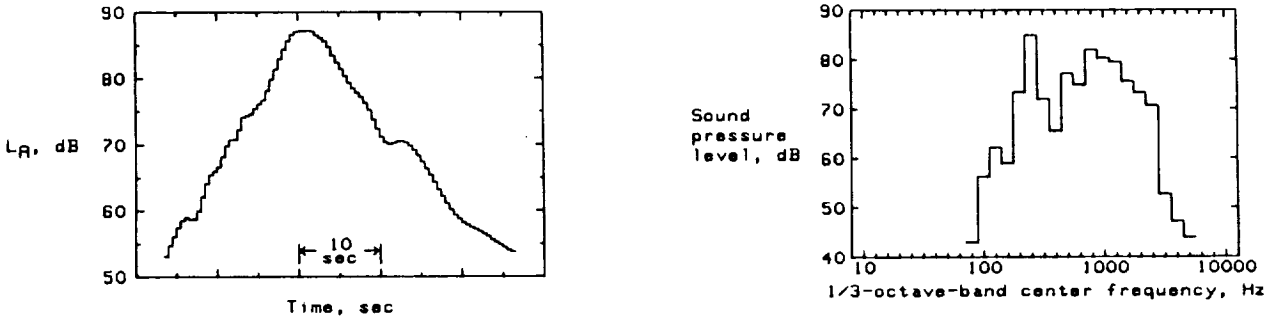

(dd) $F_{of} = 270$ Hz; $F_{oa} = 247.5$ Hz; $T/N = 30$ dB.

Figure 15. Continued.

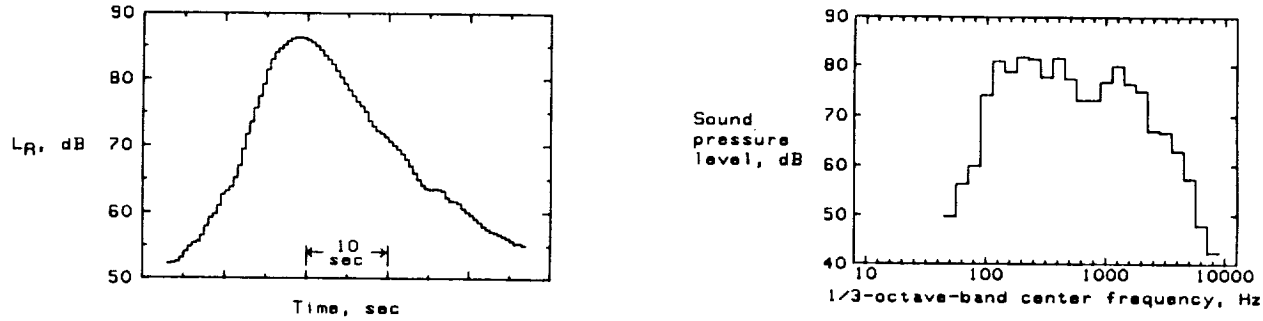

(ee) $F_{of} = 292.5$ Hz; $F_{oa} = 247.5$ Hz; $T/N = 0$ dB.

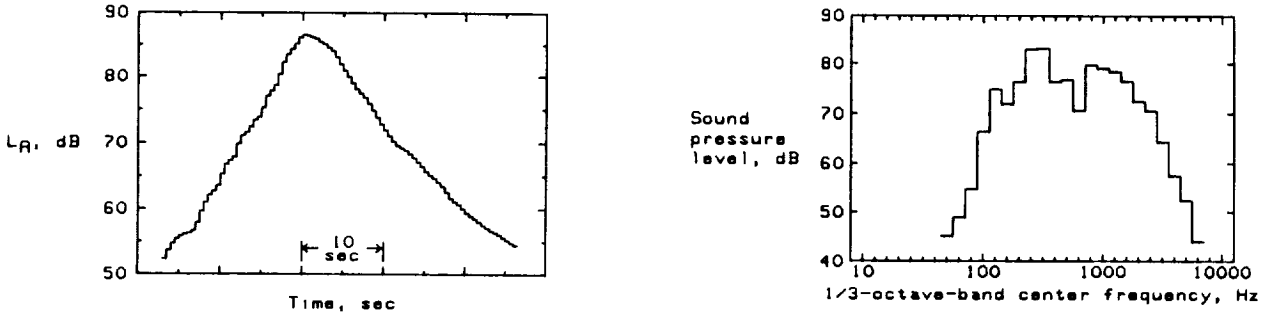

(ff) $F_{of} = 292.5$ Hz; $F_{oa} = 247.5$ Hz; $T/N = 15$ dB.

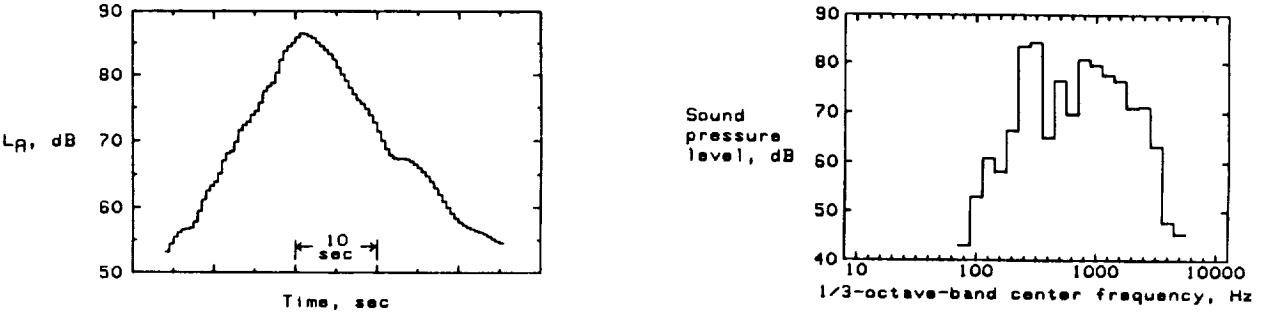

(gg) $F_{of} = 292.5$ Hz; $F_{oa} = 247.5$ Hz; $T/N = 30$ dB.

Figure 15. Continued.

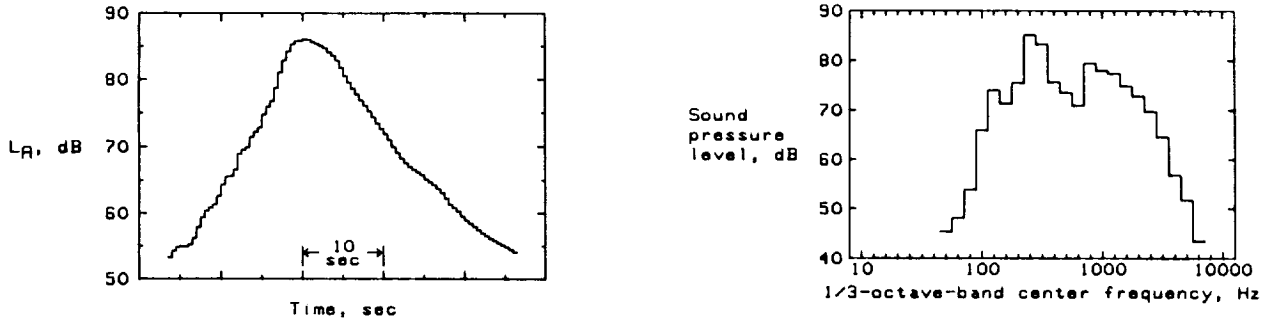

(hh) $F_{of} = 292.5$ Hz; $F_{oa} = 270$ Hz; $T/N = 15$ dB.

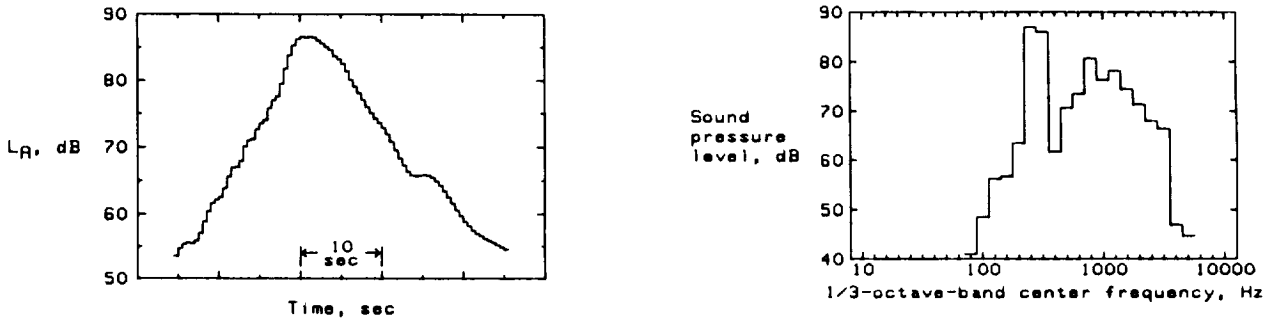

(ii) $F_{of} = 292.5$ Hz; $F_{oa} = 270$ Hz; $T/N = 30$ dB.

Figure 15. Concluded.

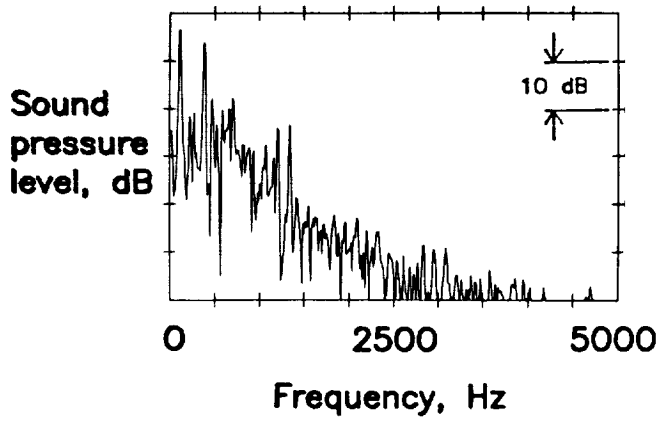

(a) F_{of} = 135 Hz; F_{oa} = 112.5 Hz.

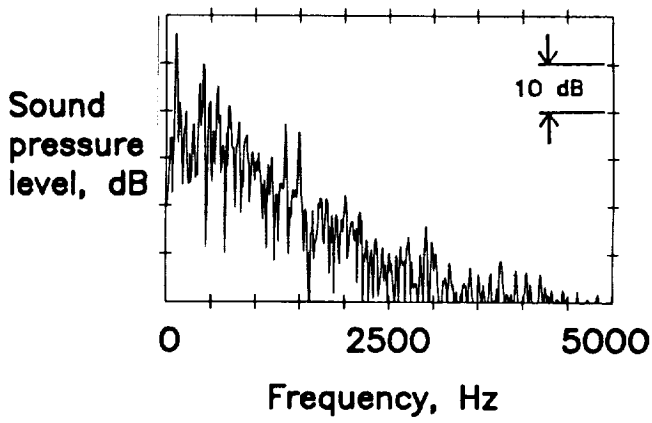

(b) F_{of} = 157.5 Hz; F_{oa} = 112.5 Hz.

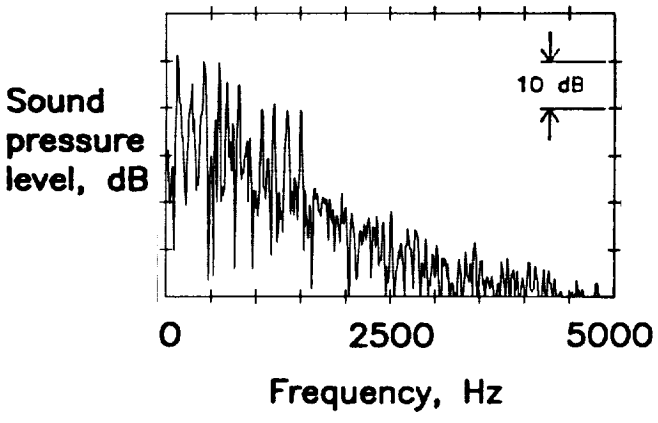

(c) F_{of} = 157.5 Hz; F_{oa} = 135 Hz.

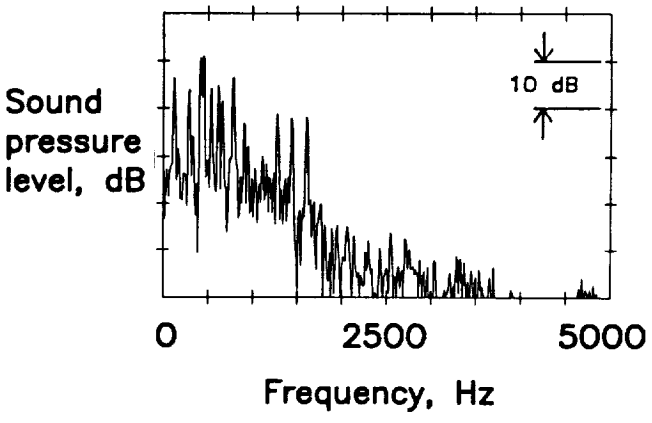

(d) F_{of} = 180 Hz; F_{oa} = 135 Hz.

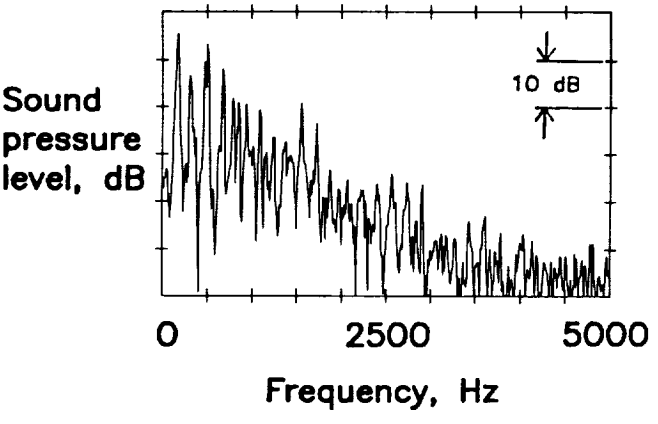

(e) F_{of} = 180 Hz; F_{oa} = 157.5 Hz.

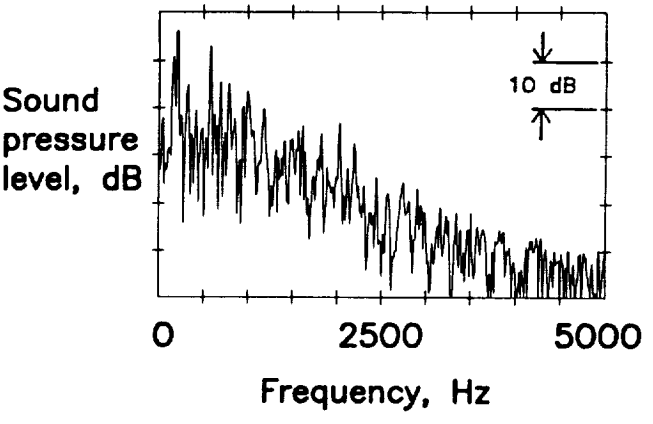

(f) F_{of} = 202.5 Hz; F_{oa} = 157.5 Hz.

Figure 16. Narrowband spectrum of each advanced turboprop flyover noise with 30-dB tone-to-broadband noise ratio in second experiment.

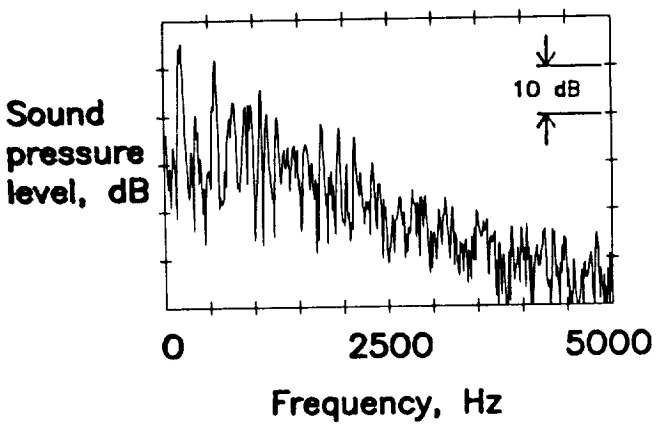

(g) $F_{of} = 202.5$ Hz; $F_{oa} = 180$ Hz.

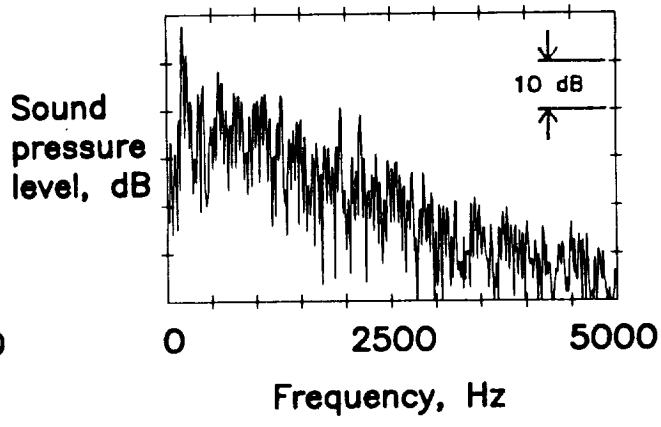

(h) $F_{of} = 225$ Hz; $F_{oa} = 180$ Hz.

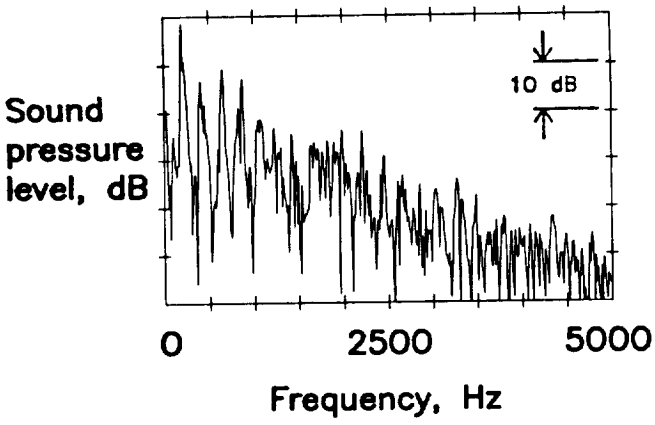

(i) $F_{of} = 225$ Hz; $F_{oa} = 202.5$ Hz.

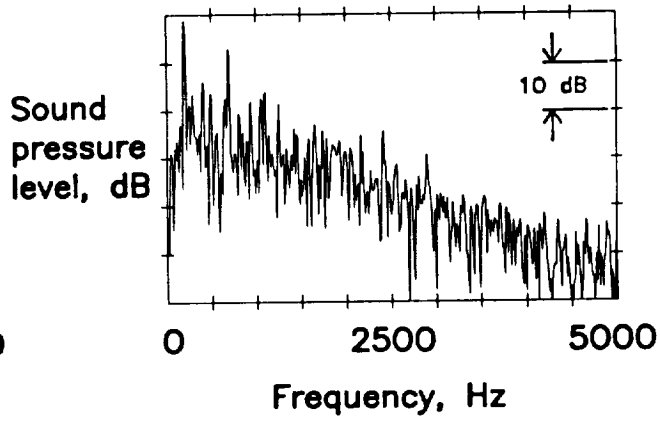

(j) $F_{of} = 247.5$ Hz; $F_{oa} = 202.5$ Hz.

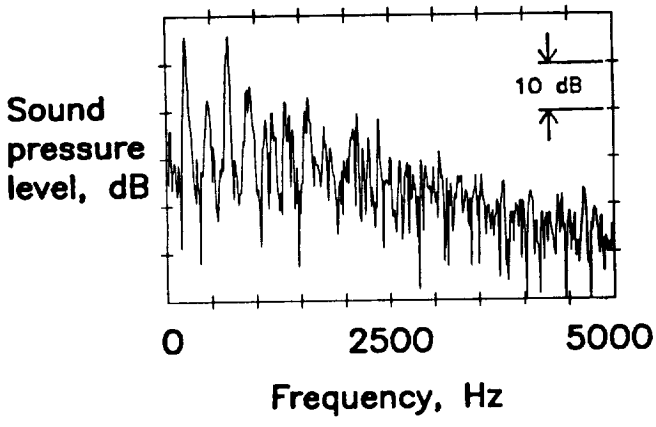

(k) $F_{of} = 247.5$ Hz; $F_{oa} = 225$ Hz.

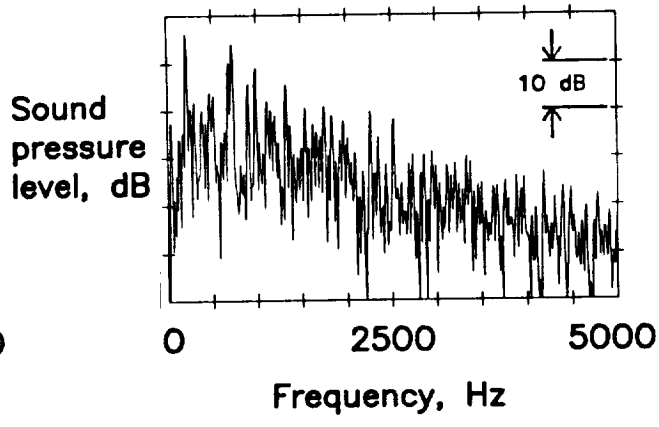

(l) $F_{of} = 270$ Hz; $F_{oa} = 225$ Hz.

Figure 16. Continued.

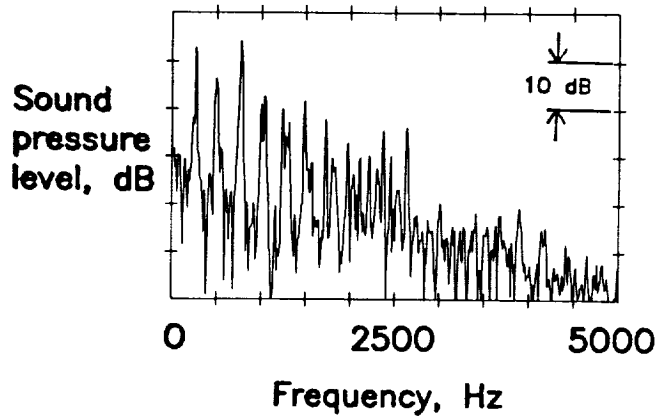

(m) $F_{of} = 270$ Hz; $F_{oa} = 247.5$ Hz.

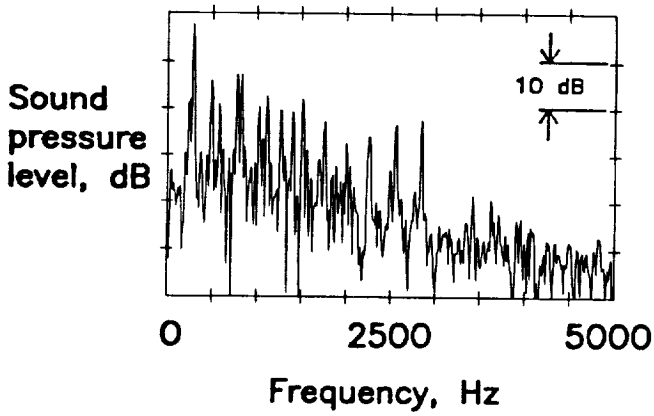

(n) $F_{of} = 292.5$ Hz; $F_{oa} = 247.5$ Hz.

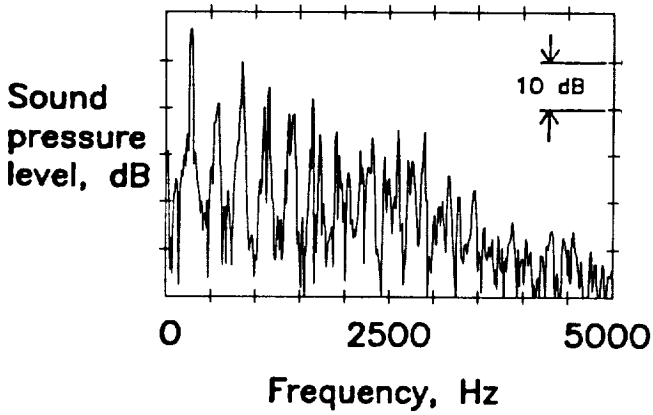

(o) $F_{of} = 292.5$ Hz; $F_{oa} = 270$ Hz.

Figure 16. Concluded.

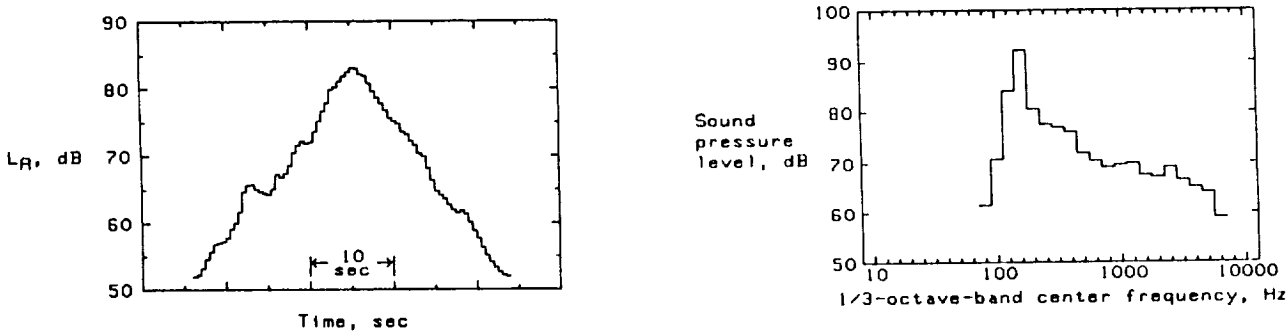

(a) de Havilland Canada DHC-7 Dash 7 takeoff.

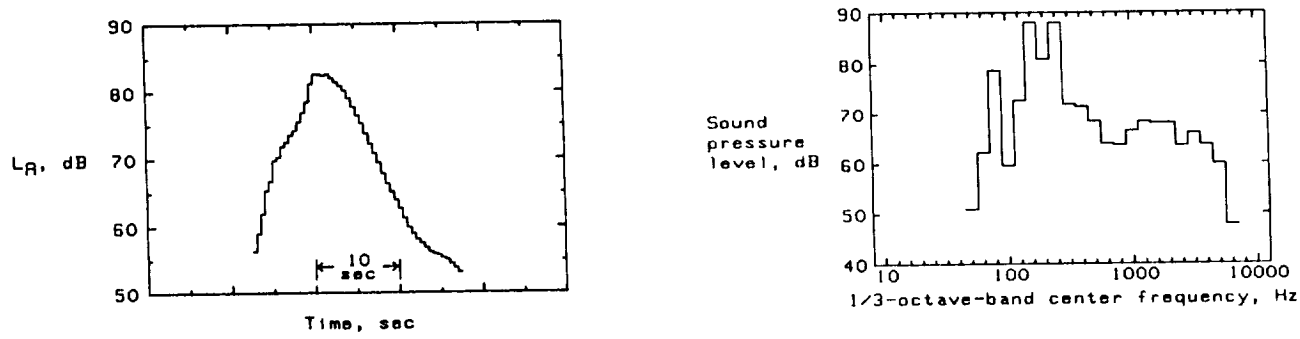

(b) Lockheed P-3 takeoff.

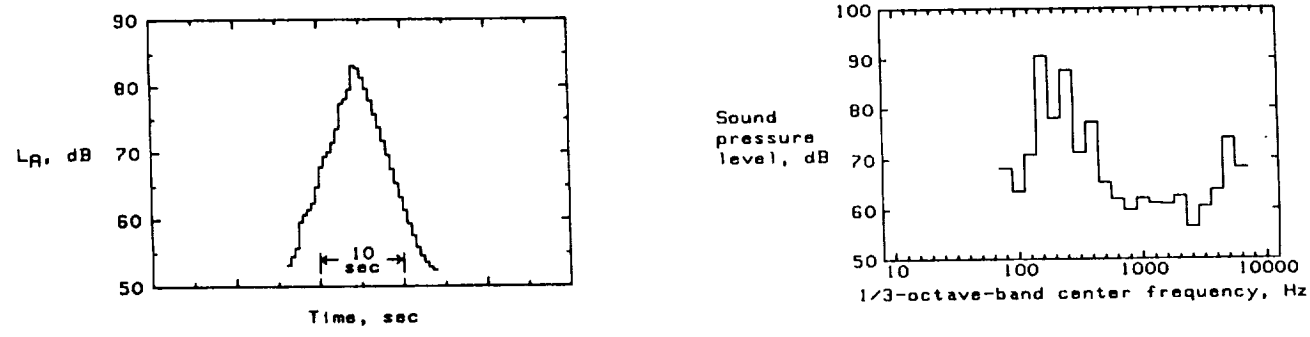

(c) NAMC YS-11 takeoff.

Figure 17. L_A time histories and 1/3-octave-band spectra at peak L_A of highest level presentations of takeoffs of conventional turboprop and turbofan aircraft.

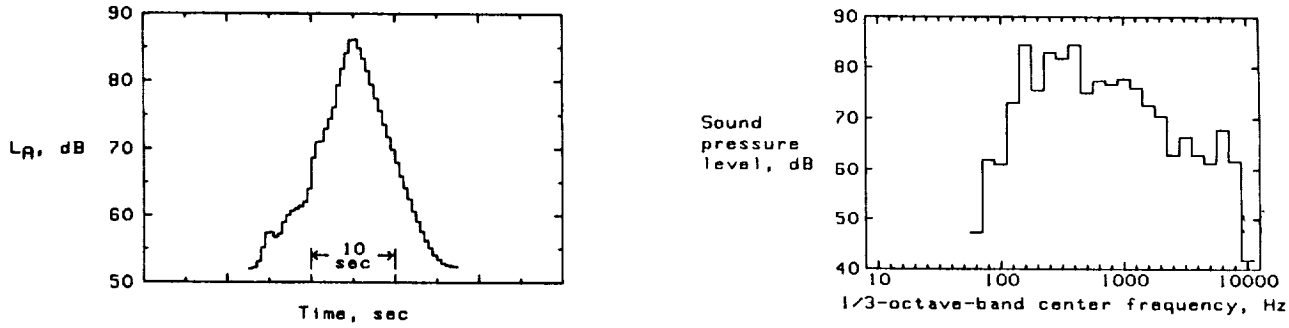

(d) Nord 262 takeoff.

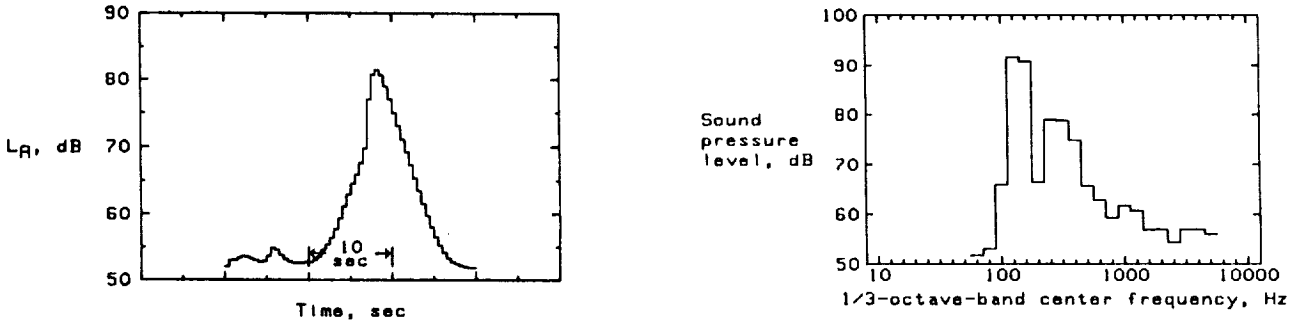

(e) Shorts 330 takeoff.

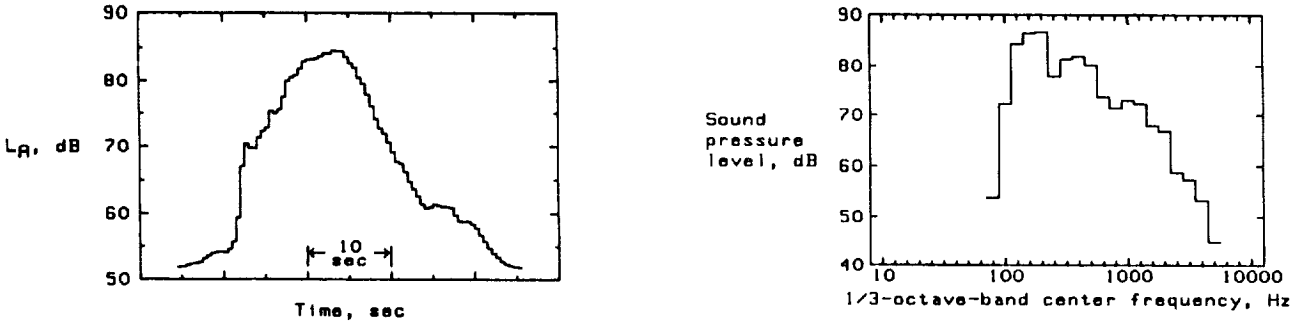

(f) Airbus Industrie A-300 takeoff.

Figure 17. Continued.

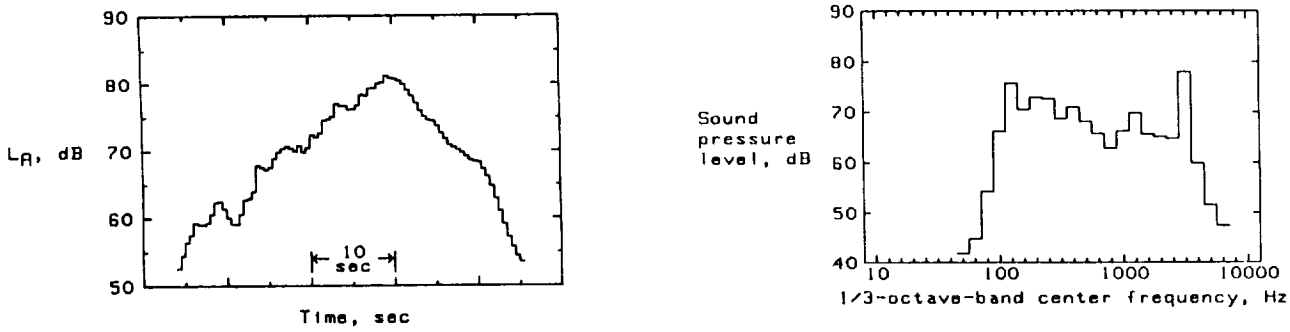

(g) Boeing 707 takeoff.

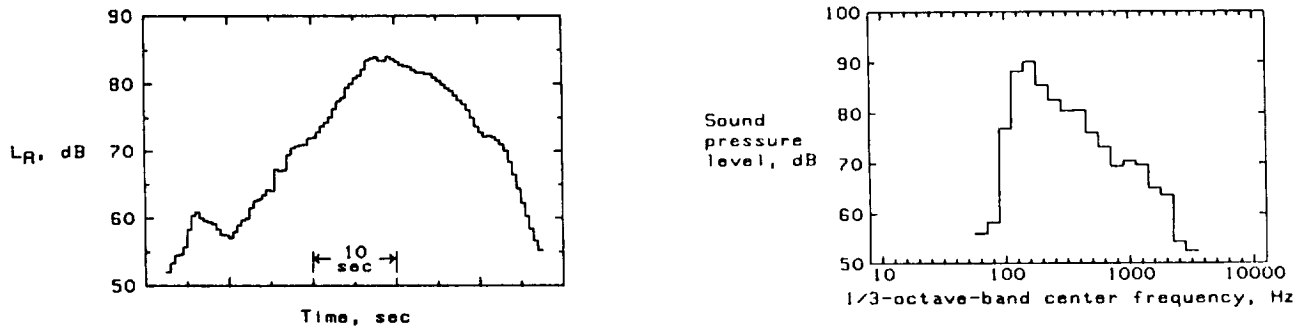

(h) Boeing 727-200 takeoff.

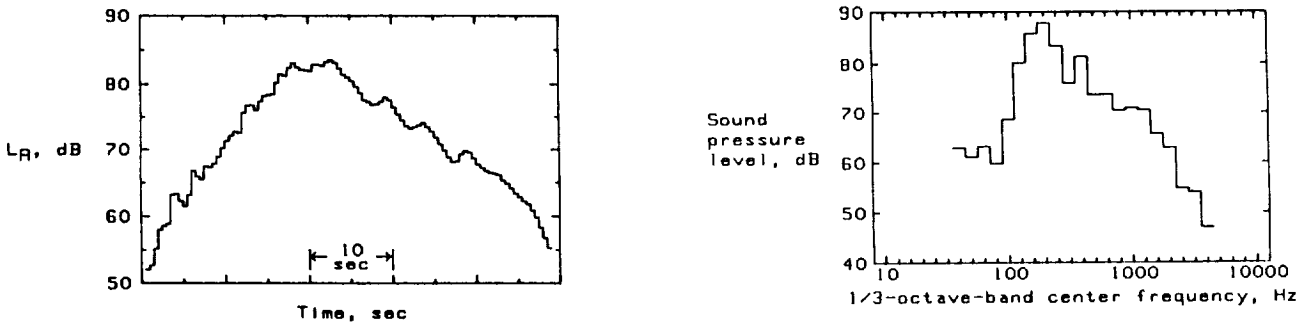

(i) McDonnell Douglas DC-9 takeoff.

Figure 17. Continued.

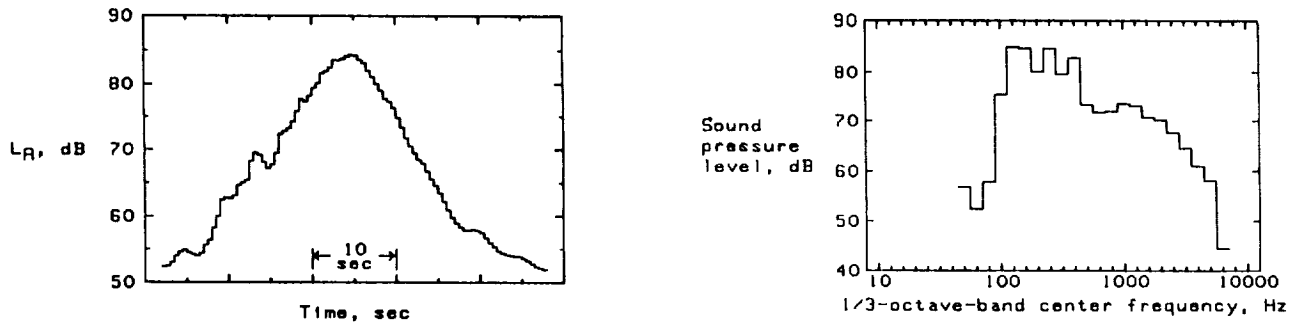

(j) McDonnell Douglas DC-10 takeoff.

Figure 17. Concluded.

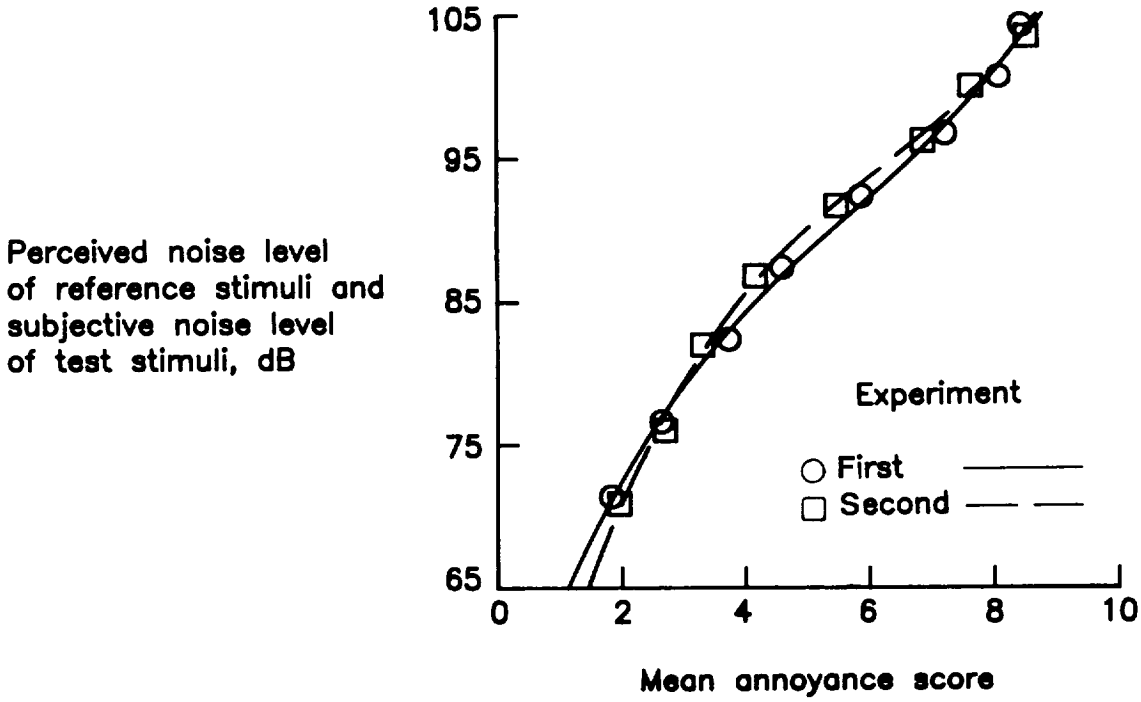

Figure 18. Regression analyses of PNL on mean annoyance scores for Boeing 727 takeoff stimuli used to convert annoyance judgments to subjective noise levels L_S.

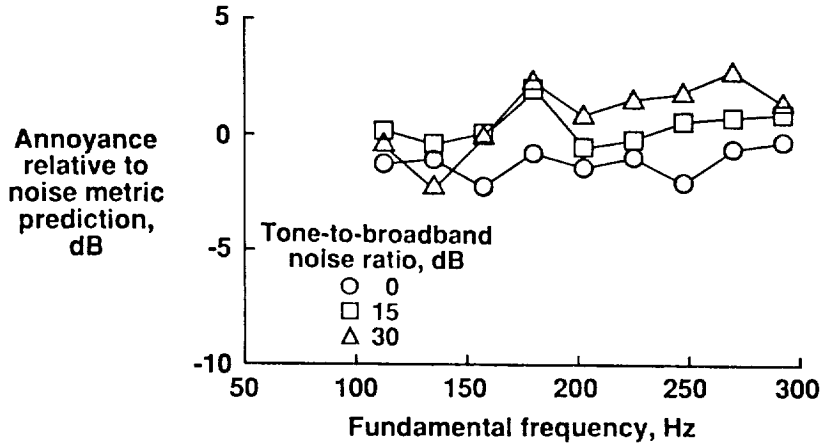

(a) L_A.

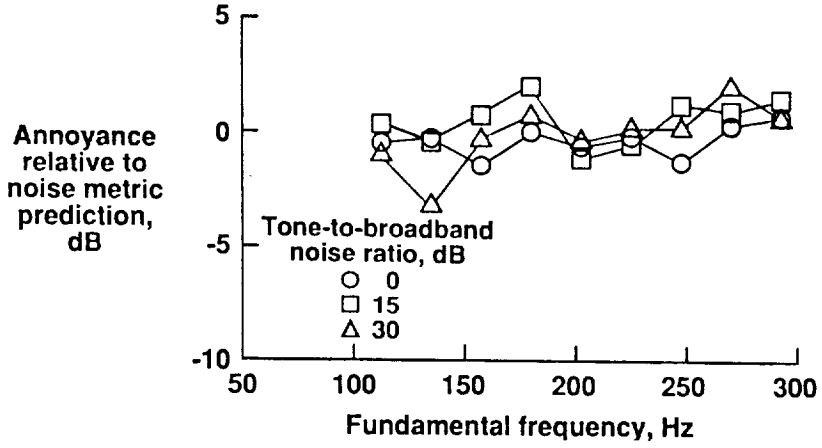

(b) L_A with T_1 tone correction.

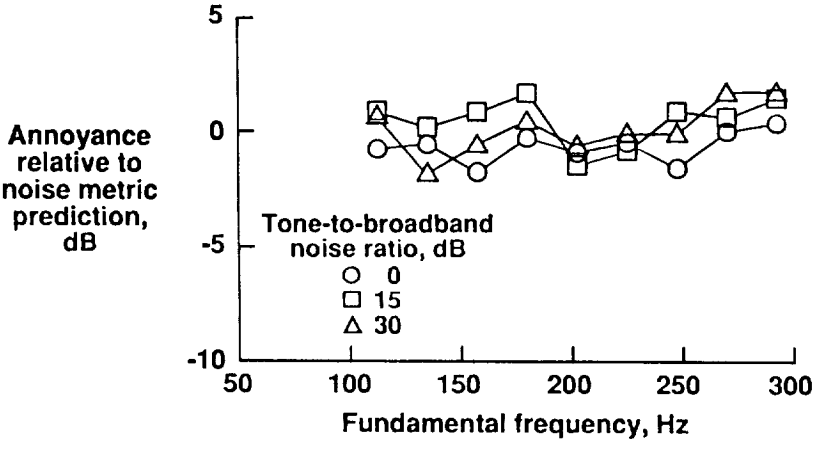

(c) L_A with T_2 tone correction.

Figure 19. Effect of interaction of fundamental frequency with tone-to-broadband noise ratio on annoyance prediction for different noise metrics in first experiment.

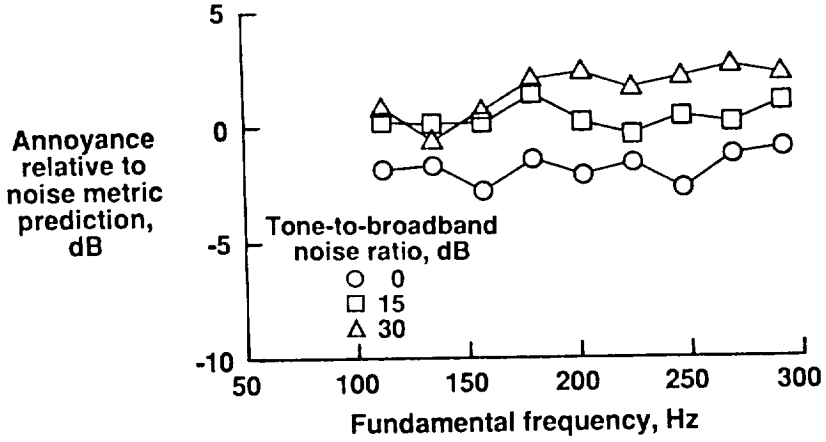

(d) Duration-corrected L_A.

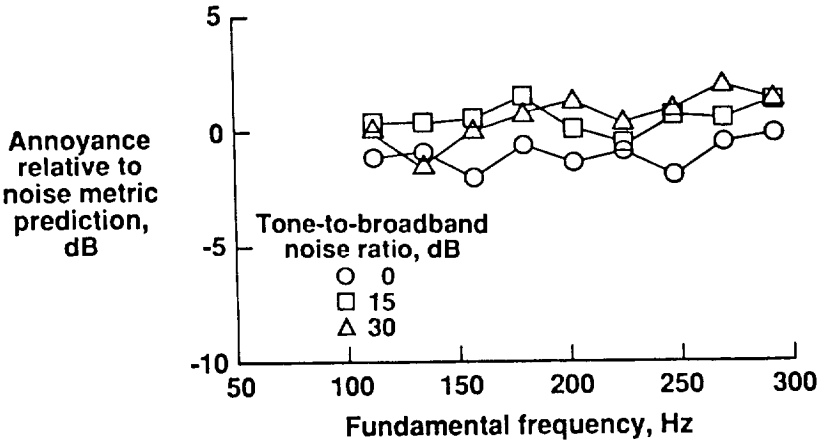

(e) Duration-corrected L_A with T_1 tone correction.

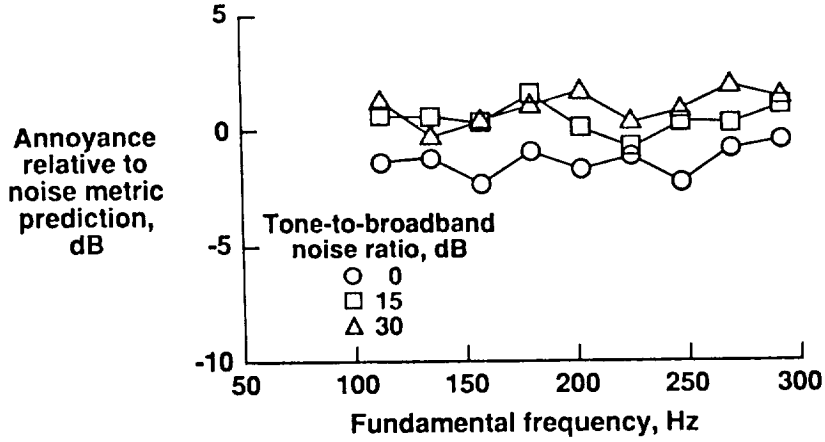

(f) Duration-corrected L_A with T_2 tone correction.

Figure 19. Continued.

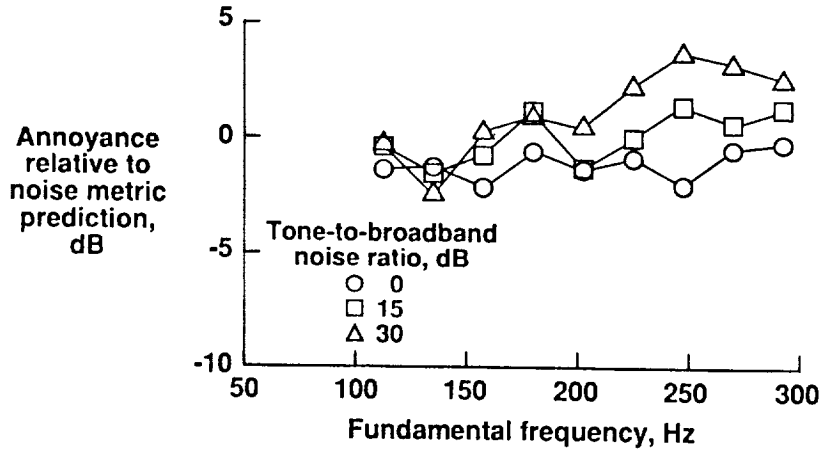

(g) PNL.

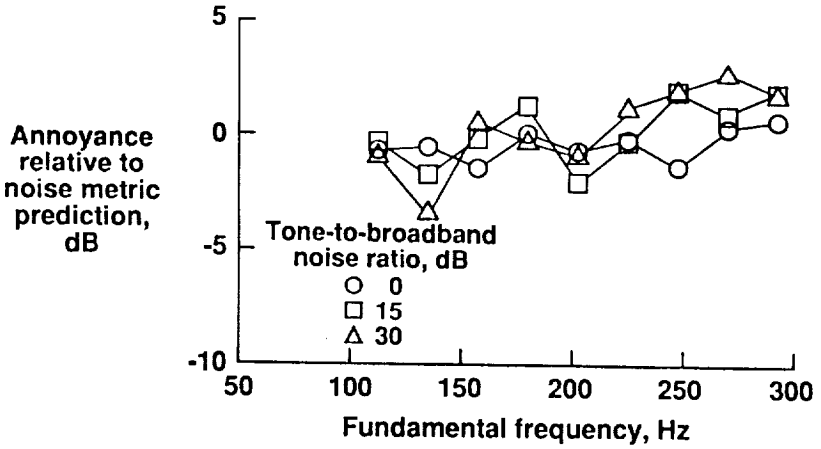

(h) PNL with T_1 tone correction.

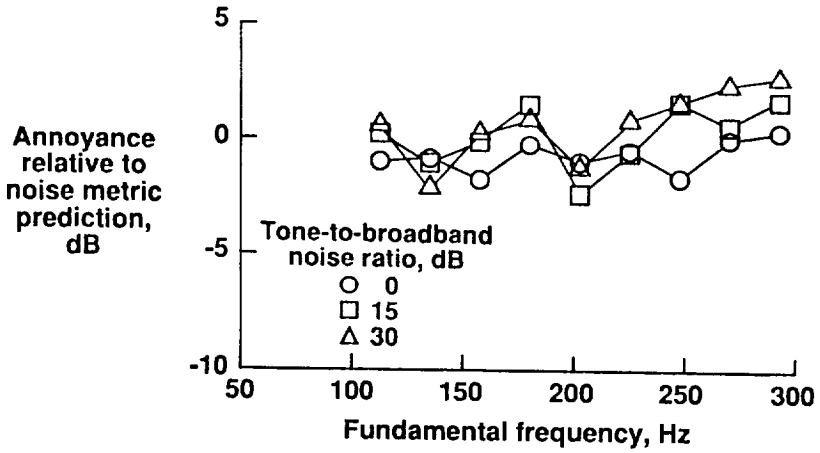

(i) PNL with T_2 tone correction.

Figure 19. Continued.

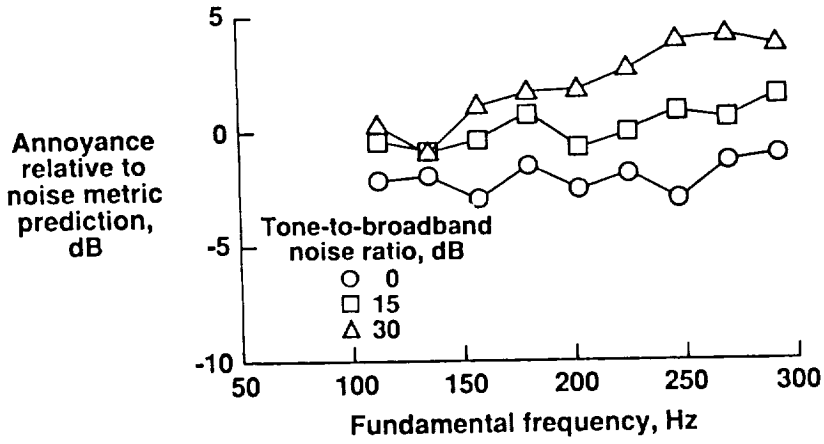

(j) Duration-corrected PNL.

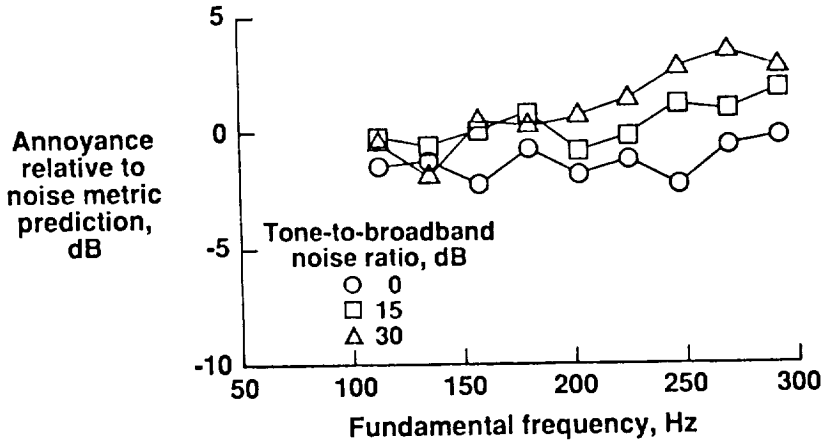

(k) Duration-corrected PNL with T_1 tone correction.

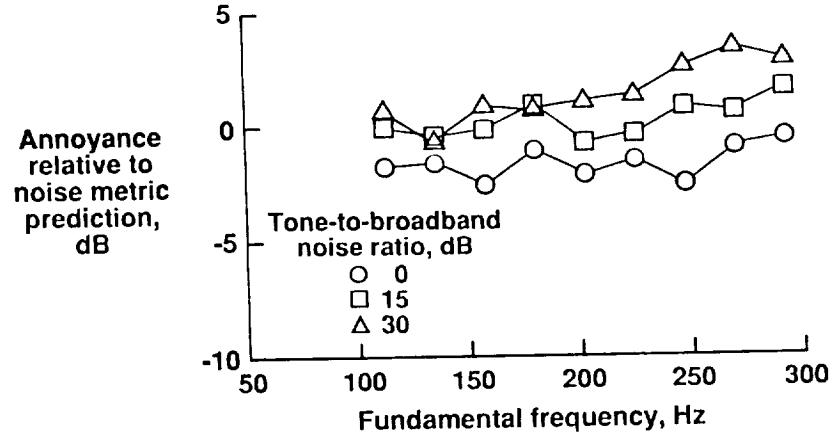

(l) Duration-corrected PNL with T_2 tone correction.

Figure 19. Continued.

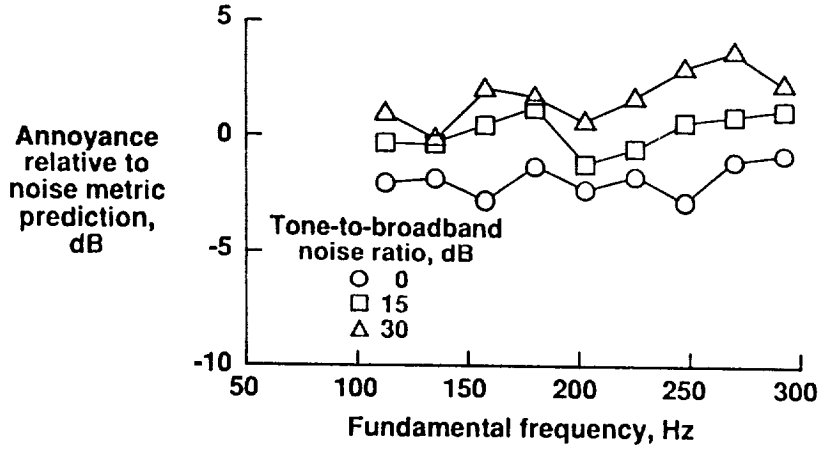

(m) LL_Z.

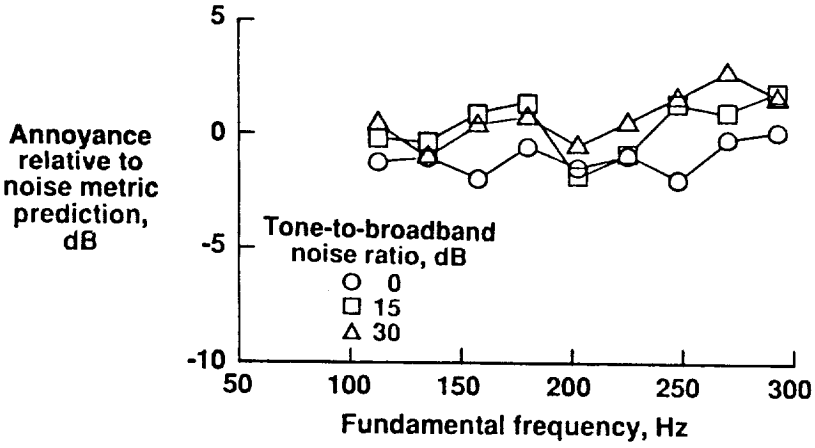

(n) LL_Z with T_1 tone correction.

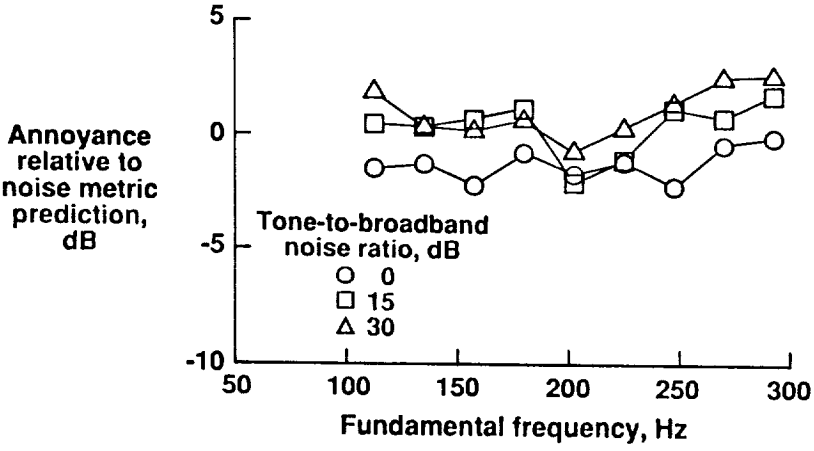

(o) LL_Z with T_2 tone correction.

Figure 19. Continued.

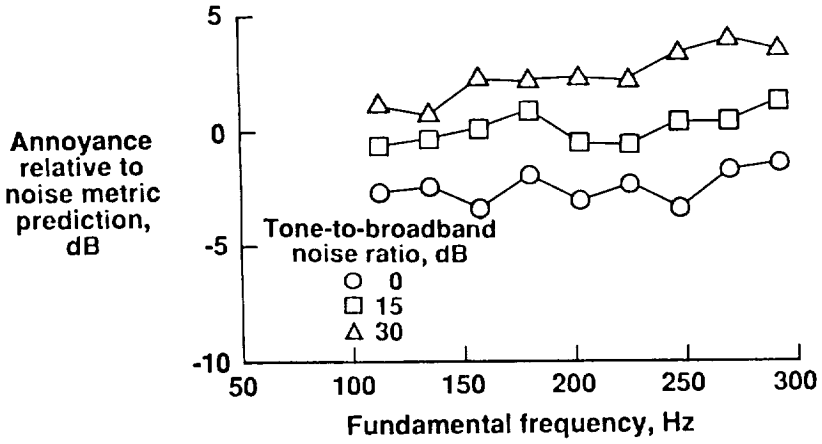

(p) Duration-corrected LL_Z.

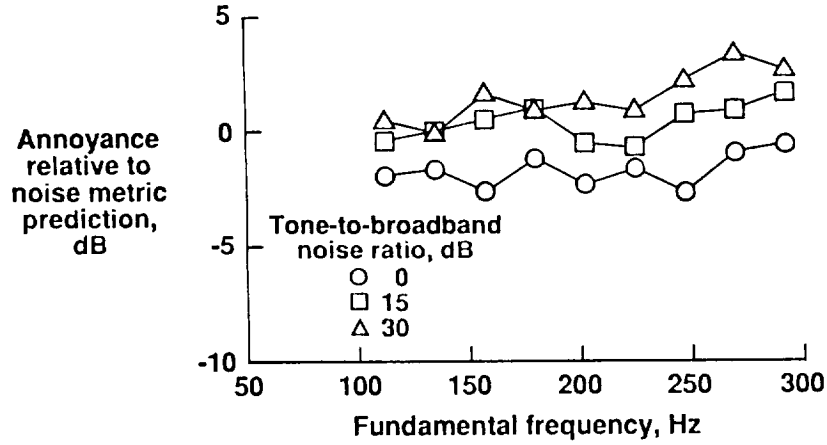

(q) Duration-corrected LL_Z with T_1 tone correction.

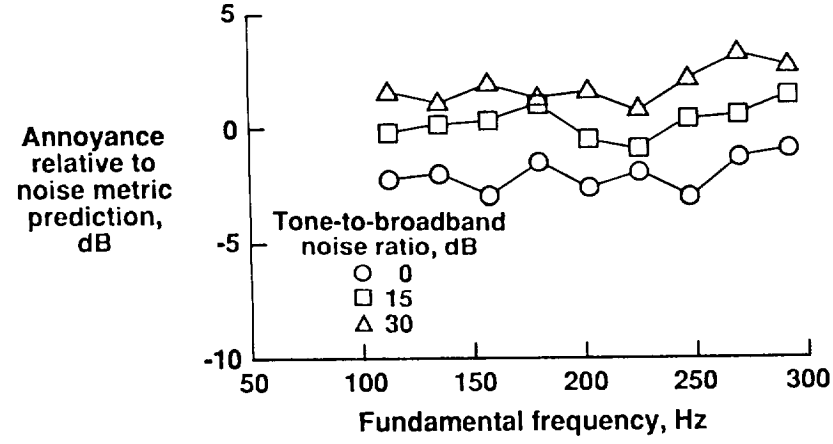

(r) Duration-corrected LL_Z with T_2 tone correction.

Figure 19. Concluded.

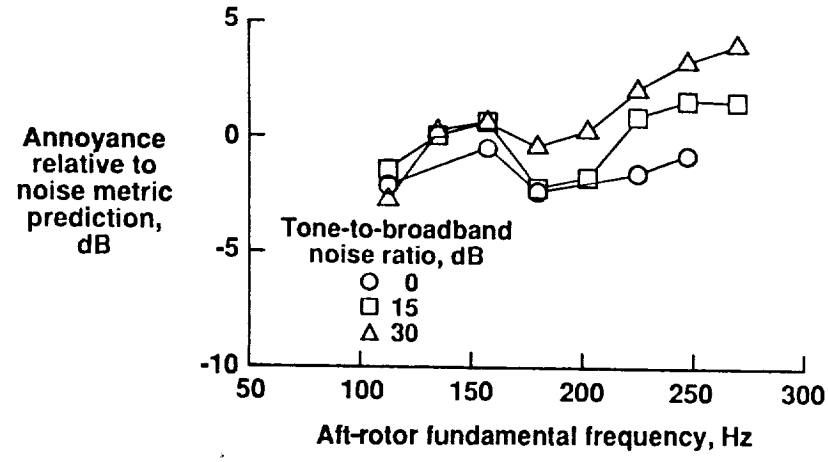

(a) L_A.

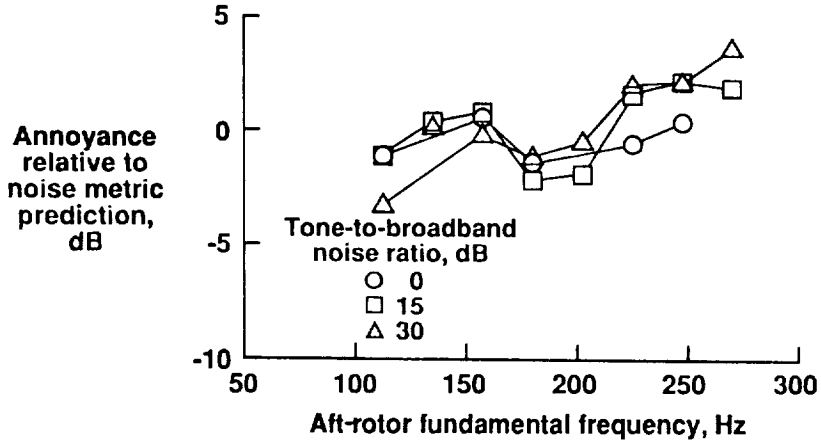

(b) L_A with T_1 tone correction.

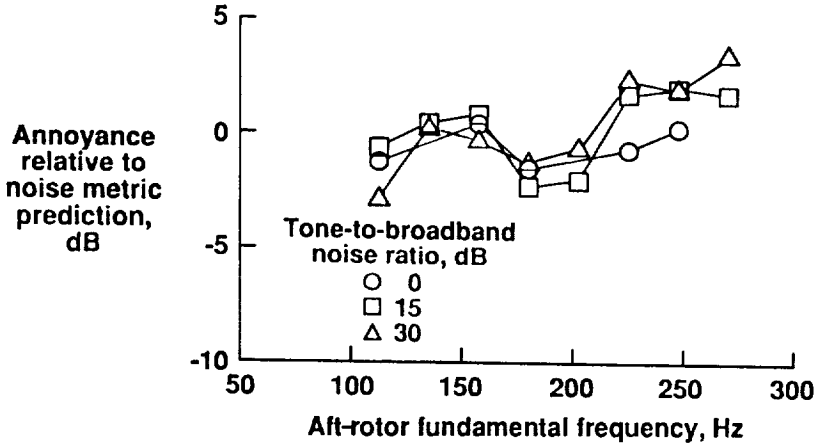

(c) L_A with T_2 tone correction.

Figure 20. Effect of interaction of aft-rotor fundamental frequency with tone-to-broadband noise ratio on annoyance prediction for different noise metrics in second experiment.

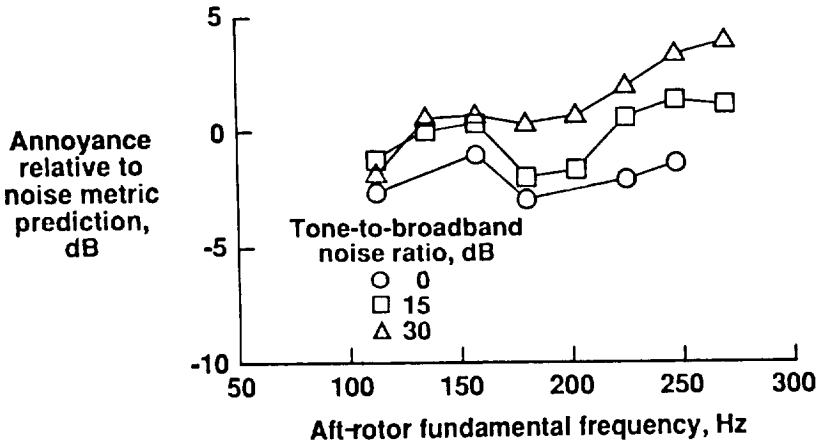

(d) Duration-corrected L_A.

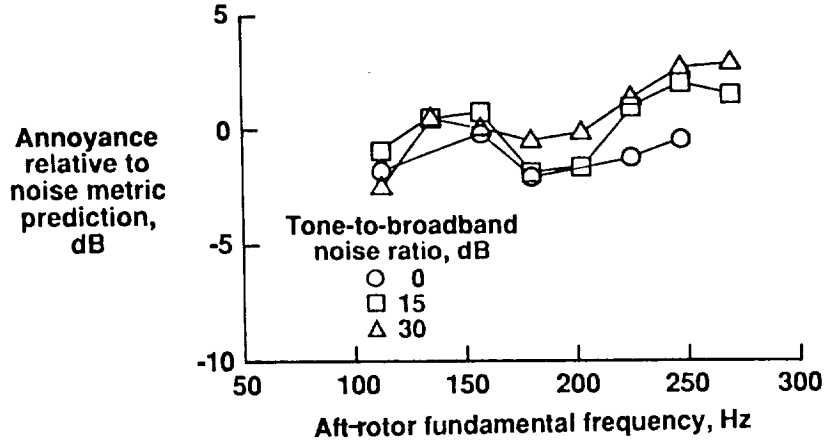

(e) Duration-corrected L_A with T_1 tone correction.

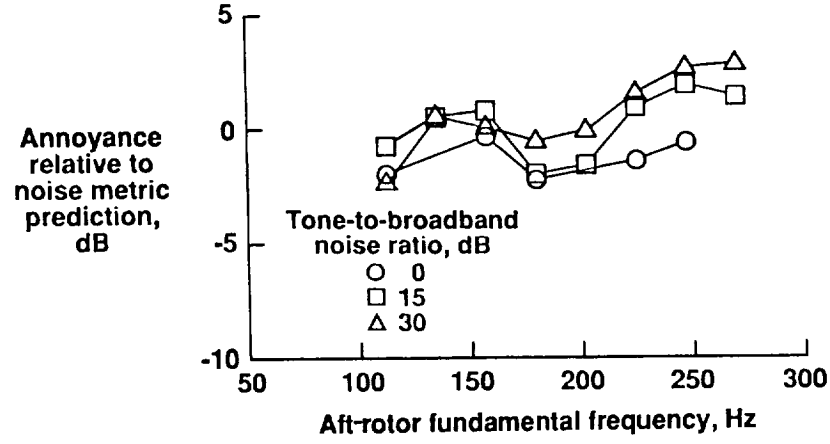

(f) Duration-corrected L_A with T_2 tone correction.

Figure 20. Continued.

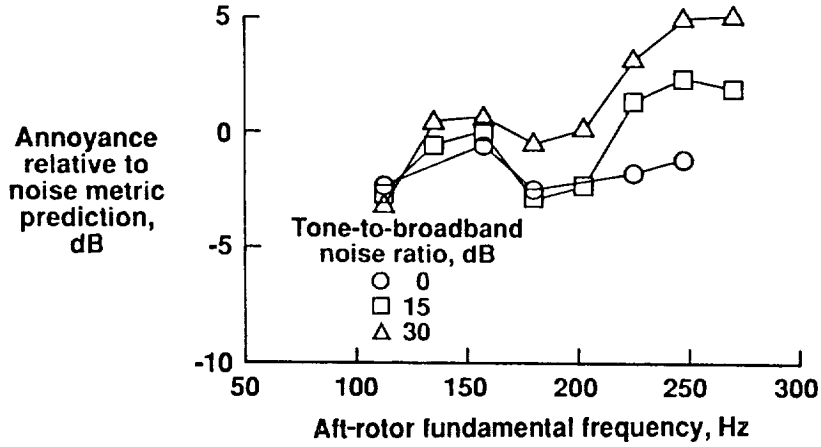

(g) PNL.

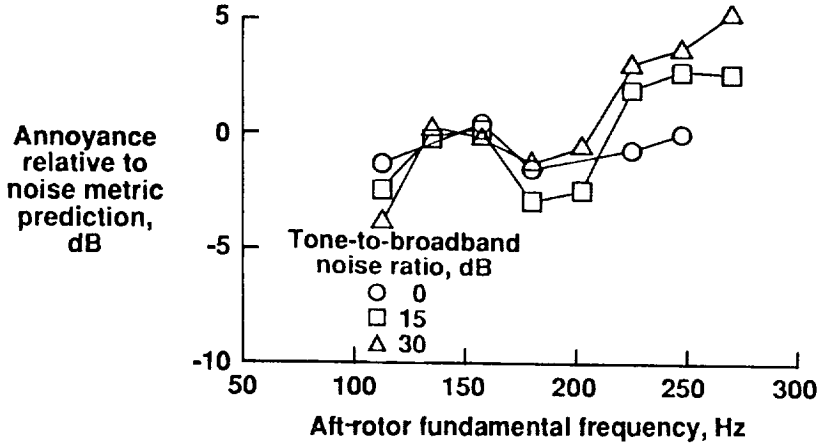

(h) PNL with T_1 tone correction.

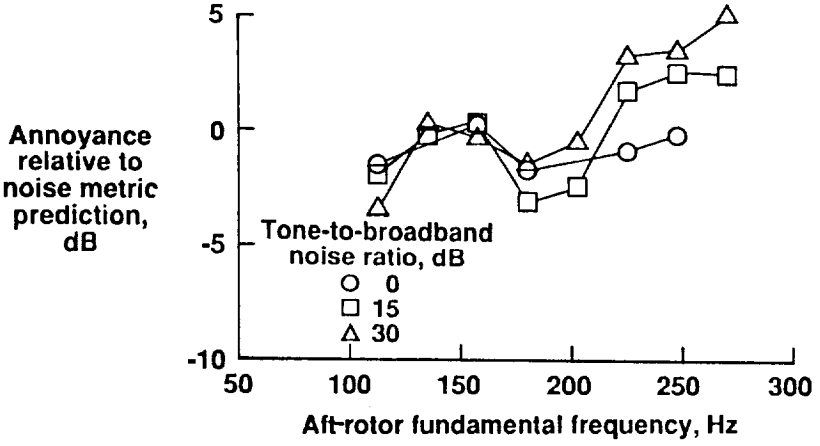

(i) PNL with T_2 tone correction.

Figure 20. Continued.

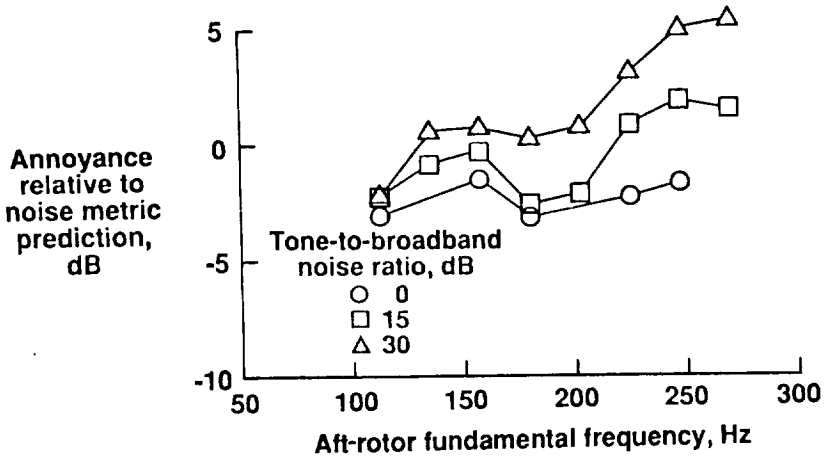

(j) Duration-corrected PNL.

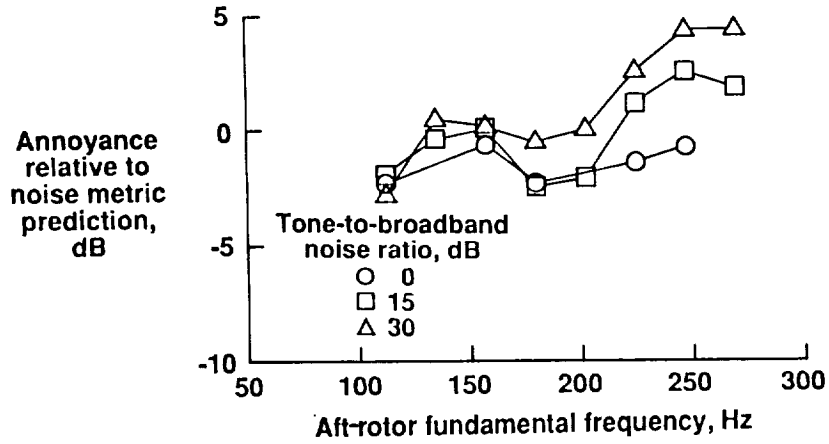

(k) Duration-corrected PNL with T_1 tone correction.

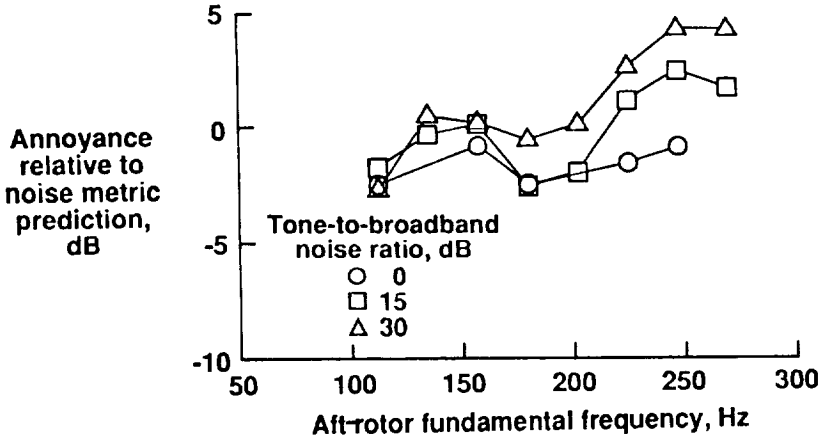

(l) Duration-corrected PNL with T_2 tone correction.

Figure 20. Continued.

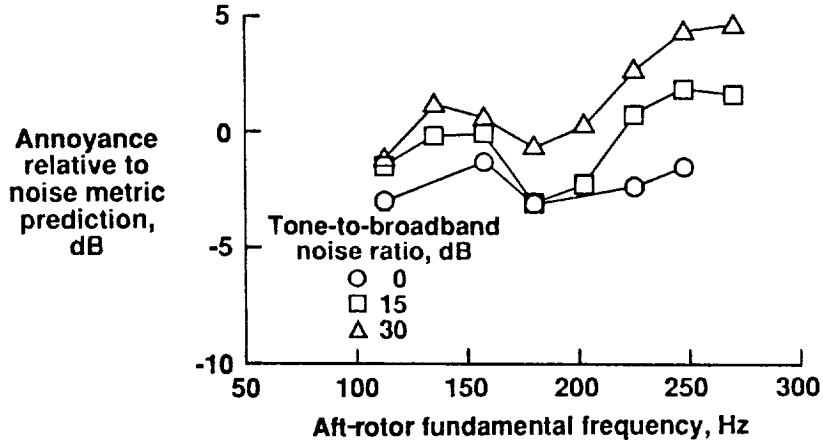

(m) LL_Z.

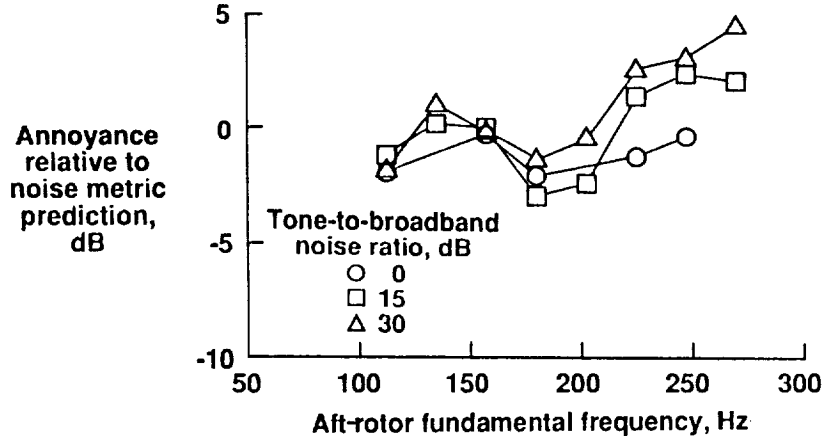

(n) LL_Z with T_1 tone correction.

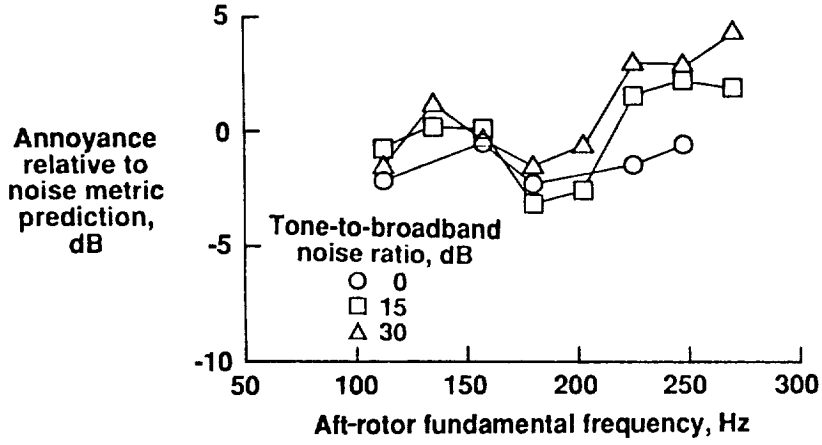

(o) LL_Z with T_2 tone correction.

Figure 20. Continued.

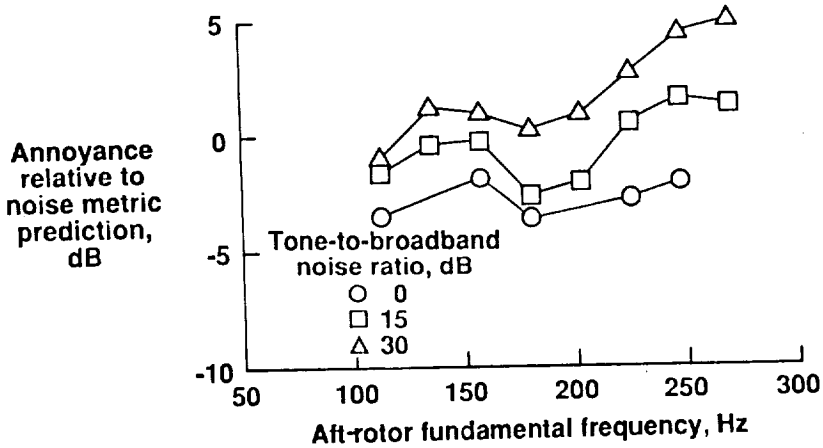

(p) Duration-corrected LL_Z.

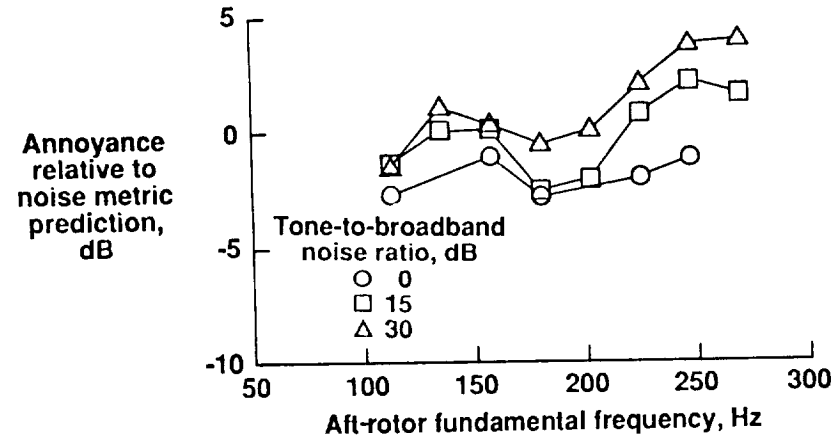

(q) Duration-corrected LL_Z with T_1 tone correction.

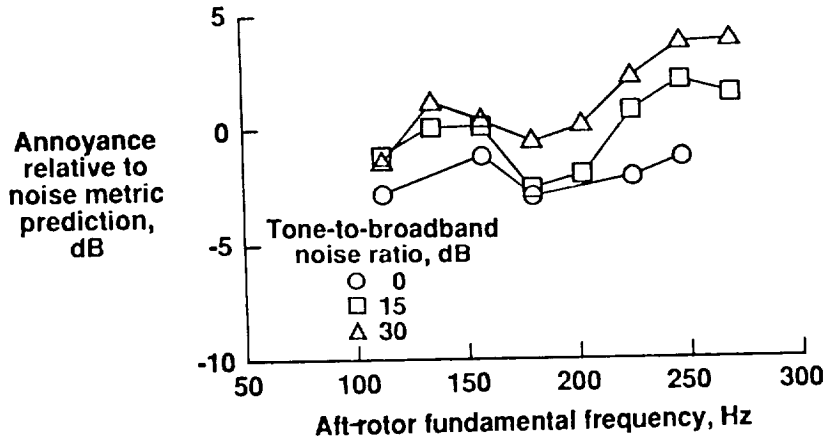

(r) Duration-corrected LL_Z with T_2 tone correction.

Figure 20. Concluded.

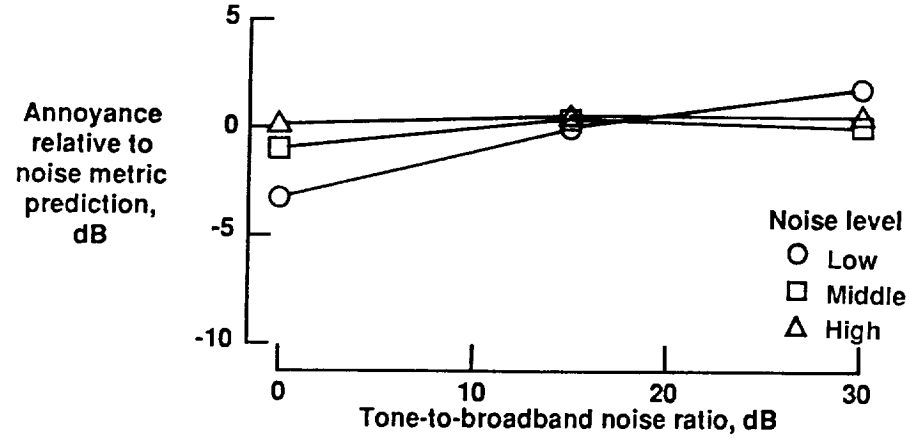

(a) L_A.

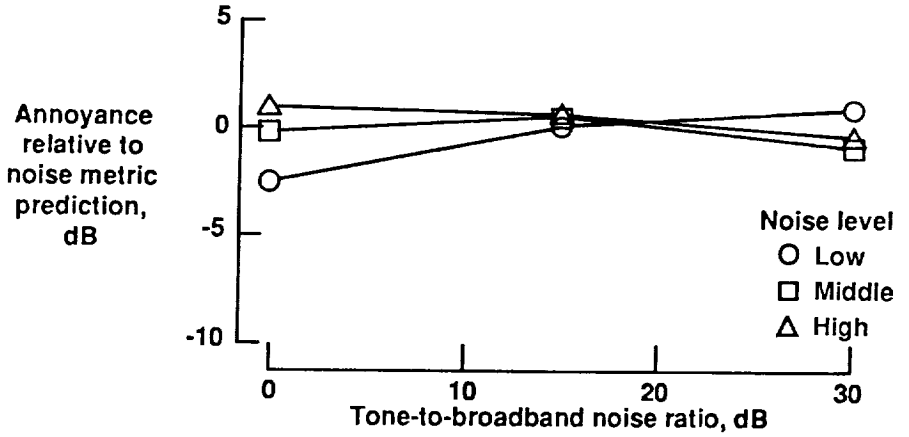

(b) L_A with T_1 tone correction.

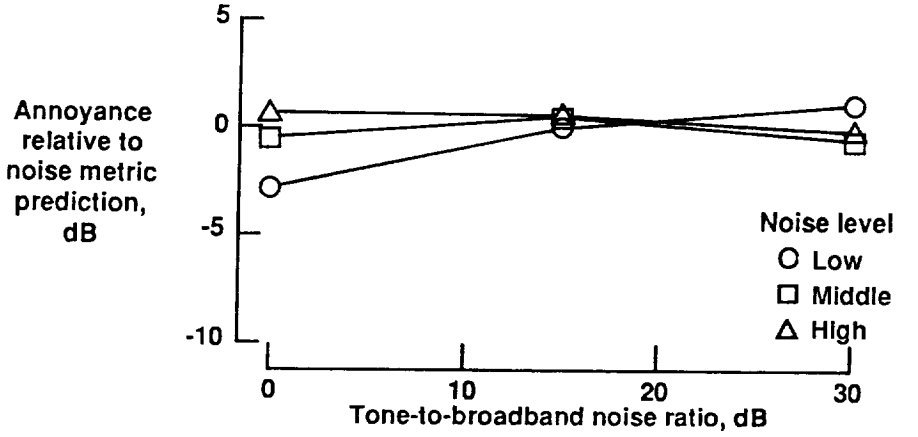

(c) L_A with T_2 tone correction.

Figure 21. Effect of interaction of tone-to-broadband noise ratio with noise level on annoyance prediction for different noise metrics in first experiment.

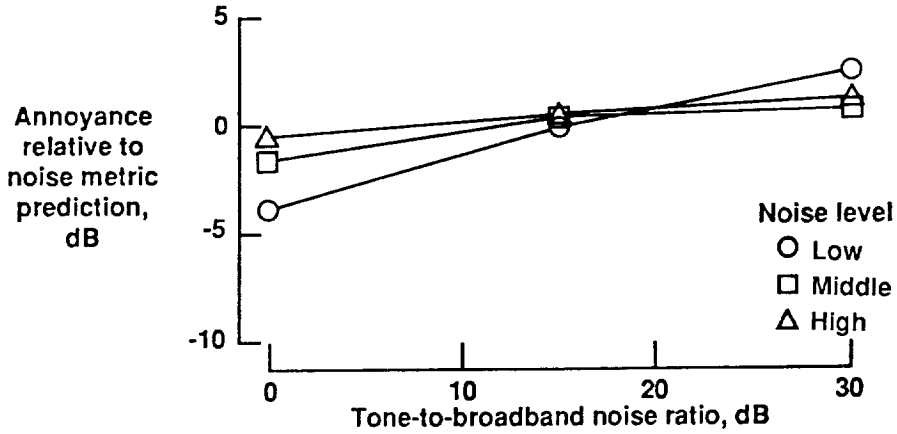

(d) Duration-corrected L_A.

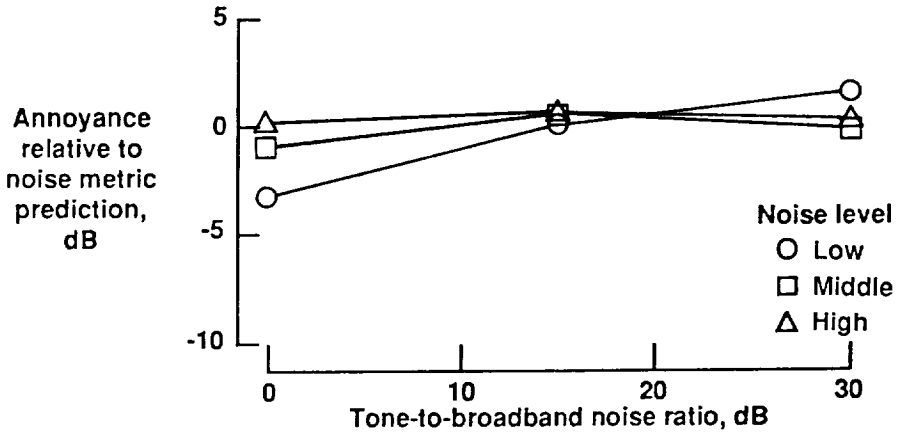

(e) Duration-corrected L_A with T_1 tone correction.

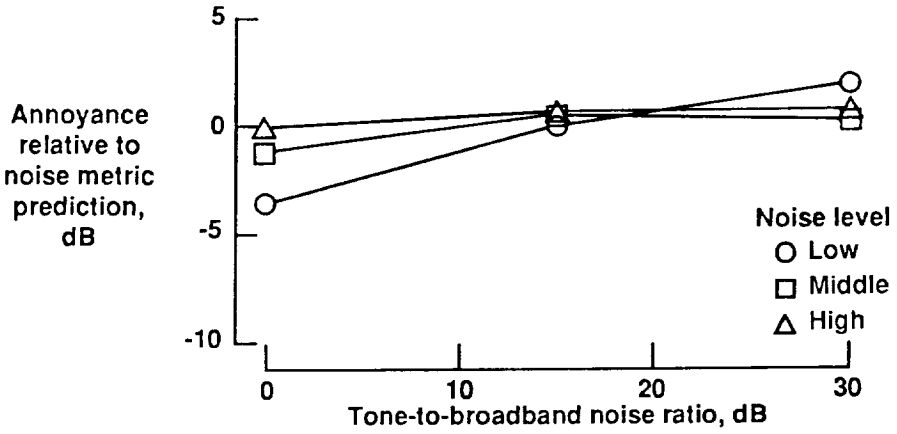

(f) Duration-corrected L_A with T_2 tone correction.

Figure 21. Continued.

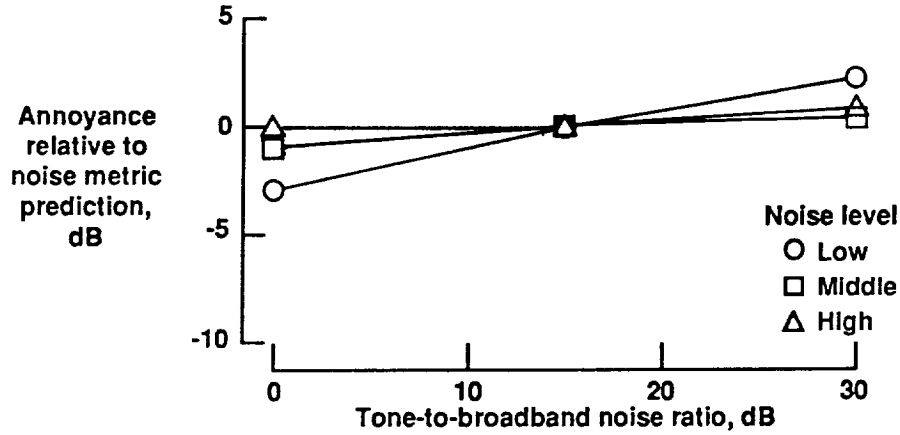

(g) PNL.

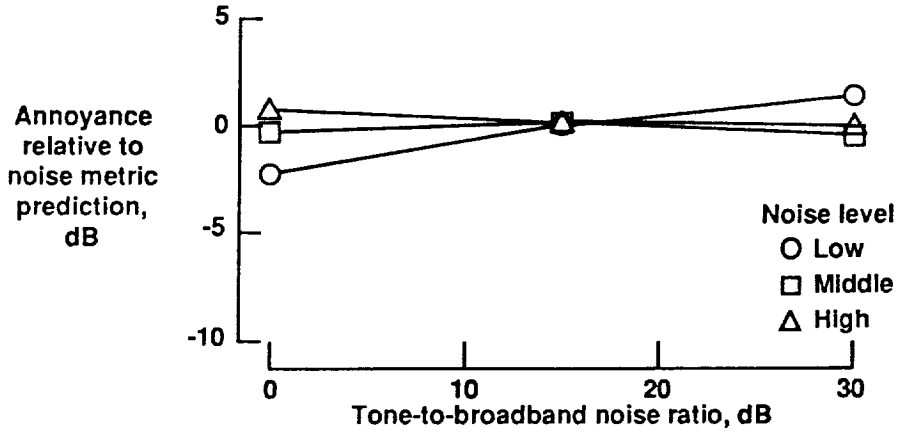

(h) PNL with T_1 tone correction.

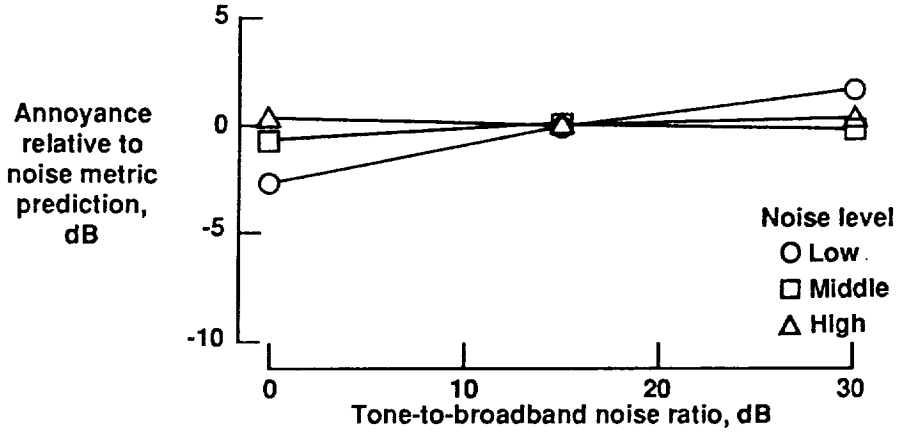

(i) PNL with T_2 tone correction.

Figure 21. Continued.

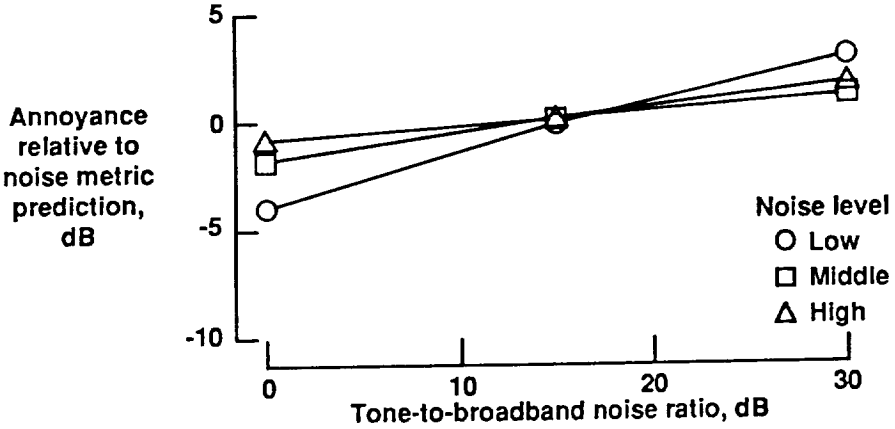

(j) Duration-corrected PNL.

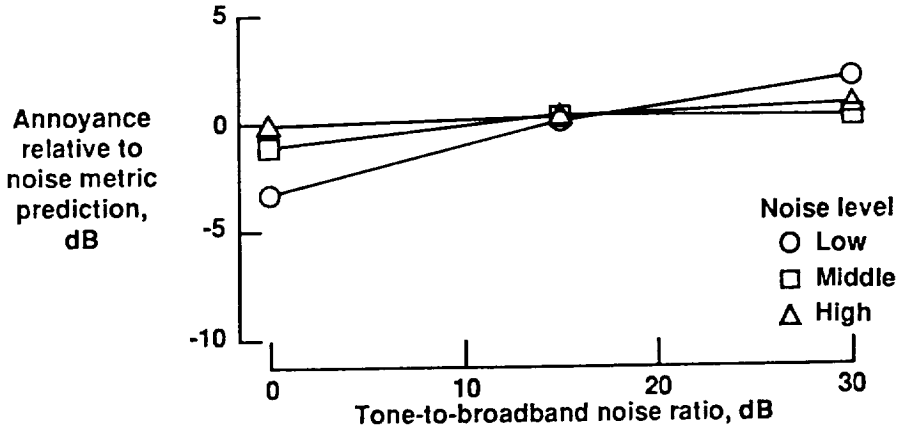

(k) Duration-corrected PNL with T_1 tone correction.

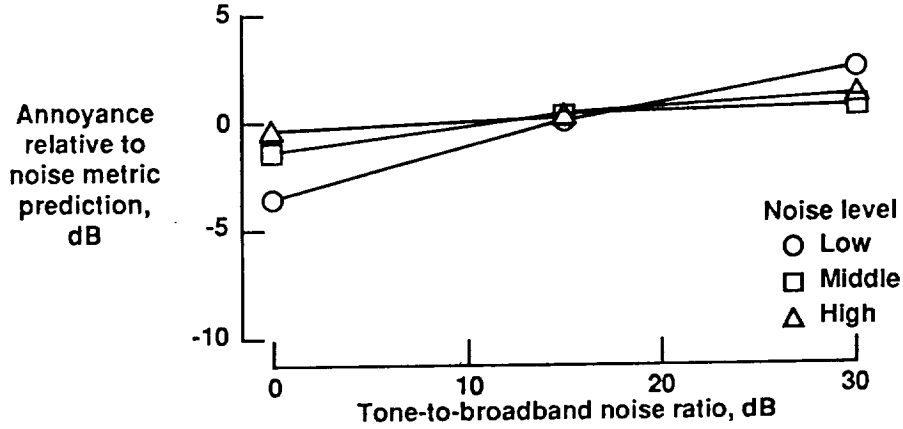

(l) Duration-corrected PNL with T_2 tone correction.

Figure 21. Continued.

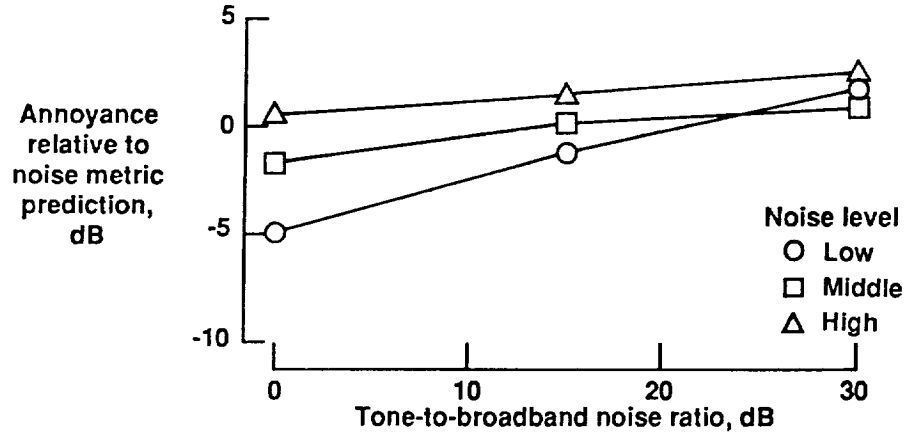

(m) LL_Z.

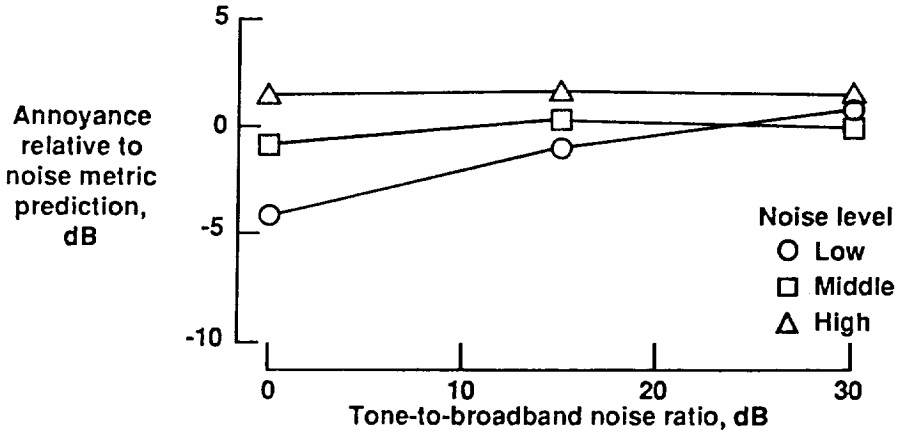

(n) LL_Z with T_1 tone correction.

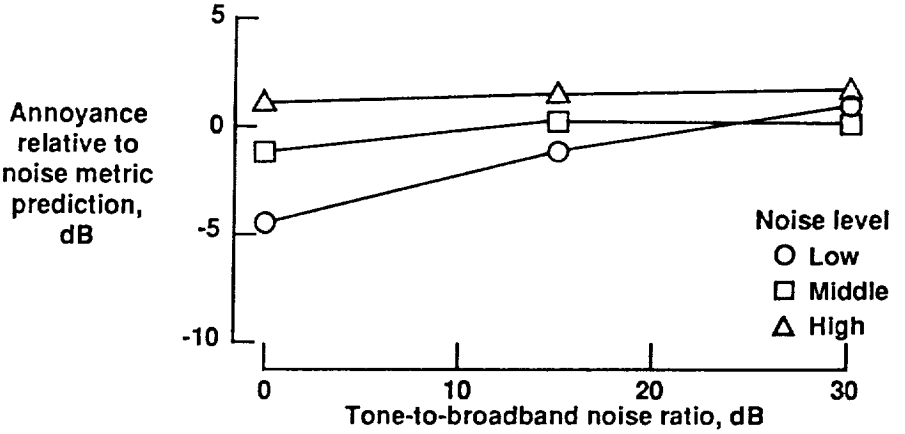

(o) LL_Z with T_2 tone correction.

Figure 21. Continued.

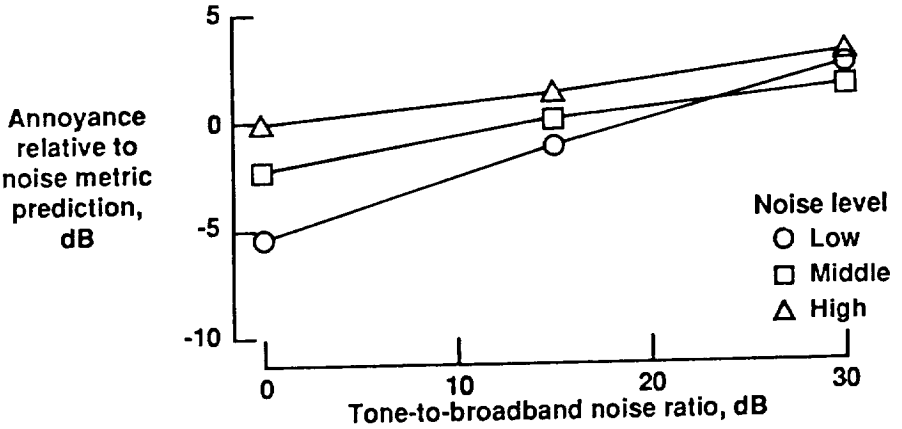

(p) Duration-corrected LL_Z.

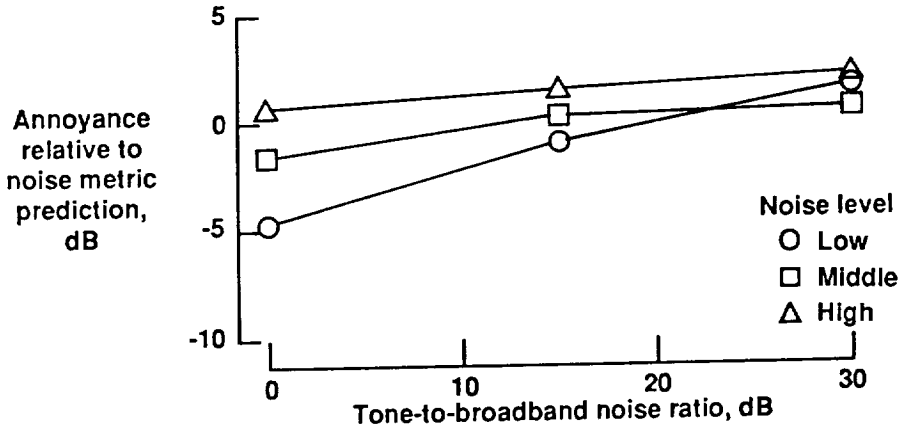

(q) Duration-corrected LL_Z with T_1 tone correction.

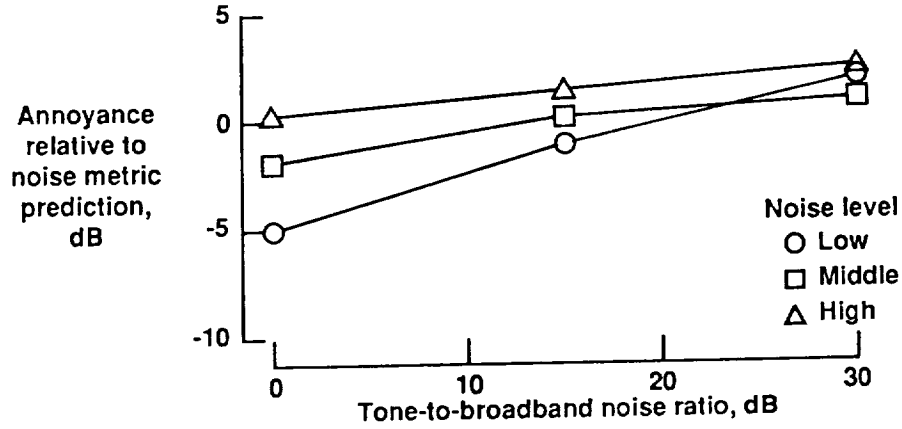

(r) Duration-corrected LL_Z with T_2 tone correction.

Figure 21. Concluded.

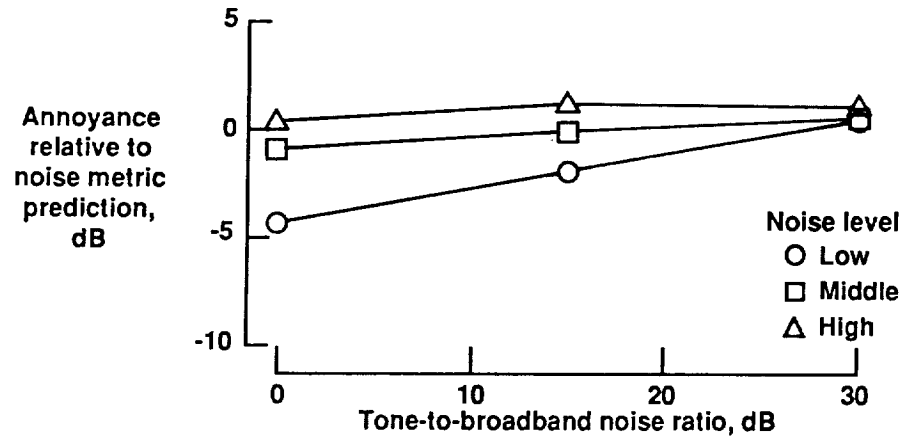

(a) L_A.

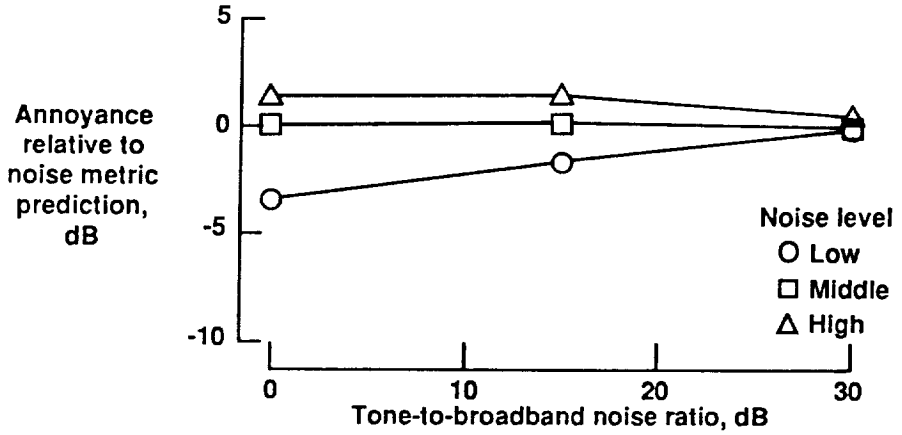

(b) L_A with T_1 tone correction.

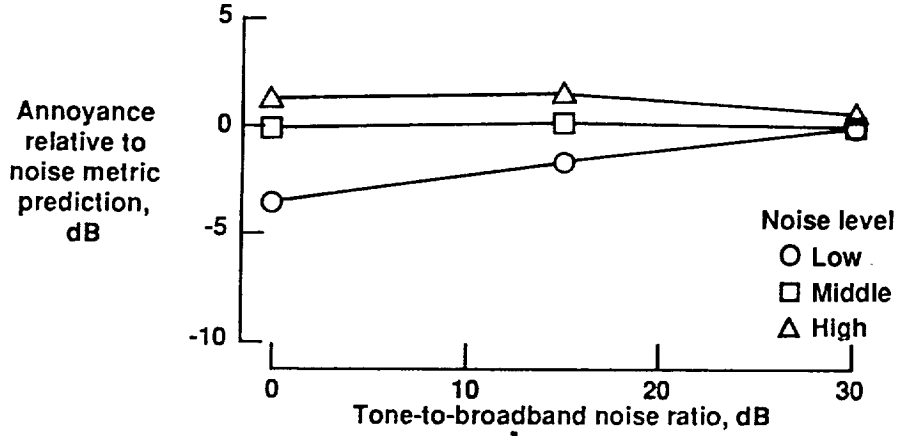

(c) L_A with T_2 tone correction.

Figure 22. Effect of interaction of tone-to-broadband noise ratio with noise level on annoyance prediction for different noise metrics in second experiment.

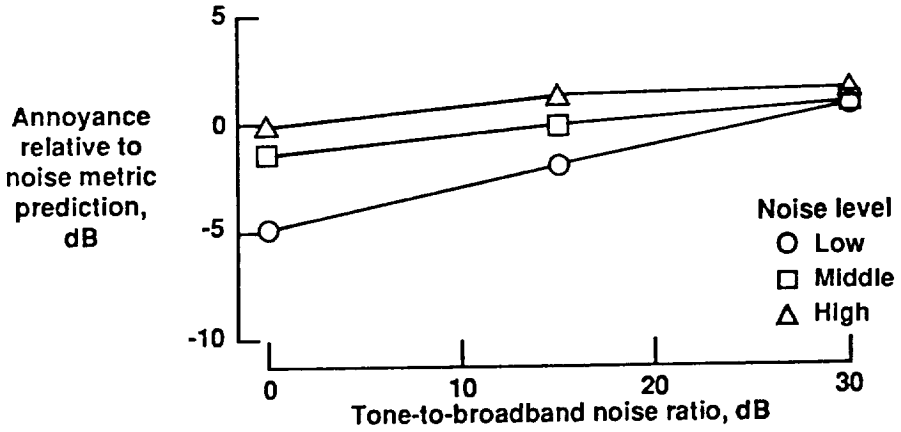

(d) Duration-corrected L_A.

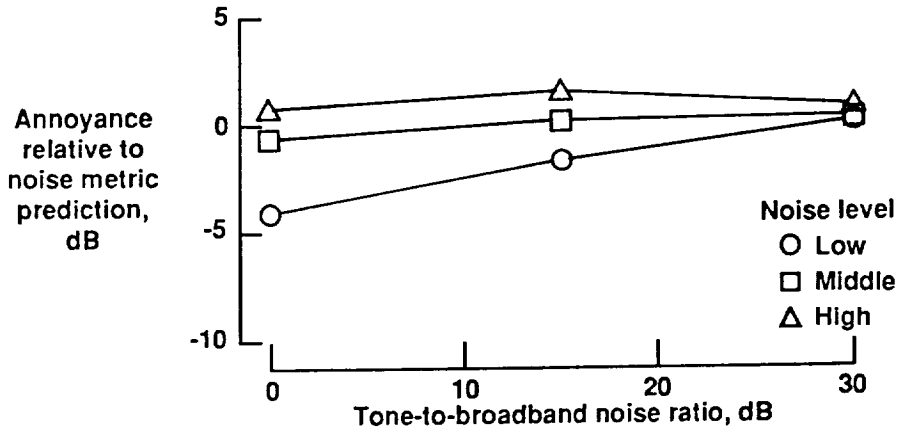

(e) Duration-corrected L_A with T_1 tone correction.

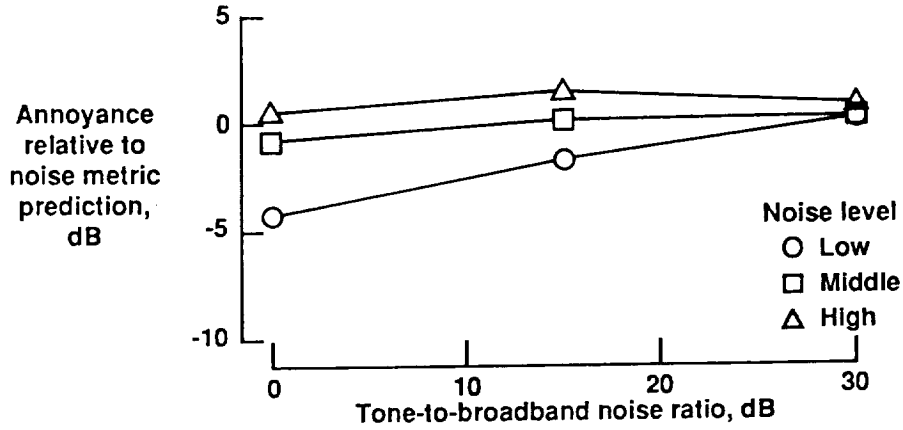

(f) Duration-corrected L_A with T_2 tone correction.

Figure 22. Continued.

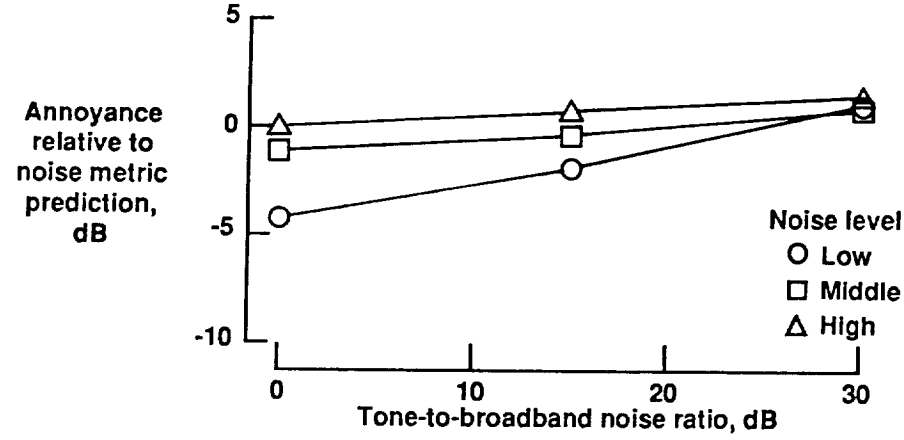

(g) PNL.

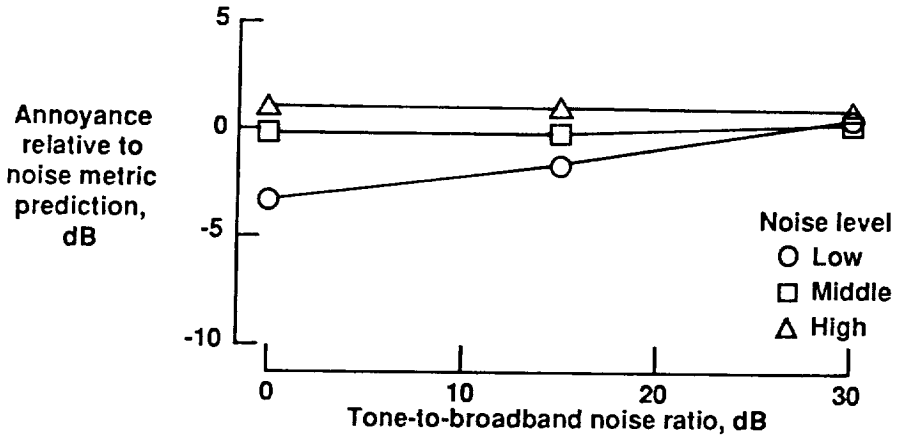

(h) PNL with T_1 tone correction.

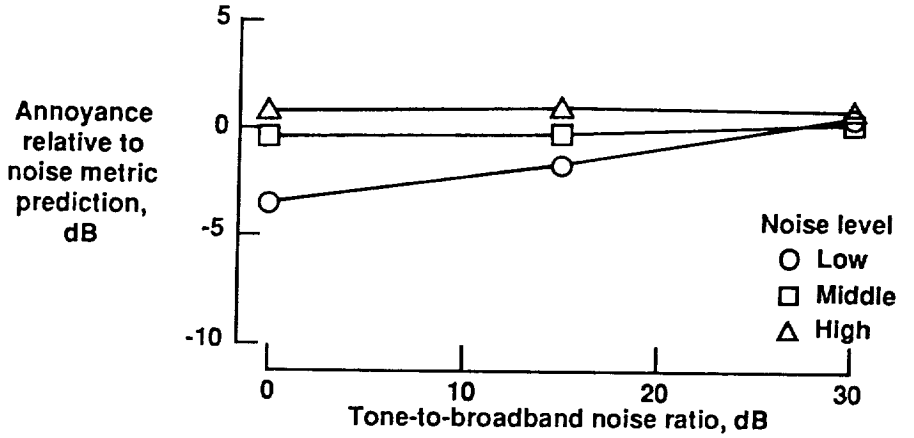

(i) PNL with T_2 tone correction.

Figure 22. Continued.

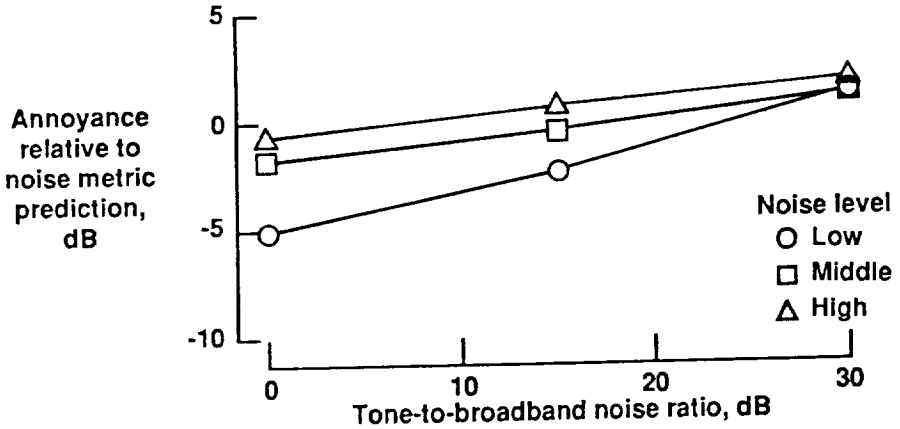

(j) Duration-corrected PNL.

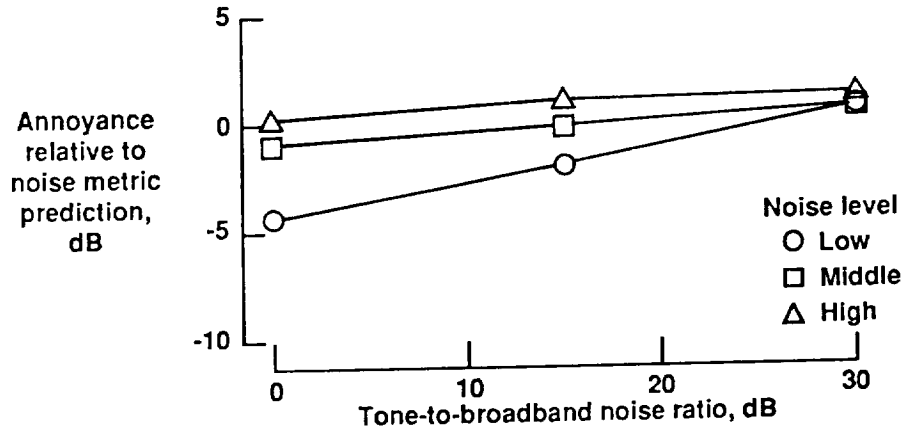

(k) Duration-corrected PNL with T_1 tone correction.

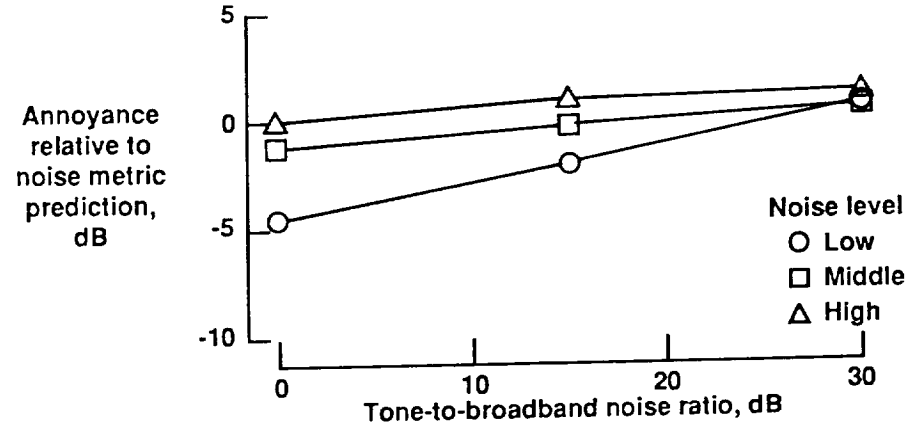

(l) Duration-corrected PNL with T_2 tone correction.

Figure 22. Continued.

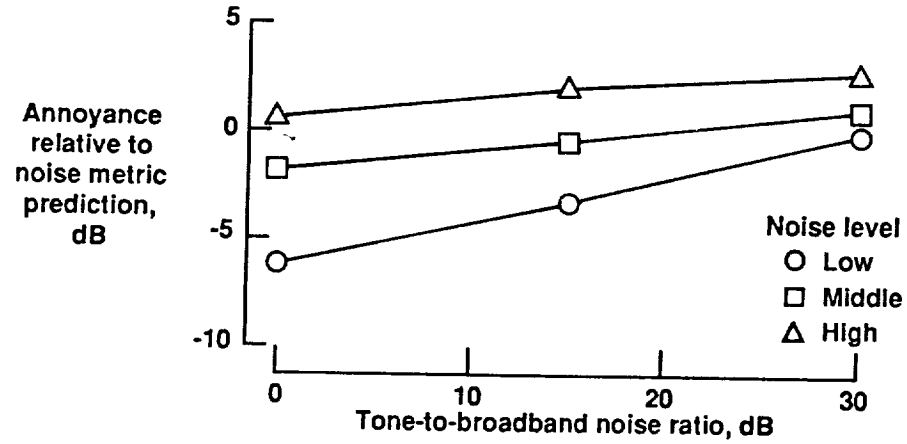

(m) LL_Z.

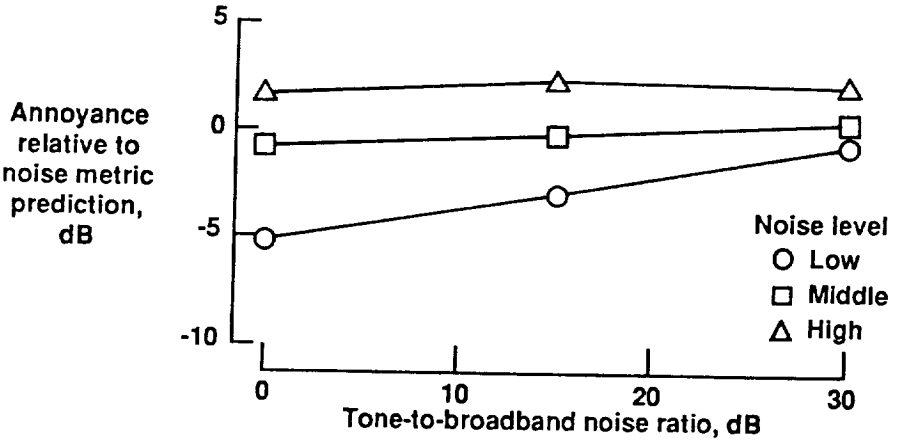

(n) LL_Z with T_1 tone correction.

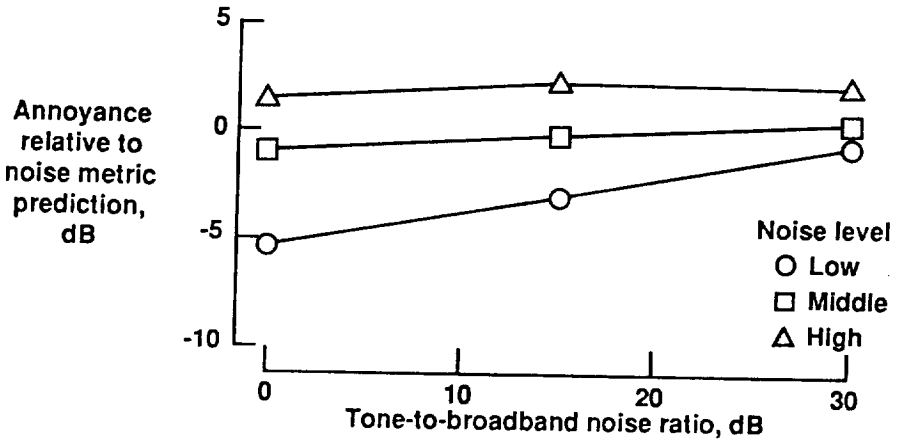

(o) LL_Z with T_2 tone correction.

Figure 22. Continued.

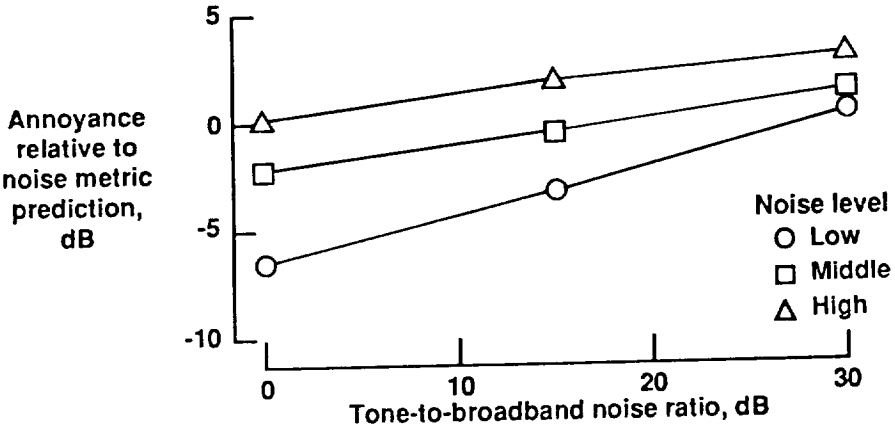

(p) Duration-corrected LL_Z.

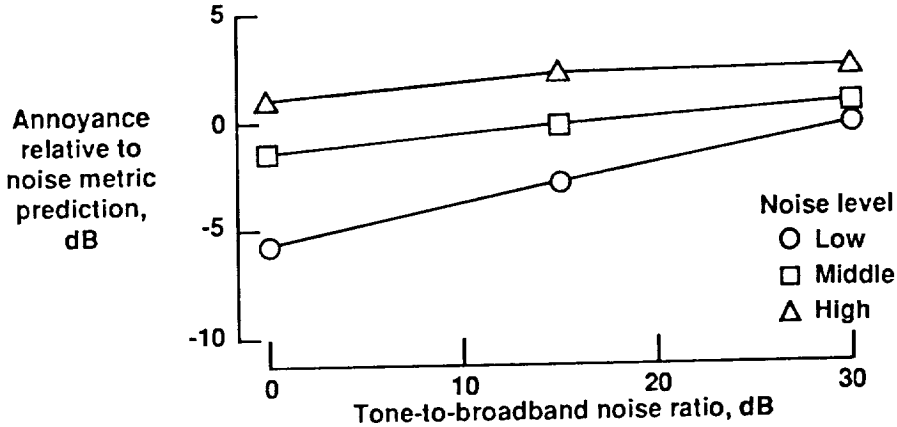

(q) Duration-corrected LL_Z with T_1 tone correction.

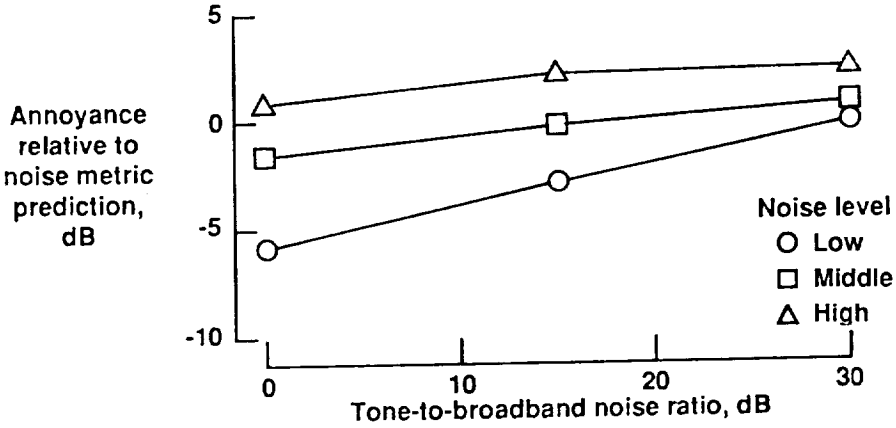

(r) Duration-corrected LL_Z with T_2 tone correction.

Figure 22. Concluded.

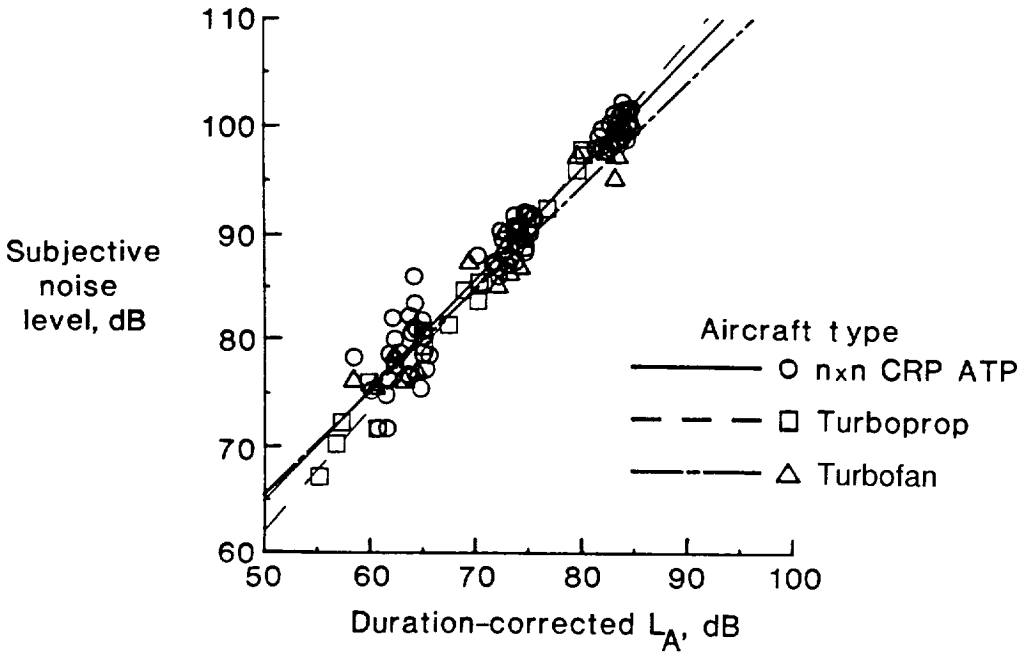

Figure 23. Comparison of annoyance responses using duration-corrected L_A in first experiment.

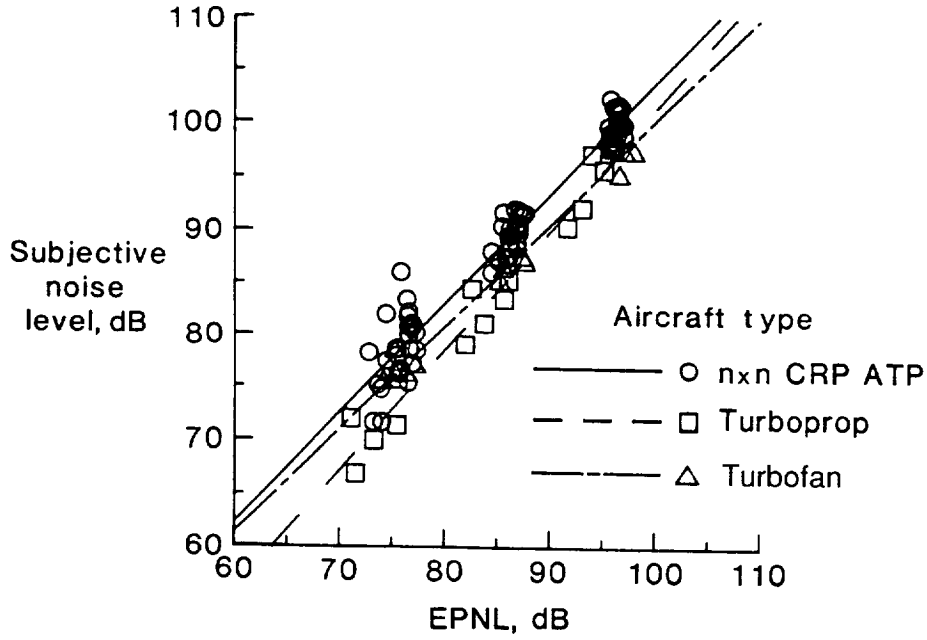

Figure 24. Comparison of annoyance responses using EPNL in first experiment.

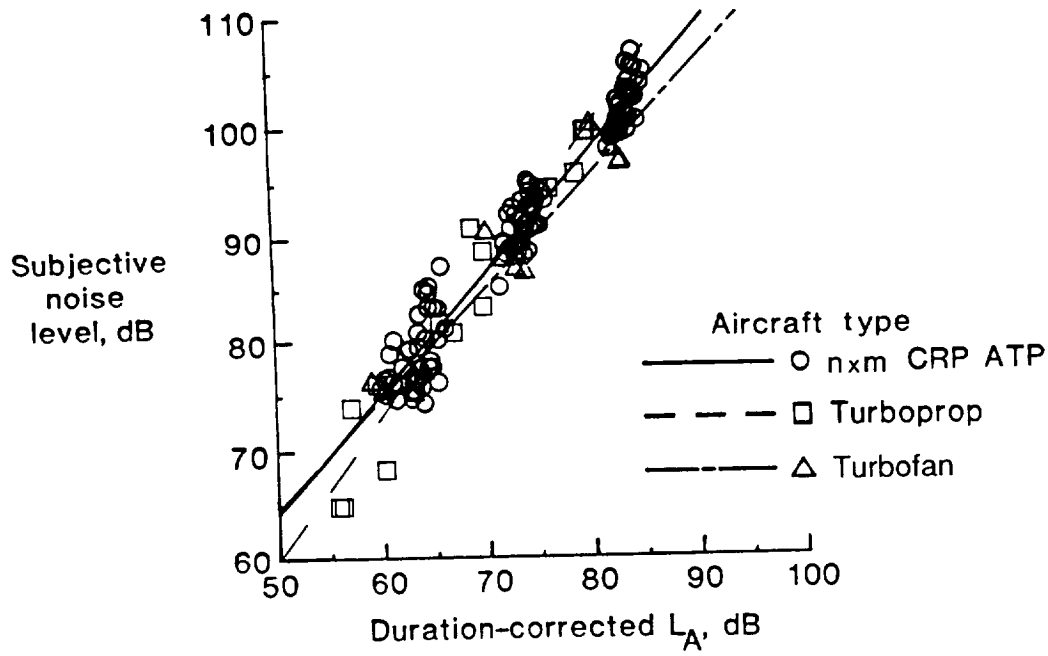

Figure 25. Comparison of annoyance responses using duration-corrected L_A in second experiment.

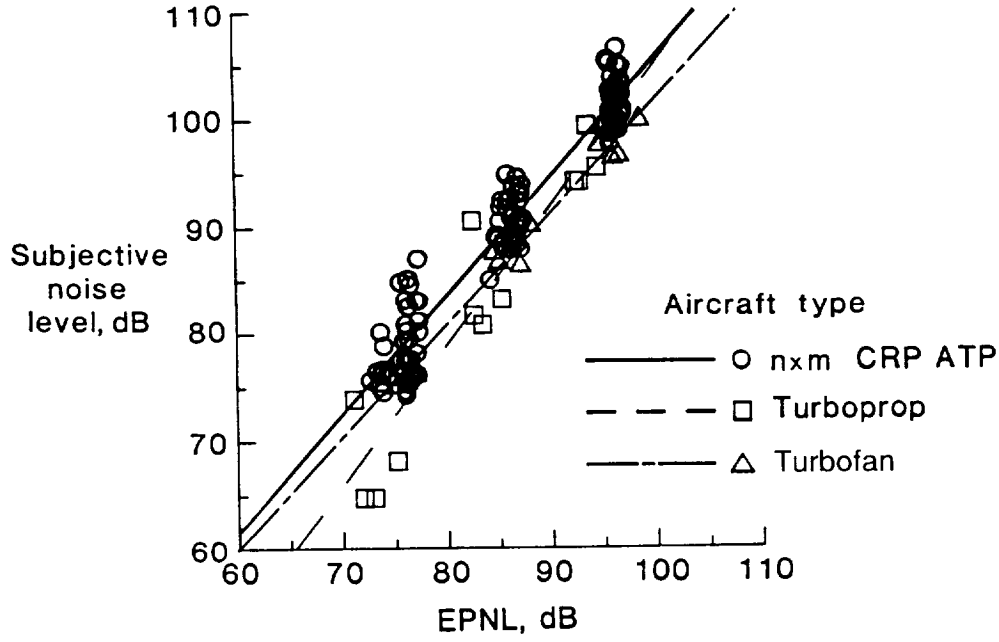

Figure 26. Comparison of annoyance responses using EPNL in second experiment.

NASA
National Aeronautics and Space Administration

Report Documentation Page

1. Report No.	2. Government Accession No.	3. Recipient's Catalog No.
NASA TP-3027		

4. Title and Subtitle	5. Report Date
Annoyance Caused by Advanced Turboprop Aircraft Flyover Noise *Counter-Rotating Propeller Configuration*	September 1990
	6. Performing Organization Code
7. Author(s)	8. Performing Organization Report No.
David A. McCurdy	L-16780
9. Performing Organization Name and Address	10. Work Unit No.
NASA Langley Research Center Hampton, VA 23665-5225	505-63-51-09
	11. Contract or Grant No.
12. Sponsoring Agency Name and Address	13. Type of Report and Period Covered
National Aeronautics and Space Administration Washington, DC 20546-0001	Technical Paper
	14. Sponsoring Agency Code

15. Supplementary Notes

16. Abstract

Two experiments were conducted to quantify the annoyance response of people to flyover noise of advanced turboprop (propfan) aircraft with counter-rotating propellers. The first experiment examined configurations having an equal number of blades on each rotor, and the second experiment examined configurations having an unequal number of blades on each rotor. The objectives were (1) to determine the effects on annoyance of various tonal characteristics, and (2) to compare annoyance response to advanced turboprops with annoyance responses to conventional turboprops and turbofans, and (3) to determine the ability of aircraft-noise measurement procedures and corrections to predict annoyance. A computer was used to synthesize realistic, time-varying simulations of advanced turboprop aircraft takeoff noise. The simulations represented different combinations of fundamental frequency and tone-to-broadband noise ratio. Also included in each experiment were recordings of 10 conventional turboprop and turbofan takeoffs. Each noise was presented at three sound pressure levels in an anechoic chamber. In each experiment, 64 subjects judged the annoyance of each noise stimulus. Analyses indicated that annoyance was significantly affected by the interaction of fundamental frequency with tone-to-broadband noise ratio. No significant differences in annoyance were found between the advanced turboprop aircraft and the conventional turbofans. The use of a duration correction and a modified tone correction improved the annoyance prediction for the stimuli.

17. Key Words (Suggested by Authors(s))	18. Distribution Statement
Advanced turboprop noise Propfan noise Propeller noise Subjective acoustics Psychoacoustics	Unclassified – Unlimited Subject Category 71

19. Security Classif. (of this report)	20. Security Classif. (of this page)	21. No. of Pages	22. Price
Unclassified	Unclassified	86	A05

NASA FORM 1626 OCT 86

NASA-Langley, 1990

For sale by the National Technical Information Service, Springfield, Virginia 22161-2171